# MATERNAL NUTRITION, PLACENTA FUNCTION AND OFFSPRING HEALTH

A Dissertation

by

ZEHUAN DING

Submitted to the Office of Graduate and Professional Studies of
Texas A&M University
in partial fulfillment of the requirements for the degree of

DOCTOR OF PHILOSOPHY

Chair of Committee, Xie, Linglin
Committee Members, Wu, Chaodong
Guo, Shaodong
Ko, Gladys
Head of Department, Threadgill, David W.

May 2021

Major Subject: Nutrition

ABSTRACT

Diabetes mellitus has become a global health concern during past decades. Consequently, diabetic pregnancies were affected in an increasing amount of population. As the one of the major factors during diabetes, maternal hyperglycemia is considered to have great adverse influences on fetal development. As a transient organ connecting the mother and the fetus, the placenta plays many important roles in fetal development. Placental development is affected in diabetes related pregnancy, which further promotes diabetic pregnancy related complications. FOXO1, a transcriptional factor in the forkhead family, plays important roles in fetal cardiovascular and placental development, as well as glucose metabolism. The aim of the project is to understand the molecular mechanism underlying how hyperglycemia disrupts placenta function and promotes birth defects of the fetus, focusing on maternal overnutrition, diabetes and the transcription factor FOXO1. Therefore, three distinct but interconnected studies are involved in this PhD project. In study 1, *in ovo* hyperglycemia was generated in a chicken egg model to study the impact of "hyperglycemia" on the embryonic development. We reported that high dose of glucose was embryonic lethal and lower dose of glucose resulted in heart and limb defects. We further demonstrated that the limb defects induced by "hyperglycemia" were an outcome of disrupted proliferation and apoptosis of the limb mesenchymal cells, associated with down-regulation of Hedgehog signaling. In study 2, wild-type (WT) or FOXO1 heterozygous mice with diabetic pregnancy were generated by streptozotocin (STZ) injections. The placental function and the embryonic heart development were examined to understand the interaction between diabetic pregnancy and FOXO1 deficiency. The results demonstrated that diabetic

pregnancy affected the placental growth and promoted angiogenesis of the placental labyrinth layer, which was further associated with the fetal overgrowth. But those effects were not observed when FOXO1 was downregulated. In study 3, we discovered the influence of maternal diet interventions on the offspring pancreatic β-cell function while the offspring were exposed to postnatal high-fat (HF) diet. The results suggested that proliferation defects and degranulation of the β-cells induced by maternal HF diet were rescued by a pre-gestational diet transition. This study could provide evidence for potential strategies to reduce the detrimental effects of maternal overnutrition. Taken together, this PhD project explored the impacts of maternal factors such as diabetes and overnutrition on placental and fetal development, and further investigated the mechanisms behind them. It provides important information that will lead to health care strategies to improve health outcomes of mothers and children.

ACKNOWLEDGEMENTS

Throughout the past five years of my PhD training, there has been lots of challenges and frustrations, but more than that, I have gained precious knowledge and experiences. Therefore, I would really appreciate those peoples who have always been supporting me and made this a fruitful and unforgettable journey, I could not have accomplished this work without them. Firstly, I would like to express my deepest appreciation to my supervisor, Dr. Linglin Xie, whose expertise and critical thinking have given me a broader insight into forming the research questions. Her support has been accompanying me while facing any challenges. Her patient guidance and instruction have helped me overcoming countless hardships and will always influent me alone my future career.

I would also like to extend my sincere thanks to all my committee members, Dr. Gladys Ko, Dr. Chaodong Wu, and Dr. Shaodong Guo for their generous advice and supports throughout my research. they have provided me with the valuable tools that were facilitative during the entire graduate path. Their insightful feedbacks have encouraged me to refine my thinking and improve my work.

I would like to acknowledge the help from my colleagues. I would like to thank Zhimin Liu for his contribution to this work, he has been a great friend and model who provided a lot of help and suggestions during my graduate life. I would also recognize Jielin Liu, Duohua Chen, Henghui Cheng, Ernest Lynch, Leya He, Zhen Li, Lin Liu for sharing their knowledge and experience in various lab techniques and trouble shootings. And I would also appreciate Yushu Qin, Naomi McCauley and Lauren Lawless for the invaluable discussion which broadened my horizon and gained me significant knowledge over my

research. Especially I would appreciate Lauren Lawless for her thoroughly proofreading on my dissertation manuscript. It really is my great honor to work with such a friendly and creative group.

Finally, special thanks to my family and my girlfriend, Hongying Wang, whose continuous encouragements have been backing me up to pass through the hardest time. They were always here for me and I would have never completed the work without their support.

## CONTRIBUTORS AND FUNDING SOURCES

### Contributors

This work was supported by a dissertation committee consisting of Professors Linglin Xie, Chaodong Wu and Shaodong Guo of the Department of Nutrition, and Professor Gladys Ko of the Department of Veterinary Integrative Biosciences.

The investigation in Chapter IV were conducted in part by Zhimin Liu of the Department of Nutrition and were published in 2020 in an article listed in the Journal of Nutritional Biochemistry.

All other work conducted for the dissertation was completed by the student independently.

### Funding Sources

This project was supported by grants from the National Institutes of Health (NIDDK 1R01DK112368-01 to Drs. Xie and Zhang) and the USDA National Institute of Food and Agriculture ([Hatch] project [1010406] to Dr Xie).

TABLE OF CONTENTS

Page

LIST OF FIGURES

Page

LIST OF TABLES

Page

# CHAPTER I

# INTRODUCTION

## Nutrition during pregnancy

Maternal nutrition is essential for fetal development and growth. Optimizing maternal nutrition requirements, that maximally benefit both the mother's health and fetal development, remains a notable issue for the public health community. To be noted, a mother's nutritional status mainly depends on her initial nutrition stores, dietary intakes, and metabolic conditions. Maternal malnutrition could affect fetal development and influence birth outcomes. Many studies have investigated the effects of maternal nutrition during the later stages of pregnancy (second or third trimesters) [1, 2], in which organogenesis is near completion. During these phases, maternal nutrient availability largely contributes to fetal growth.

### *Nutrition requirement during pregnancy*

Pregnancy is a dynamic process in which the nutritional needs of the offspring shift during the different stages in order to adequately support fetal development. Both maternal undernutrition and overnutrition during pregnancy can impair fetal growth [3-5]. To optimize the outcomes, dietary management should be employed to ensure a proper balance of nutrients. As the energy requirements of the fetus increases, the mother should gain an appropriate amount of weight based on their body mass index (BMI) and manage her calorie intake, carefully. As the major energy source of the body, carbohydrates are essential for fetal development at all stages, as glucose is the preferred

energy substrate of the offspring [6]. Except for the daily recommended intake, it is also beneficial for the mothers to consume carbohydrates with a low glycemic index [6].

Fatty acids (FAs) are also essential macronutrients in a balanced diet. FAs not only provide a large amount of energy, but also play an essential role in the transportation and storage of fat-soluble vitamins. Since fat is not the primary fuel for fetal growth, no dietary recommendation specifies the daily requirement of fat. However, based on the current guidelines for Americans, 25% - 35% of daily calories should be obtained from fat [7]. Additionally, a variety of essential FAs are recommended during pregnancy. Maternal intake of omega-3 or omega-6 fatty acids is associated with better birth outcomes [8, 9].

Protein is not usually regarded as a direct energy source, but provides necessary building blocks for fetal growth. Because of the rapid growth of the developing offspring and mammary tissue, to prepare for lactation, the demand for protein increases concurrently. The recommended dietary intake of protein for pregnant women is 40% higher than non-pregnant women [10]. Maternal protein deposition changes along gestational stages and reaches the highest during the third trimester [11]. Protein from animal sources usually satisfies this requirement during pregnancy. However, mothers should be aware of a potential essential amino acid deficiency when food accessibility becomes an issue [12].

Additionally, a balanced consumption of micronutrients, including minerals and vitamins, are necessary as well. For example, iron is a necessary mineral and its deficiency is highly associated with anemia. During pregnancy, as a result of placental

development, the maternal blood and placenta volume are significantly increased [13]. To be noted, the maternal iron status at the beginning of pregnancy is strongly associated with the risk of anemia during the third trimester [14]. Therefore, adequate iron deposition is required for the hemoglobin synthesis and oxygen delivery.

Folate, another essential micronutrient, is a member of the B-vitamin family. A folic acid deficiency can cause severe developmental complications, such as neural tube defects [15].

*Overnutrition during pregnancy*

Excessive intake of saturated FAs is one of the main factors of obesity, which is a public health concern, as its prevalence has risen over the recent decades. Women of childbearing age appear to be more prone to obesity [16]. Data from the United States in 2014 shows that half of the women at delivery were overweight or obese [17]. As a result of fetal programming and environment factors, offspring health is also under increasing risk of immediate or long-term health problems. High fat diet (HFD) feeding is widely used to mimic the inordinate intake of saturated FAs in animal studies. It has been shown that maternal HFD feeding can induce hyperglycemia, insulin resistance, chronic inflammation, and other metabolic dysfunctions [18-20]. Those changes alter the intrauterine environment and can impact the offspring growth. Increasing evidence suggests that intrauterine exposure to HFD can significantly impact the offspring by affecting growth, glucose metabolism, cognitive function and microbiota composition [5, 21-23].

*Diabetes during pregnancy*

Diabetes mellitus is diagnosed by increased blood glucose levels. In 2017, about 21.3 million babies were born to hyperglycemic mothers [24], regardless that nearly half of the people with diabetes were undiagnosed [24]. A diabetic pregnancy is strongly associated with compromised birth outcomes in both the mother and offspring, and can lead to high risk pregnancy complications, such as pre-eclampsia and miscarriage [25, 26]. For the offspring, exposure to diabetic pregnancy can cause congenital malformations, macrosomia, and higher risk of obesity and diabetes later in life [27, 28].

Placenta is a transient organ during pregnancy. It mainly originates from the trophectoderm in the blastocyst and starts to form after implantation. The placenta is considered the interactive barrier between the mother and fetus, as it functions in supporting the nutrition and gas exchange and the production of hormones. To satisfy the increasing nutritional need of the fetus, maturation of the placental villi is accomplished by well-controlled proliferation and angiogenesis within the endothelial cells. Immature vascularization can lead to fetal growth restriction and even death [29, 30]. It has been demonstrated that a diabetic pregnancy disrupts placenta development and effects the process of angiogenesis and vascular formation [31, 32].

**Birth defect in different types of diabetes**

Birth defects lead to significant infant death and affect 1 in 33 babies in the United States. Notably, gestational and pregestational diabetes are strongly associated with a higher risk of birth complications, including cardiovascular malformation, neural tube

defects, and limb reduction. Over half of the perinatal deaths are due to those major birth defects [33].

In diabetic pregnancies, hyperglycemia, caused by impaired glycemic regulation, is thought to be the main teratogen that affects organogenesis. Although there are a few mouse studies reported congenital heart defects induced by maternal hyperglycemia, the models of diabetes-induced neural tube defects are well-established [33-35]. Optimal blood glucose management before and during early pregnancy has been found to lower the rate of congenital defects in some clinical studies [36, 37]. However, the penetration rate of diabetic embryopathy seems to be incomplete, indicating the contribution of other unclear factors. Therefore, it remains a challenging question that how fetal development is affected by the maternal metabolic environment during diabetes.

*Congenital heart defects associated with diabetic pregnancies*

According to the previous reports, the most common form of birth defect is congenital heart defects (CHDs). CHDs are associated with significantly higher risks of offspring morbidity or mortality. In an epidemiology report in 2010, CHDs are diagnosed in 8 out of 1000 newborns, and is responsible for 2.4 out of 10,000 deaths of newborns in the United States [38, 39]. Moreover, it has been shown that the risk of CHDs are 2-5 times higher in women with diabetes mellitus, although there are discrepancies between different studies and specific CHD phenotypes [40]. For example, Lukas et al. reported that the incidence of transposition of the great arteries (TGA) and SV (single ventricle) were significantly higher in diabetic patients, but double-outlet right ventricle (DORV) showed the highest association with diabetic pregnancy

demonstrated by Loffredo et al. [41]. There are also results showing similar CHD incidences for type 1 and type 2 diabetes [42, 43]. Therefore, it is reasonable to speculate that the heart defects are induced by common factors in both types of diabetes, such as hyperglycemia and oxidative stress. Hyperglycemia is considered the foremost teratogenic factor [44]. A systematic review has suggested that poor glycemic control is strongly associated with compromised birth outcomes [45]. Instead, preconception care and voluntary exercise were shown to reduce the risk of CHDs in the offspring [46, 47].

*Limb defects associated with diabetic pregnancies*

Limb reduction defects are typical birth defects caused by diabetic pregnancies. They occur when the limbs cannot form normally, and manifest as a size reduction or are partially missing. Moreover, they can occur on either the arms, legs, or both. Based on an estimation in 2006, there were 3.82 out of every 10,000 babies affected by upper limb reductions and 1.91 out of every 10,000 babies affected by lower limb reductions in the United States [48].

Studies indicate that the congenital limb defects are usually observed with other bone or cardiac defects [49, 50]. A large population study reported an increased risk of hallucal polydactyly in diabetic patients [51]. Consistently, clinical practice guidelines of the Society of Obstetricians and Gynecologists of Canada (SOGC) describes that limb reduction is strongly associated with pre-existing diabetes [52]. All of this evidence indicates the correlation between diabetic pregnancy and limb defects.

*Neural tube defects and others*

Neural tube defects (NTDs) are representative congenital defects, due to a maternal folate deficiency. They severely affect the development of the central nervous system. NTDs usually arise when the neural tube fails to close during the early stages of development, although the pathological mechanisms remain unclear. Around 3.5 out of 10000 live births are affected by NTDs [53]. There are three types of NTDs: spina bifida, anencephaly and encephalocele, with the first two being the most common. A diabetic pregnancy is considered a risk factor for NTDs. A case control study involving over 7000 babies has reported that the relative risk of NTDs among infants delivered by diabetic mothers was 15.5 [54]. As one of the major metabolic complications during the diabetes mellitus, hyperinsulinemia has been observed to be a major risk factor of NTDs [55]. Besides, maternal dietary intake of high-glucose has been reported to display a strong association with NTDs in both animal studies and clinical trials [56-58]. Increased cell apoptosis and epigenetic modifications induced by high glucose are potential mechanisms for NTDs. Consistently, strict metabolic control is suggested to reduce the incidence of NTDs [56].

*Animal models of a diabetic pregnancy*

Various animal models, including mice models, have been widely used to study the embryopathy of maternal diabetes. Methods to induce a diabetic pregnancy in mice include an STZ injection and HFD [59, 60]. In such models, various birth defects similar to those in humans, were observed. Therefore, mouse models have generated abundant information to study diabetes. In addition, genomic manipulation is very frequently used

in mice to assess molecular changes in diseased states, as mice have a well-defined genome that is highly conservative to humans. Furthermore, mice share the same hemochorial placentation with humans, despite some morphology differences. Thus, a mouse model has been used to study the placenta function in a diabetic pregnancy.

Congenital limb defects have never been reported in diabetic mice models, and only a few basic studies have been carried out to understand how maternal diabetes causes defects in limb development, or combined limb and heart abnormalities. As a well-established model for limb development, the chicken embryo has been widely used, since it is easier to manipulate, and the embryo is isolated from the maternal effects [61].

In summary, both the mouse and the chicken model provide good tools for researchers to interpret the underlying mechanisms of birth defects caused by a diabetic pregnancy.

**Placental development and function in diabetic pregnancy**

The placenta is an important organ that supports the growth of the fetus during gestation. It functions as the exchange interface between fetal and maternal circulations, particularly glucose [62]. It also includes many secretory cells, and produces hormones and growth factors to regulate maternal and fetal metabolisms [63]. As the earliest organ to form during gestation, its functional defects lead to fetal growth restriction and other pregnancy-related complications (e.g., preeclampsia), and even miscarriage under severe conditions [64]. In fact, the origins of most common pregnancy disorders are usually rooted in placental defects [65]. The aim of this section is to review the overall

developmental progress of the placenta, the specific roles of different cell types of placenta, and the impacts of gestational diabetes on placental functions.

*Structure of the human placenta*

In the human, about 8 days after fertilization, the primitive polynuclear syncytium starts to contact the maternal uterine stromal cells and migrate to the decidua [66]. During migration, the syncytiotrophoblast cells produce enzymes that degrade the original cellular junction to facilitate cell invasion. As the syncytium expands, the mononuclear cytotrophoblasts start to proliferate and extend toward the maternal decidua, where the primary villi form. The villus branches develop into a highly complex network, which is similar to the labyrinth in the mouse placenta [67, 68]. Unlike the mouse, the human placental villi have only one layer of syncytiotrophoblast cells that surround the internal cytotrophoblasts and fetal capillaries. Simultaneously, the primary villi continuously expand into the decidua and remodel the maternal spiral arteries, which channel the maternal blood into the space surrounding the villous system, known as the lacunae [67]. By the end of the first trimester, the vascular connection between the maternal and fetal circulations is basically established.

*Structure of the mouse placenta*

Although the mouse placenta has a different architecture compared to the human, the developmental strategy holds many similarities. In mice, after implantation, the extra-embryonic ectoderm expands to form the chorion around E7.5. At the same time, the allantois is derived from the mesoderm at the posterior position of the embryo, and

attaches to the chorion at E8.5 [69]. This process further triggers the formation of the labyrinth layer that is composed of fetal capillaries and the maternal blood network.

At E11.5, the overall structure of the classic chorioallantoic placenta becomes distinct, and can be visualized by the placenta's sagittal plane. The layer proximal to the fetus is called the labyrinth, which is composed of an intricate vascular network of separated fetal and maternal circulation [70]. The fetal capillaries are lined by a thin layer of endothelial cells derived from the allantois, while the maternal blood lacunae are enclosed by two continuous layers of syncytiotrophoblast cells. Mononuclear trophoblast giant cells lie between the fetal capillaries and the maternal blood lacunae. They become perforated and discontinuous around E12.5 [71]. These cellular layers together form the interhemal membrane, which optimizes the mass exchange to ensure the normal development of the fetus.

Moving distally, the next layer is referred to as the junctional zone, which mainly consists of three distinct trophoblast populations: spongiotrophoblasts (SpT), glycogen trophoblasts (GlyT) and parietal trophoblast giant cells (P-TGC). This layer originates mainly from the ectoplacental cone (EPC), and is featured by the expression of trophoblast-specific protein alpha (Tpbpα) [72]. The function of SpTs remains unclear, but are likely to be essential sites of hormone secretion [73, 74]. The GlyT cells can store significant amounts of energy, in the form of glycogen, which is thought to sustain the energy supply during the late gestational stages [75]. GlyT cells also express other regulatory protein such as Connexin31 (Cx31) and matrix metalloproteinases (MMPs), suggesting its important role for cell invasion [75, 76]. P-TGCs define the border of the

junctional zone and the final layer, the maternal decidua. These cells mediate the early invasion toward the uterine endometrium [77]. and produce a variety of hormones that promote maternal adaptation to pregnancy [78]. They also deconstruct to form a connective network between maternal blood lacunae, which support the transportation and of nutrients and hormones at early stages [75].

The maternal decidua is composed of transformed endometrial stromal cells (decidual cells). The decidua also contains maternal immune cells, such as uterine natural killer cells (uNK) [79], invading trophoblast cells and GlyT cells, and maternal spiral arteries and venous sinuses [80].

*The mouse placenta is a good model for studying placental development and function*

Several *in vivo* (etc. mouse, rabbit and sheep) and *in vitro* (etc. human placenta villous explants, BeWo and JEG-3) models have been used to study placental development [81-83]. The mouse model has proven to be the most practical and beneficial due to its genetic similarity to the human and convenience for genetic modification. Although the mouse and human placenta exhibit a morphological difference, they both undergo haemochorial placentation, in which the fetal blood vessels are lined with layers of trophoblasts and are not directly exposed to the maternal blood. The mouse placenta is more similar to the human placenta when compared to some of the larger animal species, such as sheep [84]. For example, the implantation and invasion of the mouse placenta are accomplished by the migration of trophoblast giant cells, which outline the junctional zone and are functionally similar to the human invasive extravillous cytotrophoblast. Furthermore, the mouse trophoblast giant cells and

the human extravillous cytotrophoblast share a polynuclear feature [85]. In addition, inspired by the mouse embryology studies, trophoblast stem cells were generated from extraembryonic tissue, making it a powerful tool for placental studies [86].

*Major cell types of the developing placenta in the mouse*

The formation of the labyrinth requires normal folding of the chorioallantoic layer under the regulation of several signaling pathways, including Gcm1 and Fzd5 [87, 88]. The allantoic mesoderm cells migrate into the folded space, differentiate into endothelial cells, and further grow out as the fetal blood vessels. On the other hand, the chorionic trophoblast cells undergo extensive villous branching to become a condensed structure. These cells start to differentiate into two specific layers of multinuclear cells, termed syncytiotrophoblast type I and II. Taking the advantage of intact cell membranes and less cellular gaps, these two cell layers function to separate fetal and maternal circulation and facilitate nutrient and gas exchange. Another mononuclear cell type, also originating from the chorionic mesoderm, is the sinusoidal trophoblast giant cells (S-TGC). These cells line the maternal blood lacunae, and are part of the interhemal membrane, but may not play a major role in nutrients transportation. However, their abundance in organelles suggests that they may be responsible for hormone secretion and delivery [89, 90].

The EPC contains the progenitors for several trophoblast subtypes, including SpTs, GlyTs, and different types of trophoblast giant cells (TGC) [91], which are the major components of the junctional zone and maternal decidua. The maintenance and differentiation of junctional zone progenitors predominantly depend on the level of the transcription factor, Achaete-scute complex homolog 2 (Ascl2) [92]. Ascl2 drives the

cells within the EPC to punctually differentiate through the TGC lineage. On the contrary, expression of Hand1, which is majorly inhibited by Ascl2, arises outside of the EPC and promotes P-TGC differentiation from the TCG progenitors [93]. Other gene signals, such as Nodal and Erf, are also involved in the cell fate decisions of TGC progenitors in the EPC [94, 95].

At E10.5, the junctional zone forms as a flat layer, and expands from there by cell proliferation and glycogen accumulation. By E12.5, the SpT and GlyT cells start to show histological discrepancies. SpT cells appear to be small and condensed, and GlyT cells become vacuolated due to the storage of glycogen in the cytoplasm [96]. Furthermore, SpT cells are stationary and increase modestly in number, whereas GlyT cells rapidly proliferate and a subpopulation of GlyT cells migrate from the junctional zone to the decidua. In late gestation, the GlyT cell number drops dramatically [75].

Immediately after implantation, the maternal decidua starts to develop, and critical changes in vasculogenesis and the extracellular matrix are initiated in the endometrium. Simultaneously, uterine stromal cells start to interact with a variety of cytokines [97] and increase the endometrial vascular permeability [98], in a process called decidualization. To deliver the maternal blood to the placenta, a network of spiral arteries forms and connect to the maternal circulation through the myometrium [99]. While the spiral arteries are developing, trophoblast invasion begins, simultaneously, at E8.5. From the junctional zone, the SpA-TGCs also invade the arteries and replace the original endothelial cells and smooth muscle cells surrounding the lumen. As a result, the spiral arteries lose contractility and become dilated, therefore promoting placental blood flow

to meet the fetal demand. This procedure is defined as “arterial remodeling” [100]. In addition, the uterine natural killer cells (uNK) are thought to regulate the critical balance of maternal immune responses [101].

*Angiogenesis during placental development*

As the maternal and fetal blood interface forms, placental vascularization shows extreme complexity, which ensures adequate gas and nutrient exchange between the mother and the fetus, particularly in late gestation. After the vascular formation is initiated, it continues to sprout and loop under strict regulation by numerous growth factors, including both pro- and anti-angiogenic. The vascular endothelial growth factor (VEGF) family is one of the major angiogenic factors and functions throughout placental development. Ablation of one VEGFα allele or knockout of VEGF receptor 1 (VEGFR1) leads to vasculature malformation and embryonic death before E10.5 [102, 103]. Furthermore, fibroblast growth factor 2 (FGF2), angiopoietins, and placental growth factor (PIGF) and their corresponding receptors are also important for placental angiogenesis regulation.

Hypoxia is an inductive factor of angiogenesis. Normally, hypoxia occurs when the oxygen supply in the circulation is insufficient for the cellular demands. During the first trimester, the embryonic oxygen requirement increases dramatically, and hypoxia is induced under this physiological condition. Hypoxia can elevate the expression of several pro-angiogenic factors, therefore promoting endothelial cell growth and angiogenesis. Hypoxia inducible factors (HIFs) are important responsive factors that can bind to the promotor of other angiogenic genes (e.g. VEGFα) and activate their

expression [104]. Thus, placental blood circulation is mostly established at the beginning of the second trimester.

*Placental nutrient transportation in diabetic pregnancies*

Glucose is the major energy source for both the developing placenta and fetus. Because the fetal liver has not fully developed during the first and second trimester, it cannot produce enough glucose and needs to obtain it from the maternal blood circulation. The glucose transportation rate is associated with several factors, including concentration gradient, glucose transporter levels and interhemal membrane thickness. In the placenta, glucose transporter 1 (GLUT1) is the predominant member expressed by the syncytiotrophoblasts and fetal endothelial cells, with its highest expression found in the syncytiotrophoblasts [105]. Other transporters, such as GLUT3 and GLUT4, are also identified in the placenta, but with relatively lower levels [106]. Normally, the transportation capacity of GLUT1 in the placenta is far from saturated. However, during a diabetic pregnancy, maternal hyperglycemia may promote GLUT1 expression in the syncytiotrophoblasts, but not GLUT3 or GLUT4, which suggests the adaptation to the elevated glucose gradient [107]. In addition, other factors such as hypoxia and growth hormones (e.g. insulin) are also affected by hyperglycemia, as they can regulate the glucose transportation indirectly [108].

The FA transportation is a complex procedure, and is critical for fetal development, especially during late gestational stages. As relatively large molecules, FAs are required to be assembled with maternal lipoproteins prior to transportation. The transportation of lipoproteins is aided by a couple of enzymes and receptors, such as

lipoprotein lipase (LPL), fatty acid binding protein (FABP) and lipoprotein receptors [109]. During a diabetic pregnancy, it has been shown that the expression levels of several FABPs are increased, which can explain the FA accumulation in the late trimester placenta [110]. Lipid metabolism can provide an additional mechanistic correlation between maternal metabolic disorders and fetal fat accretion. GDM patients' placentas were shown to have decreased fatty acid oxidation, as well as upregulated esterification and triglyceride accumulation [111].

Amino acids are essential for protein synthesis and other metabolic activities, which are key factors to determine intrauterine growth rate. Unlike glucose, the concentrations of amino acids in the maternal blood flow are lower than in the fetal plasma. Therefore, the transportation rate is controlled by the number of transporters on the surface membrane of syncytiotrophoblasts and endothelial cells. The transporters are categorized into two families based on their specific functions: system A and L. System A transporter proteins are also called accumulative transports, which uptake amino acids from maternal or fetal circulation and store them within the syncytiotrophoblasts [112]. System L transporter proteins are in charge of essential amino acid uptake, which depends on the efflux of other amino acids in the cellular pool [113]. Both rodent and human studies have suggested that, in diabetic or obese patients, the activities of system A and L transporter proteins are upregulated in the syncytiotrophoblast membranes, and is highly associated with fetal overgrowth [114, 115]. However, the underlying mechanisms are still not fully defined.

*Effects of maternal hyperglycemia on placental angiogenesis*

The placenta is the primary interface between the maternal and fetal blood circulations in mammal. A variety of functions necessary for fetal growth and development are performed within this temporary organ, including the transportation of nutrients, oxygen, and the synthesis of many hormones, as well as growth factors that regulate fetal and placental growth [116]. Under maternal hyperglycemia conditions, such as pregnancy during overt diabetes or gestational diabetes, ample data from human and rodent studies suggest that the placental function is affected [64, 117], evidenced by pathohistological alterations.

During early stages of pregnancy, when the spiral arteries have not fully been remodeled, the placental environment is hypoxic. Hypoxia is an essential factor to stimulate arterial remodeling and angiogenesis [118]. Spiral artery remodeling, coupled with increased oxygen tension in the intervillous space, is the result of the temporary oxidative physiological stress in the trophoblast cells [119, 120]. Pregnancy under maternal obesity or diabetic conditions presents complications, as existing peripheral proinflammatory stress overlaps with this physiological oxidative stress, and can result in a retardation in trophoblast development [120].

Hyperglycemia has been reported to effect vascular modifications in the placenta, since it is the primary cause of proinflammatory and cytokine disturbances that can further affect the endothelium. Hyperglycemia upregulates the production of reactive oxygen species (ROS) and leads to oxidative stress. Many studies have shown that oxidative stress can then lead to the pro-inflammatory environment of diabetes and may

have an effect on angiogenesis [121, 122]. For example, hyperglycemia can promote TNF-α expressions in trophoblast cells, although not in fetal circulation [123, 124]. TNF-α can further contribute to a proinflammatory environment in the placenta. Moreover, TNF-α stimulates the activity of HIF1α and can upregulate the hypoxia-induced transcription [125]. Furthermore, leptin, adiponectin, and metalloproteinases (MMPs) also play regulatory roles in the placenta during pregnancy, which have been reported to have dysregulated expression patterns under hyperglycemic condition [126-128]. This suggests that placental development is affected by maternal hyperglycemia from many different aspects.

**FOXO1 signaling cascade**

There are four members in the forkhead family transcription factors, including FOXO1, FOXO3a, FOXO4, and FOXO6 [129, 130]. They are present in a wide variety of tissues and have a variety of cellular functions, including the suppression of tumor proliferation, the regulation of energy metabolism and the induction of cellular responses [131]. FOXO1 is a typical member of the FOXO family with a large presence in a various type of tissues, and its core transcription regulatory activities have been demonstrated.

FOXO1 plays an essential role of glucose metabolism, especially in hepatic gluconeogenesis [132]. Under fasting conditions, FOXO1 is dephosphorylated and translocated into the nucleus due to decreased insulin signaling [133]. As a transcriptional factor, it binds to the promotor regions of phosphoenolpyruvate carboxykinase (PEPCK) and glucose-6-phosphatase (G6Pase), which are the two rate-

limiting enzymes of gluconeogenesis. Coupled with hepatic glycogen hydrolyzation, adequate glucose is produced for physiological demand. During the postprandial state, insulin inhibits FOXO1 activity through AKT-mediated phosphorylation, and prevents excessive production of glucose [134]. Animal research has suggested that a FOXO1 deletion in the liver can significantly reduce hepatic gluconeogenesis and glycogenolysis, and the animal shows partially rescued regulation of glucose metabolic genes under diabetic condition [134, 135]. However, when insulin receptor substrate (IRS) 1 and 2 are deleted, the inhibition of FOXO1 will be blocked and FOXO1 remains hyperactive, which causes hyperglycemia, dyslipidemia, and mitochondria dysfunction [136-138].

Lipid metabolism is also regulated by FOXO1 through several pathways. Firstly, FOXO1 can affect mitochondrial oxidation. FOXO1 can bind to the promoter of heme oxygenase 1 (Hmox1) and disrupt the electron transport chain functions [139], leading to FA and triglyceride accumulation in the liver and peripheral tissues [140]. Moreover, FOXO1 can directly promote hepatic production of very-low-density lipoprotein (VLDL), though upregulating the microsomal triglyceride transfer protein (MTP) levels in liver [141].

*Effect of FOXO1 signaling over-activation in obesity and diabetes*

Overexpression of FOXO1 can induce either beneficial or detrimental effects over lipid metabolism, regarding specific tissues and organs [142, 143]. These controversial results may be a consequence of discrepancies in the duration of FOXO1 overactivation and endocrine environments. Pathological disorders, such as obesity, insulin tolerance

and diabetes, contribute to dysregulated activation of FOXO1, and can lead to metabolic disruptions and activation of apoptosis in the corresponding tissues.

During obesity, the coupled activation of MAP kinase pathways and nuclear translocation of FOXO1 are caused by excess nutrients, such as high fat or high glucose, and excessive ROS production [144]. Under insulin resistance and diabetic conditions, FOXO1 phosphorylation inhibition and insulin signaling activity have reduced, causing it to be less responsive to ubiquitination-mediated degradation [145]. In adipose tissue, p21 and PPARγ are suppressed, which are primarily involved in adipocyte differentiation. In the liver, gluconeogenesis and lipogenesis are believed to increase, which can significantly affect the energy homeostasis [146]. It has been reported that overexpression of FOXO1 in β-cells can downregulate pancreatic and duodenal homeobox factor 1 (PDX1), and induce deleterious effects related to β-cell dysfunction and death, which further leads to type 2 diabetes [147-149].

*FOXO1 deficiency and diabetes*

FOXO1 disruption has been shown to reduce insulin resistance in rodent models of T2D, caused by high fat in the liver and skeletal muscles [150, 151]. In liver specific IRS1 and IRS2 DKO diabetic mice, a FOXO1 deletion can rescue the hyperglycemia [152]. In diet-induced obese rats, induction of FOXO1 in the hypothalamus results in a reduction of appetite and body weight, and increased insulin sensitivity [153]. However, *in vivo* studies suggest that adipocyte FA exposure can cause decreasing insulin sensitivity, as well as a decreased expression of FOXO1, which further results in increased expression of adipose PPARγ and its target genes [154, 155], suggesting a

critical function of FOXO1 in adipocytes. FOXO1 levels are also found to be affected in other tissues including pancreas and muscle, which indicates a systematic alteration of FOXO1 functions during diabetes [156-159].

*FOXO1 is required for Chorioallantoic attachment during placental development*

Chorioallantoic attachment is a critical aspect of placental morphogenesis. Specific mechanisms controlling chorioallantoic attachment remain unknown. FOXO1 plays a critical role in the coordination of chorioallantoic interaction, which is vital for embryo survival. As expected, FOXO1-null embryos are not viable, and the allantois is not able to attach the chorion layer at E8.5 [160]. In addition, vascular cell adhesion molecule-1 (Vcam1) gene expression is significantly downregulated in the FOXO1-null allantois [160]. This finding is consistent with the essential interaction between allantoic Vcam-1 and chorionic integrin, which is required for normal chorioallantoic attachment [161, 162]. These findings suggest that FOXO1 is involved in placental morphogenesis at early developmental. Further investigation is needed to explore if FOXO1 deletion also affects trophoblast populations.

*FOXO1 in decidualization of the endometrium during placenta development*

Normal pregnancy involves synchronization of the growth of embryos, decidualization of the endometrium and the vascular system establishment in the placenta. Because of FOXO1's capacity to control genes related with programmed cell death, differentiation and antioxidation, it has emerged as a central mediator of cell fate [163]. In the endometrium, FOXO1 is an important key regulator of human endometrium differentiation and progesterone-dependent menstrual shedding [164].

Through decidualization, FOXO1 is significantly induced *in vivo* and *in vitro* [165, 166]. Furthermore, FOXO1 is important to induce the decidua-related marker genes, including Insulin Like Growth Factor Binding Protein 1 (IGFBP1) and Prolactin (PRL) [167].

*FOXO1 in vascularization during placenta development*

As previously mentioned, the placentation process involves an extremely high level of vascularization, due to the abundant substance exchange between the fetus and mother. FOXO1 expression has also been reported in endothelial cell and syncytiotrophoblast cells in the human placenta at later gestational ages [168] and endothelial cells in mice [169]. Therefore, it is predicted that FOXO1 may play a role in pregnancy complications, featured by abnormal vascularization and impaired angiogenesis.

FOXO1 acts as an essential endothelial growth checkpoint that strictly controls vascular development. According to some findings, FOXO1 induces endothelial quiescence by inhibiting MYC, resulting in a synchronized decrease in proliferative and metabolic function of endothelial cells [170]. The FOXO1-induced inhibition of metabolic activity can help to maintain endothelial function, as well as enforce quiescence [171]. Endothelial cells will require less energetic fuel for their homeostatic needs if their metabolism is reduced, ensuring optimal nutritional and oxygen supply. Endothelial redox equilibrium can be improved by lowering metabolic activity.

Endothelial cells, on the other hand, are long-lived cells that must defend themselves from oxidative damage, caused by elevated oxygen levels in the blood [172]. The FOXO1-induced decrease in oxidative metabolism maybe a mechanism for reducing the

generation of mitochondria-derived ROS, thus providing protection from high-oxygen environments [173].

# CHAPTER II

# *IN OVO* HYPERGLYCEMIA CAUSES CONGENITAL LIMB DEFECTS IN CHICKEN EMBRYOS VIA DISRUPTION OF CELL PROLIFERATION AND APOPTOSIS[*]

## Introduction

Diabetes mellitus is a chronic metabolic disease characterized by hyperglycemia associated with insulin deficiency or insulin resistance. As the incidence of diabetes mellitus continues to rise and the age of affected population keeps dropping, women of childbearing age have a higher rate of diabetes mellitus during pregnancy. Diabetes during pregnancy affects the health of both the mother and child. Of the two types of diabetes mellitus during pregnancy, gestational diabetes accounts for 90% while pre-gestational diabetes accounts for 10% [174, 175]. In the United States, the prevalence of gestational diabetes among pregnant women is as high as 9.2% [176]. With the introduction of insulin, diabetes-associated fetal mortality rate dropped from 70% to nearly 12% [177]. Unfortunately, the birth defect rate from diabetic pregnancies (~10%) remains higher than the general population (3%) and appears to be on the rise [176-178]. While the positive correlation between diabetes mellitus during pregnancy in women and birth defects is well established, the specific mechanism in which *in utero* hyperglycemia leads to developmental abnormalities remains unclear. In order to

[*]Reprinted with permission from "In ovo hyperglycemia causes congenital limb defects in chicken embryos via disruption of cell proliferation and apoptosis." by Ding, Z., et al, (2020). *Biochim Biophys Acta Mol Basis Dis* 1866(12): 165955. Copyright 2020 by Elsevier B.V..

formulate a preventive strategy for diabetes mellitus related birth defects, a better understanding of fetal development under hyperglycemia is urgently needed.

Diabetes during pregnancy can lead to a variety of congenital anomalies, including abnormalities of the craniofacial, cardiovascular, gastrointestinal, urogenital, musculoskeletal, and central nervous systems [177]. For over twenty years, limb defects, especially the preaxial polydactyly, have been used as markers for diabetic embryopathy due to their high association with diabetic mothers [60, 179, 180]. The longitudinal limb deficiencies in infants have also been reported to be associated with diabetes mellitus during pregnancy (OR=7.01 and 95% Crl=1.91-25.68) [181]. The Center for Disease Control and Prevention (CDC) estimates that 6 out of every 10,000 babies in the United States are born with upper limb and/or lower limb abnormalities every year [182]. Cardiovascular defects are also common congenital abnormalities associated with maternal diabetes. The risk of having a baby with congenital heart defects (CHD) is 2-5 times higher in diabetic mothers compared to non-diabetic mothers [183, 184]. A recent systematic meta-analysis study of literature from 1975 to 2012 on the association of diabetes mellitus during pregnancy and CHDs reported that 8.3% of pre-gestational diabetes mellitus/gestational diabetes mellitus women gave birth to infants with CHDs [185]. Importantly, diabetic embryopathy has been reported to be linked with VACTERL association, in which an individual exhibits a combination of vertebral, anal, cardiac, trachea-esophageal, renal, and limb defects [41, 186-189].

Previous studies have used both the STZ induced [190-193] and HF diet induced [60] pre-gestational diabetes mouse models to investigate how maternal diabetes causes birth

defects. These models contribute a considerable amount of information about the manifestations of fetal cardiovascular and central nervous system defects. In these studies, ontogeny of congenital heart defects in offspring from pre-gestational diabetic pregnancies is explained through mechanisms that involve cell proliferation defects [193, 194], excessive programmed cell death [195-197] and abnormal migration of the cardiac progenitors during early stages of heart development [198]. However, no study has examined the molecular mechanisms behind the link between diabetic pregnancies and abnormal limb development or concurrent abnormalities of the limbs and heart.

In order to investigate diabetic embryopathy, especially in the limb, we developed a novel chicken embryonic model with a high glucose environment *in ovo*. These embryos developed limb and/or heart defects that resemble those of infants born to diabetic mothers. Using this model, we studied the molecular and cellular mechanisms of how embryonic development under hyperglycemia leads to limb defects.

## Experimental methods

*Maintenance of chicken embryo*

Fertilized eggs (*Gallus gallus*, Single Comb White Leghorn) were obtained from the Poultry Science Department, Texas A&M University (College Station, TX). All chicken embryos were maintained in an egg incubator at 38°C ± 0.5°C. Special appreciation to Dr. Ko and Dr. Shi (Texas A&M University, College Station, TX) for their generous help on setting up the egg incubation and guidance of the technical details.

*Preparation of chicken saline and glucose solution*

Chicken saline (110 mM NaCl, 10 mM $BaCl_2$, 0.4 mM $MgCl_2$, 5.3 mM KCl) was used as a vehicle. Glucose was dissolved in chicken saline at 330 mg/mL then filtered through a 0.22 *um* syringe filter as a stock solution and stored at -20 °C for up to one month. Before each treatment, the stock solution was diluted with chicken saline to the respective doses.

*Chicken saline and glucose solution injection*

At embryonic day 2 (HH16 stage, 51-56 hours old) or day 4 (HH24 stage, 4.5 days old), the weight of each egg was measured with a scale. Treatments were conducted under a sterilized culture hood. The eggs were oriented with sharp ends pointing down and cleaned with 70% ethanol. A small window (less than 0.5 $cm^2$) on the shell above the air-sac was pierced open, and the shell membrane was carefully peeled away. The pre-made chicken saline or glucose solution of certain doses were pipetted onto the air sac membrane, with a volume adjusted to the egg's weight. The dosage of the glucose (g/kg) was calculated as the amount of glucose in grams per kilogram of egg being

treated. The window was sealed with medical tape to prevent contamination post-treatment and returned to the incubator.

*Yolk glucose measurement*

At each harvest, 100 µL of yolk from each sample was added to an EP tube with 500 µL of PBS by pipetting up and down several times to wash out the yolk on the tip, then vortexed and spun down. The glucose concentration of the diluted yolk was measured with Contour NEXT EZ glucose monitoring kit (Ascensia Diabetes Care US Inc, Parsippany, USA).

*Real-Time PCR*

The leg and wing bud at either HH27 or HH29 were collected and put in a 2 mL EP tube with 500 uL Trizol reagent (Thermo Fisher Scientific, Waltham, USA). The RNA extraction and real-time PCR were performed as previously established [199]. The primers used are listed in Supplementary Table 4.

*Immunohistochemistry (IHC) for proliferation and apoptosis*

Standard procedures were used for IHC. IHC was performed using the rabbit anti-mouse p-Histone-H3 (p-H3S10) (Abcam) as the primary antibody. For colorimetric staining, slides were incubated with rabbit ImmPress reagent (Vector Labs) and stained with a 3,3′-diaminobenzidine-tetrahydrochloride (DAB) substrate kit (Vector Labs), and counterstained with hematoxylin (HE). For TUNEL, an ApopTag Plus Peroxidase in-Situ Apoptosis Detection Kit was used (EMD Millipore) with DAB and HE.

*Statistical Analysis*

Data of yolk glucose concentration, histology, and real-time PCR were analyzed using Student's *t*-test. Data were considered significantly different when $p<0.05$. The limb and heart defect rates were analyzed using Chi-square test, the difference was considered significant when $p<0.05$. The two-parameter logistic function was used to analyze the survival rate data. The survival curves were generated using the following equation:

In this equation, $c$ stands for baseline response and $d$ is the largest effect achievable. If $b < 0$ the curve is increasing, otherwise, curve is decreasing. Lethal-dose 50 (LD50) is equal to $e$ when $x = e$, $y = c + \frac{d-c}{2}$.

LD50 is the estimated dosage lethal to 50% of the population.

## Results

*Glucose treatment successfully induces "hyperglycemic environment" in fertilized chicken eggs.*

Chicken saline or different doses of glucose (0.3, 0.5, 0.75, 1, 1.25, 1.5 and 2 g/kg of egg weight) were administered to the air-sac of fertilized eggs at either Hamburger Hamilton stage 16 (HH16) or HH24 (Table 1). The glucose levels in the yolk of eggs injected with chicken saline, or various doses of glucose solution were then measured at HH29 and HH35. There was only a marginal difference in yolk glucose at HH29 (1 g/kg: 159.1±21.3 mg/dL vs. saline: 118.7±6.2 mg/dL, $p$=0.084; Fig. 1A). However, injections of 1g/kg glucose into fertilized eggs at HH16 resulted in a significantly higher yolk glucose compared to the control at HH35 (1 g/kg: 196.8±5.9 mg/dL vs. saline: 139.1±10.1 mg/dL, $p$=0.0002; Fig. 1B). Injections of 1 g/kg glucose into fertilized eggs at HH24 caused significantly higher levels of yolk glucose checked at both HH29 (1 g/kg: 168±6.1mg/dL vs. saline: 112±6.9 mg/dL, $p$=0.00393) and HH35 (1 g/kg: 199.7±4.7 mg/dL vs. saline: 132.0±7.4 mg/dL, $p$=0.0000002). At HH35, fertilized eggs treated with 0.75 g/kg glucose solution at HH24 also had significantly higher yolk glucose levels compared to the control (0.75 g/kg: 159.1±6.2 mg/dL vs. saline: 132.0±7.4 mg/dL, $p$=0.025; Fig. 1B). Therefore, we confirmed the success of creating a hyperglycemic environment *in ovo* through glucose treatment that simulates "*in utero* hyperglycemia".

*Embryo survival rate decreases with increasing glucose treatment, especially in later exposures.*

The survival rates of glucose treated chicken embryos were determined at both HH29 and HH35 (Table 1). At the time of embryo collection, all the embryos treated with saline were normally developed, but some of the embryos treated with glucose solution were found dead at an earlier stage, especially at higher glucose doses (Fig. 1C, D). A dose-survival rate curve was fitted with a sigmoid function for logistics model analysis for HH35 embryos. Treatment at both stages resulted in-reverse "S" shaped curves which indicated that embryos survived at lower doses of glucose while their survival rate dropped within a narrow range of dosage until it plateaued (Fig. 1E) or approached to zero as glucose levels increased (Fig. 1F). The effective dose that caused the death of 50% of treated embryos (LD50) was higher in embryos treated at HH16 (LD50=1.57 g/kg) compared to HH24 (LD50=0.93 g/kg). This trend implies that the sensitivity to glucose varies at different developmental stages. The sharp decrease in survival rate of HH24 treated embryos indicates that embryos in later stages of development are more susceptible to the effects of hyperglycemia.

*Hyperglycemia increases rate of OFT heart defects.*

The presence of heart defects was examined in surviving HH35 embryos treated with 0.75 g/kg or higher glucose dosage at HH16 or HH24. The heart structure was examined via histological evaluation on serial sections.

Embryos treated at HH16 with 1 g/kg glucose displayed ventricular septum defects (VSD) where the ventricular septum is partially missing (Fig. 1K and Table 2, 5/12,

*p*=0.037), DORV where both the aorta and pulmonary artery connect to the right ventricle (Fig. 1L and Table 2, 4/12, *p*=0.093), and persistent truncus arteriosus (PTA) where the truncus arteriosus failed to separate into the aorta and pulmonary artery (Fig. 1M and Table 2, 1/12, *p*=1). The total incidence of outflow tract (OFT) defects, including VSD, DORV and PTA, was five out of 12 embryos (Fig. 1 and Table 2, *p*=0.037). The percentile of myocardium area relative to the area of ventricular chamber and the thickness of compact myocardium on the ventricular wall of the glucose group were similar to the control group, suggesting neither hypoplastic nor hyperplastic myocardium in these embryos (Fig. 2).

When 1 g/kg glucose was given at HH24, we observed VSD (Fig. 1O and Table 2, 6/9, *p*=0.0015) and DORV (Fig. 1P and Table 2, 5/9, *p*=0.0062) at HH35. PTA was not observed. Valve malformation was found in one of the embryos (Fig. 1R and supplementary Table 2, 1/9, *p*=0.429). This embryo displayed four leaflets instead of a tricuspid valve. The total incidence of outflow tract defects (OFT), including VSD and DORV, and valve abnormality was six cases out nine embryos (Fig. 1 and Table 2, *p*=0.0015). There was no significant difference in percentile of myocardium area relative to the area of ventricular chamber, nor thickness of compact myocardium between the glucose and the control group (Fig. 2). This indicates that neither hypoplastic nor hyperplastic myocardium was induced by glucose treatment at HH24, similar to observations of HH16 treated embryos. These results suggest that hyperglycemic conditions during development leads to increased rates of congenital heart defects, especially at the OFT.

*Hyperglycemia increases the rate of limb defects.*

Among the surviving HH35 embryos exposed to high glucose at HH24, the presence of leg/wing reduction was observed with an incident rate of 13% when exposed to 0.75 g/kg glucose (Fig. 3 and Table 3, 4/30, $p$=0.2091) or 44% when exposed to 1 g/kg glucose (Fig. 3 and Table 3, 4/9, $p$=0.0058). Specifically, in the 0.75 g/kg group, limb reduction applied to the leg only in three of the four observed cases, and one case had reductions in both wing and leg. At the dose of 1 g/kg glucose, two of the four cases were in the leg only, and the two other cases had both wing and leg reductions. To be noted, we did not observe any embryos with only wing defects but with normal legs. We then speculated if hyperosmolarity, instead of hyperglycemia, caused these defects. Thus, we treated eggs with L-glucose at two different does, 0.75 g/kg and 1 g/kg, at HH24 (Table 1) to induce hyperosmolarity. Neither limb defects nor heart defects were observed in these chicken embryos. Thus, we ruled out the possibility of hyperosmolarity to be the cause of the observed limb and heart defects with glucose treatment.

*High level of glucose causes proliferation defects in the limb bud at HH27-29.*

We then investigated if the limb reduction was due to decreased numbers of proliferating cells. Immunohistochemical (IHC) staining for p-H3S10 were performed on limb buds at HH27 or HH29 (24- or 48-hours post-treatment) of HH24 1 g/kg glucose treated embryos (Fig. 4A-D). At HH27, there were significantly lower numbers of p-H3S10+ cells in the wing bud of 1 g/kg glucose treated embryos compared to the saline (Fig. 4E, 1 g/kg: 666±56/mm$^2$ vs. saline: 916±66/mm$^2$, $p$=0.045). In the leg, the

numbers of p-H3S10+ cells were not different between glucose treated and saline treated embryos at HH27 (Fig. 4F). At HH29, treatment with 1 g/kg glucose resulted in a two-fold decrease of p-H3S10+ cells in the leg bud compared to the saline (Fig. 4H, 1 g/kg: 181±5.7/mm$^2$ vs. saline: 583±25/mm$^2$, $p$ =0.00009). However, there was no significant difference in the number of p-H3S10+ cells observed in the wing buds of glucose treated and saline controls at HH29 (Fig. 4G).

The expression levels of several key genes involved in cell proliferation, including *p21, p16, CycD and CycE,* were measured in both wings and legs at HH27 and HH29 after 1 g/kg glucose injection at HH24. In the HH27 wings, the expression of *CycD* in the glucose treated embryos was significantly lower than that of the control. However, this level of difference faded over time and the glucose induced reduction of *Cdk1* expression in the wing was only marginal at HH29 ($p$<0.1). These expression changes are consistent with the decrease in proliferation rates marked by lower pH3S10+ count observed in HH27 wing, but not the HH29 wing (Fig. 4I and K). Unlike the wing, expression levels of these genes in the HH27 leg were not statistically different between glucose and saline treated embryos (Fig. 4J). However, *CycD* expression was significantly lower in the HH29 leg exposed to glucose compared to saline (Fig. 4L). *CycE* expression in the glucose treated HH29 leg was also lower with a marginal significance ($p$<0.1).

Taken together, these results suggest that “hyperglycemia” hinders proliferation in the wing at an earlier stage (HH27) and the leg at a later stage (HH29).

*Hyperglycemia causes abnormal patterns of cell survival in the limb bud at HH27.*

One of the crucial steps of limb development, specifically the digit formation, is the degeneration of interdigital tissue via controlled cell death patterns [200]. We hypothesized that glucose-induced limb truncation could be accounted by abnormal cell survival. TUNEL staining was performed to evaluate if glucose treatment (1 g/kg) result in changes in programmed cell death patterns in the developing HH27 limb buds.

In the control wing bud, three regions were shown to be undergoing programmed cell death: the apical ectodermal ridge (AER) (Fig. 5A and E, region "a"), the posterior necrotic zone (PNZ) (Fig. 5A, E; region "b"), and the opaque patch (OP) (Fig. 5A, E; region "c"). Apoptotic cells were also observed in the same three regions of glucose treated wing buds. The number of apoptotic cells was quantified at each region in all the serial sections through the wing. There were no significant differences in the numbers of apoptotic cells in each individual region of the wing or in total between the saline controls and glucose treated embryos (Fig. 5B, E; 1 g/kg: 56±7 vs. saline: 49±9, $p$=0.597).

In the control leg bud, two major regions were shown to be undergoing programmed cell death: the PNZ (Fig. 5C, F; region "a") and the OP (Fig. 5C, F; region "b"). Interestingly, in the glucose treated embryos, the PNZ region showed no apoptotic cells while the OP region had an increased number of apoptotic cells (Fig. 5D, F; region "a" and "b"). In control leg buds, no apoptotic cells were observed in the AER (Fig. 5C, region "c") or in the region opposite to AER (Fig. 5C, region "d"). In contrast, the glucose treated leg bud had a significant count of apoptotic cells in both of these regions

(Fig. 5D, “c” and “d”; Fig. 5F). Despite the presence of ectopic apoptosis, the total number of programmed cell deaths was not different between the glucose treated leg bud and control leg bud (Fig. 5D and F, 1 g/kg: 103±6 vs. saline: 70±29, $p$=0.33).

Next, we examined the expression of several key genes involved in cell survival, including *Casp2, Casp3, Casp8, Apo2L, Api5, Bcl, Bid, Bcl2L Bak1, Bax* and *Grp78.* In the wing buds, the expression levels of *Grp78* and *Apol2L* significantly decreased in the glucose treated embryos compared to their saline controls (Fig. 5F). In the leg buds of glucose treated embryos, all genes, except for *Casp2* and *Casp3,* had significantly decreased expression levels compared to the control embryos (Fig. 5G). Interestingly, these include *Bak1, Bax, Casp8, Apo2L* and *Bid* that promote apoptosis as well as *Grp78, Bcl, Bcl2L* and *Api5* that are anti-apoptosis.

*Hyperglycemia affects the integrity of Shh signaling in the limb bud at HH27.*

Sonic hedgehog (Shh) is required for both posterior-distal limb skeleton and the posterior digit development in vertebrate animals [201-203]. Therefore, we investigated if high glucose (1 g/kg) would affect the integrity of Shh-signaling in the developing limb buds by measuring changes in expression of its key modulator genes. In the wing buds, glucose treatment significantly lowered the expression of *Shh* (Fig. 6A, 1 g/kg: 0.58±0.0349 vs. saline: 1.00±0.0017, $p$=0.000159), but not its downstream key modulator genes (Fig. 6A). In the leg buds, the *Shh* modulator genes, including *Smo, Gli1, Gli3* and *Ptch1* were expressed at significantly lower levels in the glucose treated leg buds compared to the control leg buds (Fig. 6B). These results suggest that hyperglycemia disrupts the integrity of Shh-signaling in limb buds.

*Hyperglycemia induces expression changes in genes involved in chondrogenesis and digit patterning at HH27.*

In order to understand how high glucose causes defects in limb outgrowth, we further assessed expression changes in chondrogenic gene markers (*Sox9, Col2a1*), early osteogenic gene markers (*Runx2*), and patterning gene markers (*Hoxd10, Hoxd11, Hoxd12* and *Hoxd13*) by RT-PCR. At HH27, the expression of *Col2a1* decreased in both the wing and leg bud of glucose treated embryos (Fig. 6C, D). Unique to the wing bud, *Hoxd13* expression was significantly lower in glucose treated embryos compared to the control (Fig. 6C). There were significant decreases in expression of all patterning genes including *Hoxd10, Hoxd11, Hoxd12* and *Hoxd13* in the leg bud of glucose treated embryos compared to the control (Fig. 6D). There was no difference in *Runx2* expression in either wing or leg buds between glucose and saline treated embryos (Fig. 6C, D).

## Discussion

In the current study, we established a novel "in ovo hyperglycemia" model using chicken embryos to mimic fetuses exposed to hyperglycemia in mothers with diabetes. By administering the glucose solution into the air-sac of fertilized eggs *in ovo*, the chicken embryos were exposed to higher glucose levels in the yolk that simulates an *in utero* hyperglycemic environment.

Recent studies report that diabetes during the first trimester, which expose the early embryo to hyperglycemia, closely relates to birth defects. Higher fasting glucose level in the first trimester [178, 204-208], even within the normoglycemic range [205, 208], is an early predictor of gestational diabetes mellitus. Indeed, fetuses can be exposed to amniotic fluid with elevated glucose levels as early as gestational week 15 which is before screening takes place for gestational diabetes mellitus [204]. Thus, fetuses can already be exposed to a high-glucose environment in the early developmental stage far before diagnosis of gestational diabetes mellitus in the third trimester. Unlike STZ-induced Type-I diabetes [190-192, 209] or HF diet induced Type-II diabetes [60] models of pre-gestational diabetes mellitus, our chicken embryonic model allows for the specific investigation of dose and temporal effects of elevated glucose levels. In our study, post-fertilization hyperglycemia was induced at HH16 or HH24, which is equivalent to the human embryonic day 24 or 42, respectively (at gestational week 5 or 8). Moreover, treatment of 1 g/kg glucose at HH16 or 0.75 g/kg glucose at HH24 increased glucose levels in the HH35 egg yolks by 21% and 51%, respectively. Considering HH35 as equivalent to human embryonic day 56 or gestational week 10, our data mimics the 44%

glucose elevation detected in amniotic fluids of gestational diabetic pregnancies compared to normal glycemic pregnancies [204]. Thus, the chicken embryonic model used in this study resembles both temporal and clinical glucose levels that embryos are exposed to during the first trimester of gestational diabetic pregnancies.

Although a handful of studies report an increased risk of congenital defects in infants born to women with gestational diabetes [54, 210-212], conflicting reports exist [213-216]. A recent systematic review of 768 potential articles to assess observed associations between gestational diabetes mellitus and birth defects found no evidence for consistent association of gestational diabetes mellitus with birth defects [217]. There is only a weak association between gestational diabetes mellitus and congenital heart defects [217]. Considering that gestational diabetes mellitus is always diagnosed after the critical developmental period of various organs, the data in these studies could be confounded by factors such as obesity and undiagnosed prediabetes before conception. Consistently, the same systematic review reiterated this paradox by reporting an increased risk of selected birth defects among offspring of women with both obesity and gestational diabetes mellitus [217]. With this discrepancy, the direct link between *in utero* hyperglycemia and birth defects remains to be addressed. In our study, we showed that glucose treatment (0.75 g/kg at HH16), even at a dose unable to maintain a prolonged high glucose level in egg yolks, was substantial enough to be teratogenic and induce embryopathy. At treatment doses that maintain high glucose levels in yolks, embryos displayed increased incidences of birth defects. Our data demonstrates that exposure to abnormal glucose levels during development is an important risk factor for heart and

limb abnormality. Importantly, both the STZ induced [190-192, 209] and HF diet induced [60] pre-gestational diabetes mellitus mouse models have contributed a considerable amount of information about the manifestations of fetal cardiovascular defects and central nervous system defects. However, neither of the two mouse models nor other vertebrate animal models reported phenotypes of limb defects in offspring of gestational diabetes mellitus mothers. From our knowledge, this study is the first to report phenotypes of limb abnormality caused by exposure to "hyperglycemia" during development.

However, it also needs to be cautious that in our novel egg model there are lack of stimulation over other factors changed during maternal diabetes, which also affect the glucose metabolism and embryo development. For instance, insulin and insulin-like growth factors (IGFs) play essential roles in regulation of cell metabolism, proliferation and differentiation [218, 219]. Although insulin secretion initiates at mid-gestational stage, IGF-1 and 2 are detectable at early stage of gestation. There have been studies showing that alterations in the plasma or serum concentrations of IGF have been identified in pregnancies complicated by diabetes and preeclampsia, and fetal growth were reduced [220, 221].

Common features of birth defects resulting from gestational diabetes mellitus pregnancies are variable expressivity and incomplete penetrance [181]. The basis for this variability is presently unclear. In our study, a hyperglycemic environment was induced at two different time points that were selected based on a previous study designed to investigate the effect of maternal hyperglycemia on offspring myocardium development.

The stage HH16 is when chicken embryos start myocardium trabeculation, and at the stage HH24, myocardium compaction starts [222]. Neither hypoplastic nor hyperplastic myocardium were induced with the glucose treatment. However, structural heart defects including VSD and OFT defects were observed in embryos treated at either timepoint. Although DORV was observed in HH16 glucose treated embryos, the rate was not statistically significant. Consistently, limb defect rates were higher with glucose administration at HH24, but not HH16. These results might suggest that the OFT and limb development were more sensitive to "hyperglycemia" at a later stage than an earlier stage. In addition, we reported association of "hyperglycemia" with a certain spectrum of CHD phenotypes, which is consistent to previous findings in human [223]. Similar as their reports, we observed much more outflow tract malformations than the inflow tract malformations in our model, suggesting that the cardiac precursor cells located at the anterior second heart field are more sensitive to "hyperglycemia" than the posterior second heart field. Unfortunately, Oyen et al. did not provide data to evaluate if GDM is associated with hypoplastic or hyperplastic myocardium. Because hyperglycemia may consistently affect the ventricular wall thickness through the entire embryonic stage and after birth, we could not conclude that hyperglycemia is not associated with hypoplastic or hyperplastic myocardium based on our observation at HH35. Furthermore, several key points should be noted. First, the major OFT defects induced by glucose were DORV which are caused by disruptions in alignment. During chicken heart development, the OFT septation starts at HH27 [222]. Secondly, the glucose administration was only given once, therefore, the glucose levels at HH27 could be different between the HH16

and HH24 treated groups. Our results and previous knowledge of OFT developmental timeframe suggest the mechanistic etiology of embryopathy under gestational diabetes mellitus to involve both dose and timing of "hyperglycemia" as elements of variability. Thus, our data provides a potential explanation why clinical gestational diabetes mellitus is associated with incomplete penetrance and variability of amongst offspring phenotypes.

Our data suggests that "hyperglycemia" during development causes limb defects by disrupting cell proliferation and apoptosis in the limb bud. First, glucose treatment caused more leg reduction than wing reduction, as wing reduction was always concurrent with the leg reduction. Consistent with the aforementioned phenotype, the leg buds showed both ectopic apoptosis and disrupted cell proliferation, while the wing bud only displayed proliferation defects. These results suggest to us that normal regulation of both cell proliferation and cell survival patterns is required for proper limb development. Second, the glucose treatment disrupted normal patterns of apoptosis rather than reducing the total number of apoptotic cells during limb development. This finding is consistent with previous knowledge that suggest major areas of programmed cell death in the limb bud mesenchymal cells to be a part of programmed limb growth [200]. Third, exposure window to "hyperglycemia" is critical to affect cell proliferation in the wing bud vs. the leg bud. The proliferating cells in the leg are more sensitive to elevated glucose between HH27 and HH29, evidenced by lower expression of *CycD* and *CycE* and lower count of pH3S10+ cells observed only at HH29, but not HH27. In contrary, stages before HH27 are more important to wing bud cell proliferation as lower pH3S10+

cell count and suppression of *CycD* was observed only in the HH27 wing, but not the HH29 wing.

Shh signaling is required for the limb bud outgrowth by controlling the width of the limb bud and by regulating the antero-posterior length of the AER [201-203]. Mechanisms involve regulation of mesenchyme cell proliferation and apoptosis [202]. In our study, the hyperglycemia-induced abnormalities in proliferation and apoptosis of limb buds were associated with depressed Shh-signaling pathway. Glucose treatment disrupted the integrity of Shh-signaling which depressed expressions of cell cycle regulators such as *CycD,* consistent with previous reports [202, 224]. This signaling is likely to be independent of AER, the signaling region required for laying down structures that drive limb bud outgrowth along the proximal-to-distal axis [202, 224]. However, decreased cell survival in the AER of the glucose treated leg bud directly affected the proximal-distal growth evidenced by limb reduction in our samples. In addition, the interaction between AER and the polarizing region, PNZ, is required for the formation of both anterior-posterior and proximal-distal patterning [202]. The number of cells in the polarizing region is controlled by Shh signaling which regulates BMP2 signaling, that in turn determines the size of the PNZ [225]. In our study, decreased Shh signaling could have promoted apoptosis in PNZ, possibly via inhibition of BMP2 signaling, leading to fewer cells in that region. Our data points to potential candidates for preventing diabetic embryopathy. Future studies can test if applying a chemical agonist for Shh-signaling could prevent hyperglycemia induced limb defects by rescuing the Shh/BMP and Shh/CycD levels.

In summary, our study established a novel chicken embryonic model with a high glucose environment *in ovo*. Using this model, the important mechanisms of how gestational diabetes mellitus increases the risk for birth defects were investigated. Findings of this study will guide efforts to explore interventional approaches to reduce diabetes-induced embryonic malformations.

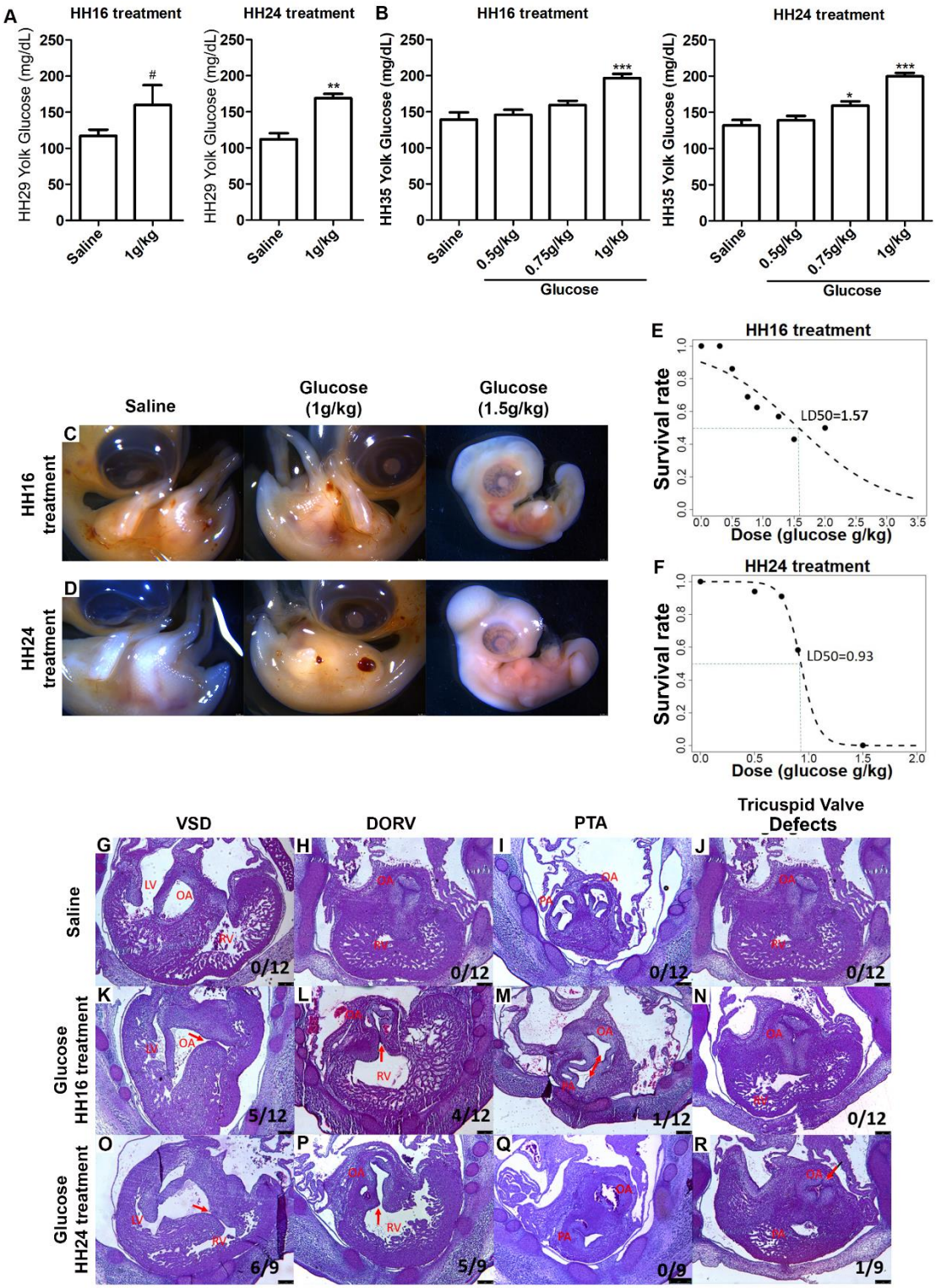
A
HH16 treatment
HH24 treatment
HH29 Yolk Glucose (mg/dL)
Saline
1g/kg
B
HH16 treatment
HH24 treatment
HH35 Yolk Glucose (mg/dL)
Saline
0.5g/kg
0.75g/kg
1g/kg
Glucose
C
D
Saline
Glucose (1g/kg)
Glucose (1.5g/kg)
HH16 treatment
HH24 treatment
E
HH16 treatment
Survival rate
LD50=1.57
Dose (glucose g/kg)
F
HH24 treatment
Survival rate
LD50=0.93
Dose (glucose g/kg)
VSD
DORV
PTA
Tricuspid Valve Defects
Saline
Glucose HH16 treatment
Glucose HH24 treatment
LV
RV
OA
PA
0/12
5/12
4/12
1/12
0/12
6/9
5/9
0/9
1/9

Figure 1. Embryo survival rate decreases with increasing glucose dose, especially in later exposures.

A. At HH16 or HH24, eggs were treated with either glucose (1g/kg) or saline (control). The yolk glucose levels was measured at HH29.

B. At HH16 or H24, eggs were treated either glucose (0.5g/kg, 0.75g/kg, or 1g/kg) or saline (control). The yolk glucose levels was measured at HH35.

C. For embryos at HH35 with treatment at HH16, most of the embryos treated with saline or 1g/kg glucose group survived, 57% embryos treated with 1.5g/kg glucose died.

D. For embryos at HH35 with treatment at HH24, most of the embryos treated with saline or 1g/kg glucose group survived, all embryos treated with 1.5g/kg glucose died.

E. Dose-survival rate curve of HH16 injection. LD50 is 1.57g/kg at this treatment stage.

F. Dose-survival rate curve of HH24 injection. LD50 is 0.93g/kg at this treatment stage.

G-R. H&E staining of HH35 embryo sections shows VSD (G, K, O), DORV (H, L, P), PTA (I, M, Q), tricuspid valve regurgitation (J, N, R). AO, aorta; DORV, double outlet right ventricle; LV, left ventricle; RV, right ventricle; PTA, persistent truncus arteriosus; VSD, ventricular septal defect. Read arrows indicates defects.

Data is presented as Mean±SE, N=6-30; #$p<0.1$, *$p<0.05$, **$p<0.01$, ***$p<0.001$.

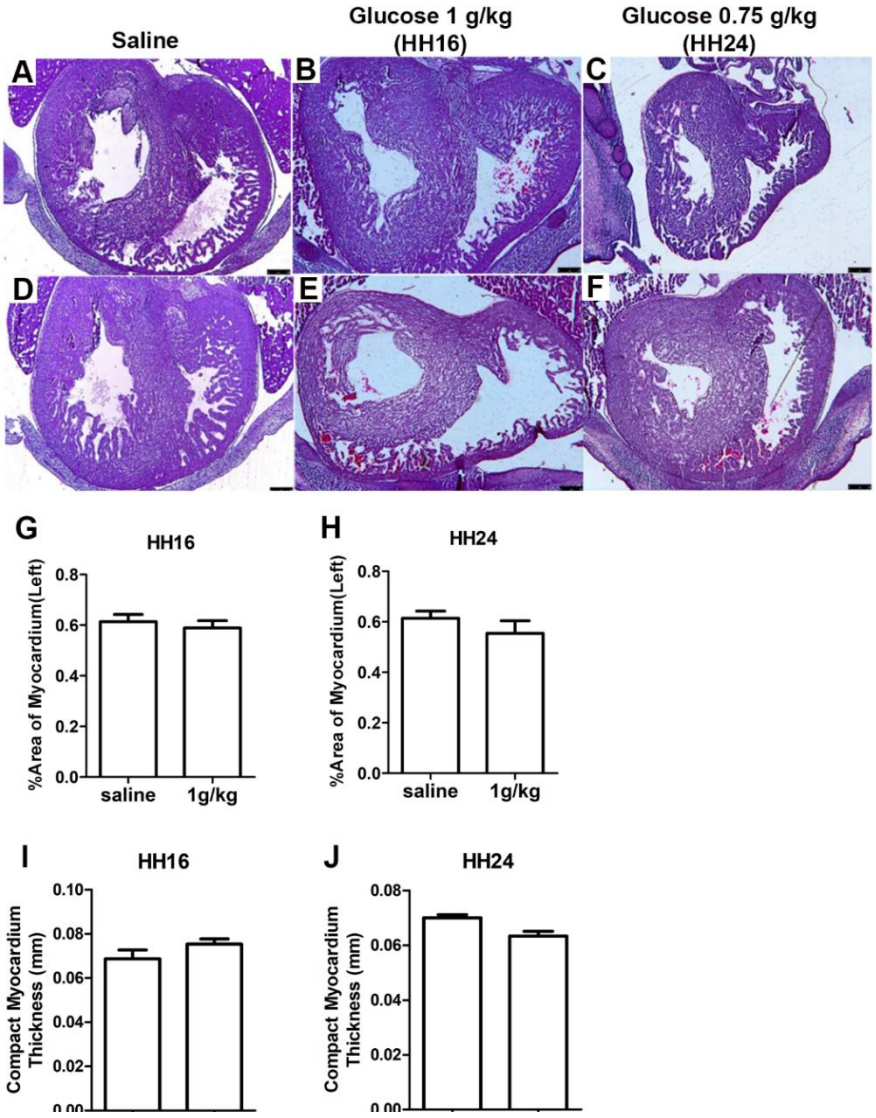


Figure 2. Glucose treatment at HH16 or HH24 does not cause hypoplastic nor hyperplastic myocardium in HH35 embryos.

A-F. H&E staining of hear sections from HH35 embryos treated with saline (A, D), 1g/kg glucose at HH16 (B, E), 0.75g/kg glucose at HH24 (C, F).

G. Percent myocardium occupancy of left ventricle in HH35 embryos treated at HH16.

H. Percent myocardium occupancy of left ventricle in HH35 embryos treated at HH24.

I. Thickness of compact myocardium on left ventricle in HH35 embryos treated at HH16.

J. Thickness of compact myocardium on left ventricle in HH35 embryos treated at HH24.

Data is presented as Mean±SE, N=3.

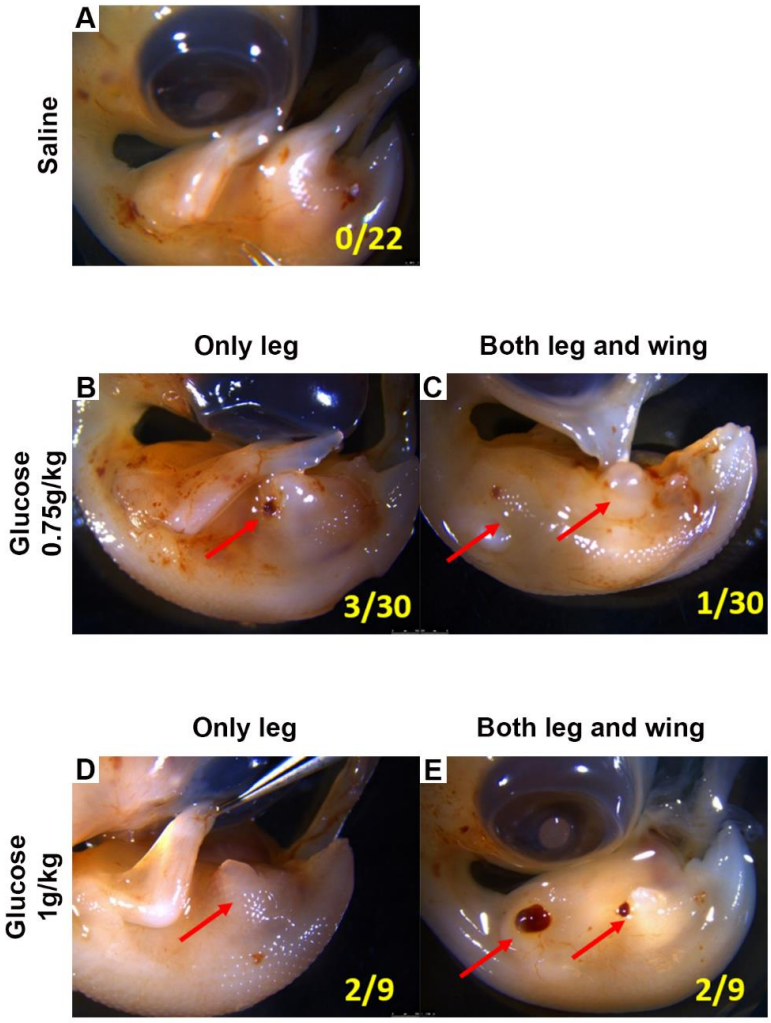


Figure 3. High glucose treatment at HH24 causes limb defects.

A. The embryos displayed normal limbs with saline injection.

B-E. For HH24 injection of 0.75 or 1 g/kg glucose, embryos showed defects at only leg (B, D) or at both leg and wing (C, E). Red arrows show the malformed limbs.

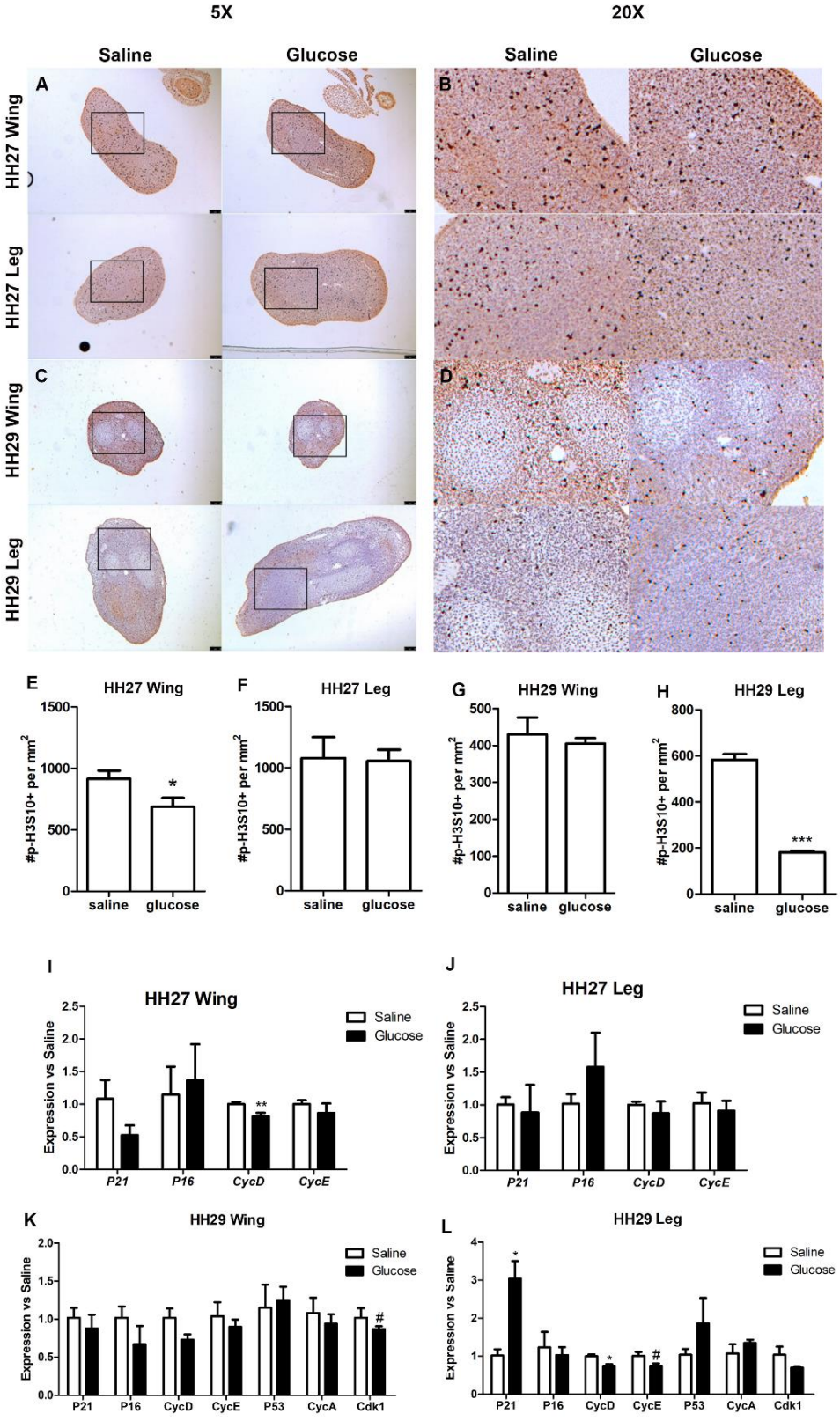
5X
20X
Saline
Glucose
Saline
Glucose
A
B
C
D
HH27 Wing
HH27 Leg
HH29 Wing
HH29 Leg
E
HH27 Wing
#p-H3S10+ per mm2
saline
glucose
F
HH27 Leg
G
HH29 Wing
H
HH29 Leg
I
HH27 Wing
Expression vs Saline
Saline
Glucose
P21
P16
CycD
CycE
J
HH27 Leg
K
HH29 Wing
P21
P16
CycD
CycE
P53
CycA
Cdk1
L
HH29 Leg

Figure 4. High glucose treatment at HH24 cause proliferation defects in limbs at HH27-29.

A-B. IHC staining for p-H3S10 in wing and leg of 1g/kg glucose injected embryo at HH27.

C-D. IHC staining for p-H3S10 in wing and leg of 1g/kg glucose injected embryo at HH29.

E-H. The number of p-H3S10+ cells in 1mm2 of wing or leg tissue.

I-J. Expression levels of cell cycle related gene in wing and leg tissue at HH27.

K-L. Expression levels of cell cycle related gene in wing and leg tissue at HH29.

Data is presented as Mean±SE, N=3-5, #$p<0.1$, *$p<0.05$, **$p<0.01$, ***$p<0.001$.

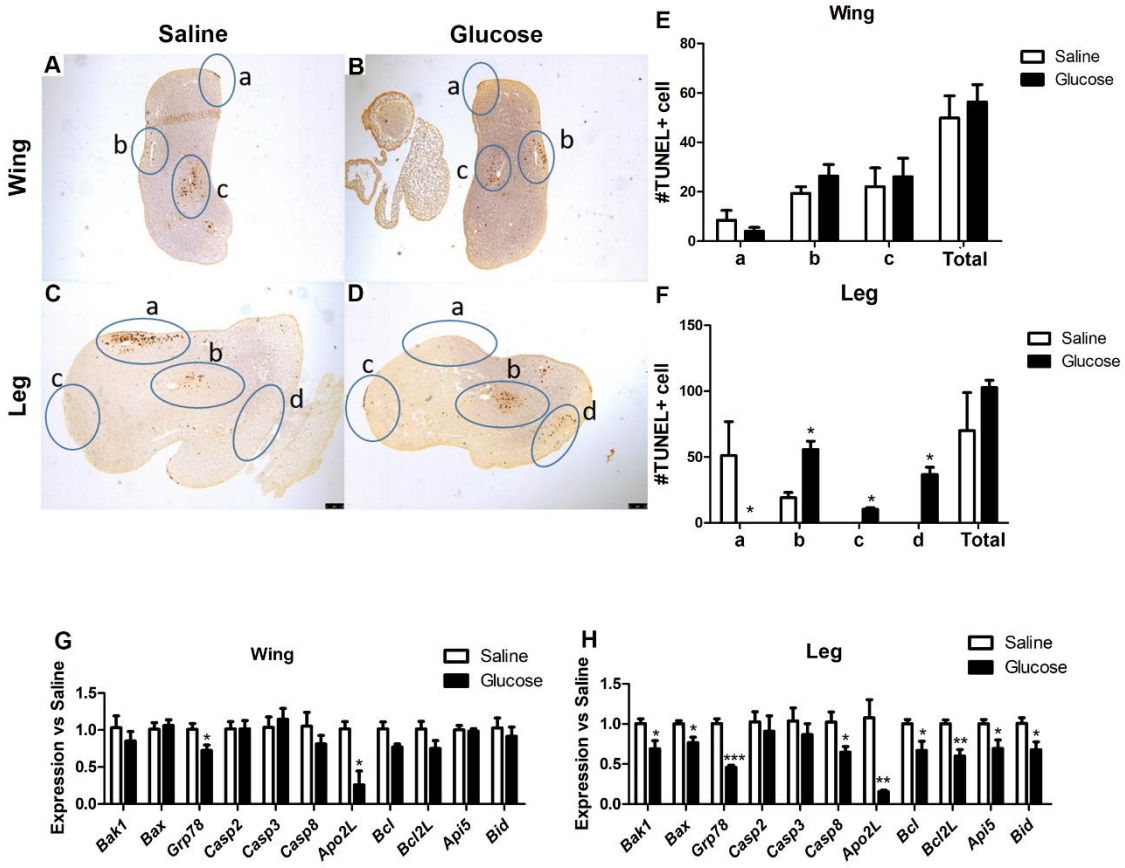


Figure 5. High glucose treatment at HH24 caused ectopic apoptosis in the leg at HH27.

A-D. TUNEL staining in leg and limb tissue at HH27 embryo. a, b, c or d indicate corresponding region of apoptotic cell of different tissue.

E-F. The number of TUNEL+ cells in each region. Data is presented as Mean±SE, N=3-5, *p<0.05.

G-H. Expression levels of apoptosis related gene in wing and leg tissue at HH27. Data is presented as Mean±SE, N=3-4; #p<0.1,*p<0.05, **p<0.01, ***p<0.001.

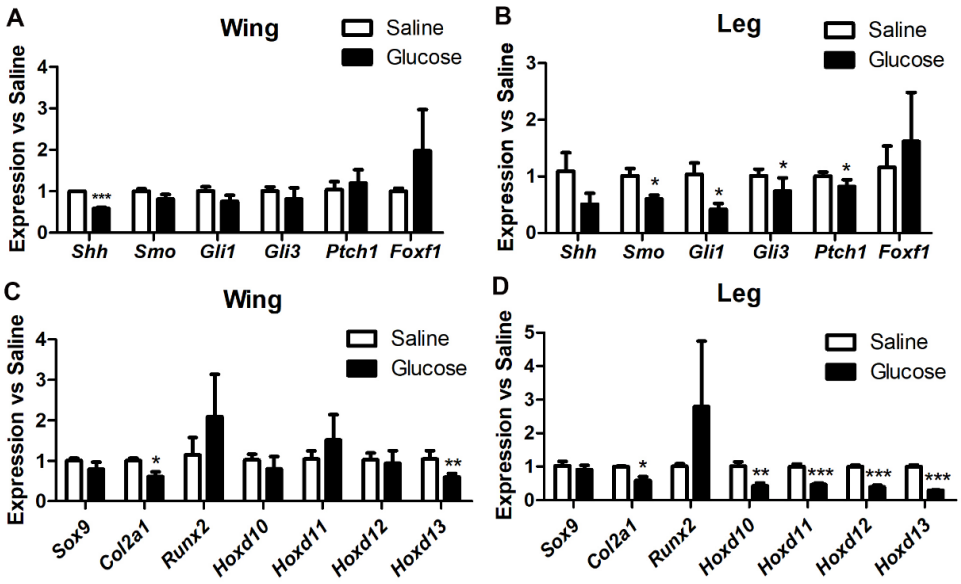


Figure 6. High glucose treatment at HH24 disrupted the integrity of Shh signaling pathway and the expression of genes for chondrogenesis and digit patterning in HH27 limbs.

A-B. Expression levels of *Shh, Smo, Gli1, Gli3, Ptch1, Foxf1* in limb tissue of saline or glucose treated embryos.

C-D. Expression levels of *Sox9, Col2a1, Runx2, Hoxd10, Hoxd11, Hoxd12, Hoxd13* in limb tissue of saline or glucose treated embryos.

Data is presented as Mean±SE, N=3-4, *p<0.05, **p<0.01, ***p<0.001.

Table 1. Survival rates with glucose injections.

Various doses of glucose or L-glucose were injected into the eggs at HH16 or HH24, and the embryos were collected at HH29 or HH35.

| Injection stage | Collection stage | Treatment | Dose (g/kg body weight) | Total | Alive (survival%) | Limb defect | Heart defect |
|---|---|---|---|---|---|---|---|
| HH16 | HH29 | Saline | | 8 | 8(100%) | 0 | NA |
| | | Glucose | 1 | 6 | 5(83%) | 0 | NA |
| | | Glucose | 1.5 | 6 | 2(33%) | 0 | NA |
| | HH35 | Saline | | 9 | 9(100%) | 0 | 0/5 |
| | | Glucose | 0.3 | 4 | 4(100%) | 0 | 0/4 |
| | | Glucose | 0.5 | 12 | 11(90%) | 0 | 0/3 |
| | | Glucose | 0.75 | 10 | 7(70%) | 0 | 3/6 |
| | | Glucose | 1 | 20 | 12(60%) | 0 | 5/12 |
| | | Glucose | 1.25 | 7 | 4(57%) | 0 | NA |
| | | Glucose | 1.5 | 14 | 6(43%) | 0 | NA |
| | | Glucose | 2 | 6 | 3(50%) | 0 | NA |
| HH24 | HH29 | Saline | NA | 11 | 11(100%) | 0 | NA |
| | | Glucose | 1 | 16 | 6(37.5%) | 0 | NA |
| | | Glucose | 1.5 | 16 | 4(25%) | 2 | NA |
| | HH35 | Saline | NA | 27 | 27(100%) | 0/22 | 0/22 |
| | | L-Glucose | 0.75 | 10 | 10(100%) | 0 | 0/10 (0%) |
| | | L-Glucose | 1 | 8 | 8(100%) | 0 | 0/8 (0%) |
| | | Glucose | 0.5 | 18 | 17(94%) | 0/17 | NA |
| | | Glucose | 0.75 | 33 | 30(91%) | 4/30(13%) | 4/10(40%) |
| | | Glucose | 1 | 24 | 9(37.5%) | 4/9(44%) | 6/9(67%) |
| | | Glucose | 1.5 | 14 | 0(0%) | NA | NA |

Table 2. Evaluation of embryos with various types of heart defects.[#]

| | Saline | HH16 glucose (1g/kg) | p-value (vs. Saline) | HH24 glucose(1g/kg) | p-value (vs. Saline) |
|---|---|---|---|---|---|
| VSD | 0/12 | 5/12 | 0.03726708* | 6/9 | 0.001547988** |
| DORV | 0/12 | 4/12 | 0.0931677 | 5/9 | 0.00619195** |
| PTA | 0/12 | 1/12 | 1 | 0/9 | 1 |
| Valve malformation | 0/12 | 0/12 | 1 | 1/9 | 0.4285714 |
| Total | 0/12 | 5/12 | 0.03726708* | 6/9 | 0.001547988** |

[#]p value is calculated by Chi-square test.
*p<0.05, **p<0.01.

Table 3. Evaluation of embryos with limb defects.[#]

| | Saline | 0.75g/kg glucose | p-value (vs. Saline) | 1g/kg glucose | p-value (vs. Saline) |
|---|---|---|---|---|---|
| Leg | 0/22 | 3/30 | 0.2533937 | 2/9 | 0.07741935 |
| Wing & leg | 0/22 | 1/30 | 1 | 2/9 | 0.07741935 |
| Total | 0/22 | 4/30 | 0.2091 | 4/9 | 0.005773** |

[#]p value is calculated by Chi-square test.
**$p<0.01$.

Table 4. Primer used for Real-time PCR.

| Gene | Forward (5’-3’) | Reverse (5’-3’) |
|---|---|---|
| Gapdh | AGATGCAGGTGCTGAGTATG | CTGAGGGAGCTGAGATGATAAC |
| Shh | CCCGTTAGCCTATAAGCAGTTT | CTCTCGGAGTTTCTTGTGATCTT |
| Gli1 | GAGAAATCGGAGGGTGACATT | CCATCCCAGTAGCAGTTTGT |
| Gli3 | CTGTCCCTAGAGTCCAACATTTC | GGGTACAGTTCTGAAGGACAAG |
| Ptch1 | GCAGAGGTTGGTCATGGTTAT | GCTACATCAAGAGGCTTGGTAG |
| Smo | CTGCCACTTCTACGACTTCTTC | CACACTCTGGGATGGGTTTATT |
| Foxf1 | CGGAGAAACCGCCCTATT | GGCTCTGTAAGAACTGGTAGAT |
| Sox9 | AGAGCGACGAGGACAAATTC | GTTCTTGCTGGATCCGTTCA |
| Runx2 | TGATCAGTCGTACCCGTCCT | GGGAGTCGTGGAGTGAATGG |
| Col2a1 | TGGATGCCACCCTCAAATCC | ACTCGGGATGGCAGAGTTTG |
| P21 | CAATGCCGAGTCTGTAGTTCCC | TTCCAGTCCTCCTCAGTCCCTT |
| P16 | GCGGGATGAACTAGCCAACG | GTCCGACCGAAGGAGTTGAC |
| CycD | GACTTTTGTGGCTCTGTGCG | GCGATCATGGAAGGTGGGTT |
| CycE | GGCTGGGCAAACAGAGATGA | TTAGGTTGCAGGAGAGGGTG |
| Hoxd10 | GACCTACGCCACTGGGAAAA | GCCGCGAGGGTTTAACTGTA |
| Hoxd11 | GGTGAGGCTGTTGCAGAGAA | TCCTCGATCGCTGAGGAACT |
| Hoxd12 | GCAGTCCAGTCATGCCTCAG | ATTCGGCGATTTGCTGTTTT |
| Hoxd13 | CACAGAGCTCGCACTTCTGG | ATCTCGGGCTGGTTTAGTGC |
| Bid | GGAGCGCATGCTTCTCTTTG | TGGCTTTGTAGGGATGGCAG |
| Bcl2 | ATGACCGAGTACCTGAACCG | AGGCCTCATACTGTTGCCGT |
| Apo2L | CGCAGAAGAAACAGTGCTGC | CCAGAGCTGTTCCACGCTTA |
| Caspase3 | TGAAGGAACACGCCAGGAAA | GTCGAGTGGAGCAGGATTCA |
| Caspase2 | ATGGTCCTCCGATTCCTCCA | TAAGCCTCGGGGCTCTGATA |
| Grp78 | TTGATGCCAAGCGGCTCATA | CACCACCAACATCGACCTGA |
| Bax | GTGATGGCATGGGACATAGCTC | TGGCGTAGACCTTGCGGATAA |
| Caspase8 | TGGGAAAGTGGACAAGAGCC | ACAGTTGCCCAGAGAATCGG |
| Api5 | CCAGATTGCGTGGACAGACT | TCAAAGCACTGAGGTTCGGA |
| Bcl2L1 | GCTTTGAGCAGGTAGTGA | CAAGTACGTGGTCATCCAA |
| Bak1 | GCCCTGCTGGGTTTCGGTTA | AATTCGGTGACGTAGCGGGC |

# CHAPTER III

# INTERACTION BETWEEN GDM AND FOXO1 DISRUPTION ON PLACENTA DEVELOPMENT

## Introduction

Diabetes mellitus is diagnosed by high blood glucose levels. In 2017 there were an estimated 21.3 million babies born to hyperglycemic mothers [24]. Moreover, nearly half of the people with diabetes remain undiagnosed [24], leading to a greater number of mothers and newborns affected by diabetes or hyperglycemia.

The placenta is a transient organ during pregnancy, which mainly originates from the trophectoderm in the blastocyst, and starts to develop after implantation. The placenta is considered to be the interactive barrier between the mother and fetus. Its role is to not only support nutrient and gas exchanges, but also generate a substantial variety of hormones that regulate and maintain normal development of the embryo. To satisfy the increasing nutritional fetal requirements, maturation of the placental villi is accomplished by well-controlled proliferation and angiogenesis within the endothelial cells. Immature vascularization usually leads to fetal growth restriction and even death [29, 30]. It has been demonstrated that pregnancy affected by maternal diabetes can obstruct the development of the placenta by impacting many different aspects, such as placental weight, angiogenesis, vasculature maturity and inflammation levels [226-228]. Those changes can further affect nutrient transportation and endocrine functions, and compromise the health of the mother and fetus [229]. However, the physiological progress of pregnancy during diabetes is complicated by many factors, including

hyperglycemia and insulin resistance, as well as the onset timing of the disease. Therefore, more studies are urged to unveil the specific mechanism of how diabetes affects the development of placenta and fetus.

FOXO1 is an essential transcription factor, involved in many developmental and metabolic processes, including cell differentiation, proliferation, programmed cell death and gluconeogenesis. FOXO1 is mainly regulated through the IRS-PI3K-AKT pathway, as an increase in blood insulin causes the deactivation of FOXO1 through phosphorylation and nuclear translocation [230]. FOXO1 also plays an important role in placental development. FOXO1-null embryos are not viable due to an absence of chorioallantoic fusion at E8.5 [160]. FOXO1 expression has also been reported in endothelial cells and syncytiotrophoblast cells in the human placenta at late gestational ages [168] and endothelial cells in mice [169]. It has been reported to regulate angiogenesis via mediating angiogenic factors, such as VEGFA and AKT [231, 232].

In this study, an STZ-induced FOXO1 transgenic mouse model with hyperglycemia during pregnancy, was used to study the morphological and functional changes in the placentas. The effects of FOXO1 disruption on placental weight and angiogenesis, as well as the underlying mechanisms were also investigated. Overall, this study aimed to examine the interaction of FOXO1 and GDM during placenta development.

**Experimental methods**

*Mice*

*FOXO1*$^{fl/+}$ mice were obtained from Dr. Shaodong Guo's lab (Department of Nutrition, Texas A&M university, College Station, TX) as a gift, and they were crossed with *EIIa-Cre* mice to generate mice with a germline knock down of FOXO1. *FOXO1*$^{+/-}$*; EIIa*$^{Cre/+}$ mice were then crossed with WT mice to exclude the *EIIa-Cre* allele.

*Mouse model of gestational diabetes*

WT or *FOXO1*$^{+/-}$ female mice at age of 9-10 weeks were maintained on a chow diet (9%) and water *ad libitum* under a 12 h light/dark cycle throughout the experiment. Before treatment, mice body weight, basal blood glucose levels and age were recorded (Fig. 7A-C). Then mice were randomly selected and administered with STZ (Sigma) at a dose of 100 mg/kg per body weight, prepared in citrate buffer (pH 7.4) (HG)or citrate buffer only (NG) on day 1 and day 4, injected intraperitoneally. After the second injection, the female mice were mated overnight with WT male mice, the day after was considered as embryonic day 0 (E0) if vaginal plugs were observed. Random blood glucoses were measured every day after the first injection to identify the initial time point of diabetes induction. Maternal blood glucose levels were higher than 198 mg/dL, level set up to define diabetic status, 5 days after injection in both WT and *FOXO1*$^{+/-}$ mice after the STZ treatment (Fig. 8A), and hyperglycemia was maintained until the day of sacrifice (Fig. 8B).These results defined and validated the six treatment groups in our study. Under NG, we had placentas from WT fetus from WT mothers (WT-WT NG), from WT fetus from *FOXO1*$^{+/-}$ mothers (F-WT NG) and from *FOXO1*$^{+/-}$ fetus from

*FOXO1*$^{+/-}$ mothers (F-F NG). Similarly, under HG, we had WT-WT HG, F-WT HG and F-F HG. Consistently, glucose levels in the amniotic fluid of the embryos were also significantly higher in STZ treated groups. Notably, the amniotic fluid glucose levels were lower in the F-F group compared with WT-WT group without STZ treatment (Fig. 8C).

Embryos and placentas were collected and weighed at E10.5, E12.5, E14.5, E16.5 and term. Placentas were bisected and half of the placenta were then dissected across junctional zone to separate the labyrinth or decidua, and stored at -80 °C, while the remaining half was fixed with 10% formalin. Amniotic fluid glucose levels were measured during sample collection.

*Human sample of placenta from normal pregnancy and diabetic pregnancy*

Decoded human placenta sections were obtained from Dr. Lanjing Zhang, Director of Gastrointestinal and Liver Pathology, Princeton Medical Center (Plainsboro Township, NJ).

*Histology and evaluation of human placenta*

Immunohistochemistry (IHC) was performed on the human placenta slide. The slides were then photographed, and the positive stain intensity was evaluated in the villi and basal plate, under a single-blinded evaluation. The staining intensity was scored as 1, 2, or 3, with 1 being low and 3 being high.

*Histology of mouse placenta*

Routine procedures were used for H&E staining and (IHC). The following antibodies were used for IHC:

Anti-Histone H3 (phospho S10) antibody (Abcam)

Anti-Tpbpα rabbit antibody (Abcam)

Anti-CD31 rabbit antibody (Cell Signaling Technology)

Anti-Cytokeratin mouse antibody (Abcam)

The In-Situ apoptosis detection kit (EMD Millipore) was used for TUNEL staining.

*Western blot*

Total protein from the labyrinth or decidual tissues were extracted using Cell Lysis buffer (Cell Signaling Technology). Protein concentrations were measured using the Pierce™ BCA Protein Assay Kit (Thermo Fisher Scientific). 15-30μg proteins were loaded on a 7–12% SDS-PAGE electrophoresis gels and transferred onto PVDF membranes (Bio-Rad). The membranes were then blocked with 5% fat-free milk, and incubated in the primary antibodies overnight at 4 °C. After incubation with anti-rabbit secondary antibodies (Cell Signaling Technology) for 1 h, the signal was detected with the HRP substrate, and analyzed with the ImageJ.

*Realtime-qPCR*

Total RNA was extracted from the labyrinth or decidua using RNA spin columns. 500ng of total RNA was reverse transcribed using a SuperScript III Reverse Transcriptase kit (Invitrogen). qPCR was performed using a SYBR Green PCR master mix (Bio-Rad), with designed primers. Results were analyzed using the comparative C(T) method with *Cyclophilin A* as a normalization control [233]

## Results

*FOXO1 expression was increased in the term placenta of maternal diabetes.*

In the human, FOXO1 expression was observed in the placental villi and the maternal basal plate. Within the villi, FOXO1 was localized in the fetal vascular endothelial cells and the cytotrophoblasts near the syncytiotrophoblast layer. In the decidua, FOXO1 was strongly expressed in the spiral artery endothelial cells. The endometrial stromal cell also displayed a weak expression of FOXO1, when compared to the endothelial cells (Fig. 9A).

To understand if the placental FOXO1 expression is affected under gestational diabetes, a FOXO1 IHC staining was performed on term placentas from women who were either healthy (CTL) or diagnosed with gestational diabetes (GDM) (Fig 9B and C). In both the placental villi and basal plate, the intensity scores were significantly higher in GDM group compared to the CTL group (Fig 9D and E). These results suggest that gestational diabetes induces FOXO1 upregulation in term human placentas.

*FOXO1 expression was increased in the mouse placenta with hyperglycemia.*

To test if FOXO1 expression in the mouse placenta is affected similarly, a western blot was performed with protein from the WT-WT NG and WT-WT HG groups. FOXO1 expression was observed to be significantly upregulated in the WT-WT HG placentas (Fig 9C). This result was consistent with that in human placentas.

*FOXO1 expression was dynamic through the gestational period.*

Next, the expression and localization of FOXO1 in the mouse placenta were evaluated. FOXO1 IHC staining performed on sagittal sections of WT-WT NG placentas

collected at different gestational stages. From E10.5 to term, FOXO1 expressions were always observed in the labyrinth and the decidua, but not in the junctional zone. In the decidua, FOXO1 expression was mainly localized in the spiral arterial endothelial cells (Fig. 10A). In the labyrinth, besides the fetal vascular endothelial cells, FOXO1 was also identified in the syncytiotrophoblasts (Fig. 10A). The IHC staining also showed a temporal expression pattern of FOXO1 between E10.5 and term. Among the different gestational stages, FOXO1 expression steadily increased after E10.5 and reached its maximum expression at E14.5, followed by a dramatic decrease afterwards (Fig. 10B).

*FOXO1 heterozygous mice expressed a lower level of FOXO1 in the placenta.*

FOXO1 expression was then evaluated in E14.5 *FOXO1*+/- placentas. Compared to the WT-WT NG group, the F-WT NG group showed a marginal decrease of FOXO1 expression, while the F-F NG group showed a significant downregulation of FOXO1 (Fig. 11A and B). Consistent with the western blot result, FOXO1 IHC staining also exhibited a decreased staining intensity in the F-F NG group, compared with the WT-WT NG group (Fig. 11C).

*Changes in embryonic weight, placenta weight and placenta efficiency under maternal hyperglycemia and by FOXO1 disruption.*

Embryonic and placental weights were measured, and placental efficiency defined by the ratio of the embryo weight to placenta weight was calculated. At E14.5, the embryo weight of WT-WT offspring was significantly increased when treated with STZ, and no significant difference was observed between the different genotypes (Fig. 12A). Within the F-F group, the HG placentas showed a decreased weight when compared to the NG

placentas (Fig. 12B). No significant difference of the placental efficiency was observed among the groups at E14.5, except for the F-F HG group, which displayed a marginally increased placental efficiency when compared to the F-F NG group. Similarly, at both E16.5 and term, the embryo and placenta weights of the WT-WT offspring were increased under a maternal hyperglycemic condition (Fig D, E, G and H). Notably, the placenta weights of the F-F NG group were significantly higher compared to the WT-WT NG group at both E16.5 and term (Fig. 12E and H), but a significant increase in embryonic weight for the F-F NG group was only observed at term (Fig. 12D and G). Together, this could indicate that FOXO1 disruption may impact the placenta development, which then compromises embryonic growth in late pregnancy. However, the placenta efficiencies showed no significant difference between any two groups at either E16.5 or term (Fig. 12F and I). Litter size differences were not observed between any two groups (Fig. 12J).

*FOXO1 heterozygous placenta showed increased labyrinth volume under normal conditions.*

To test whether the placental weight changes were due to increased size of the decidua, junctional zone or labyrinth layer, Tpbpα IHC staining was performed on the E14.5 placentas. Tpbpα is a specific marker for the spongiotrophoblasts of the junctional zone. As a result, the junctional zone volume was not different between all of the groups (Fig. 13B). The labyrinth layer volume, however, was significantly increased in the F-F NG group when compared to the WT-WT NG group (Fig. 13A).

*Decreased apoptosis and increased proliferation were observed in the labyrinth of FOXO1 heterozygous placenta under normal conditions.*

To understand the mechanisms underlying the increased labyrinth volume of the FOXO1 heterozygous placenta, a TUNEL and pH3S10 staining were performed to examine the apoptosis and proliferation levels, respectively. At E12.5, the number of apoptotic cells per given area of the labyrinth was significantly less in the F-F NG group compared to the WT-WT NG group, and the number also showed a decreasing trend after STZ treatment. However, no difference was observed among groups under the HG condition (Fig. 14A-B). Apoptotic cells were not observed in the E12.5 labyrinth in all groups.

Assay to detect pH3S10 staining was used to evaluate cell proliferation at E12.5. The number of pH3S10+ cells per given area was significantly increased in the F-F NG group compared to the WT-WT NG group (Fig. 15A-B). Under hyperglycemic condition, all three groups showed no difference in the number of pH3S10+ cells (Fig. 15A-B).

*Hyperglycemia caused fetal vascularization increase and maternal lacunae decrease in the labyrinth.*

The formation of a sufficient fetal vascular system and maternal lacunae area in the labyrinth is necessary to ensure the normal growth of the embryos. Therefore, the fetal vasculature and maternal blood lacunae were further evaluated by PECAM-Cytokeratin co-IF stating. By analyzing the area of fetal vasculature and maternal lacunae, as defined by PECAM and Cytokeratin staining, respectively, there were significantly larger fetal blood spaces in the WT-WT HG group compared to the WT-WT NG group (Fig. 16A),

suggesting that maternal hyperglycemia can promote fetal angiogenesis. Interestingly, the fetal blood spaces of F-WT HG and the F-F HG were not different from that of the WT-WT NG, suggesting a potentially partial rescue by FOXO1 disruption under HG. For the maternal lacunae area, significant decrease was also only observed in WT-WT HG group compared with WT-WT NG group (Fig. 16B), which indicated that hyperglycemia damped the development of maternal blood network. Similar as the fetal blood space, F-WT HG and F-F HG groups have similar area of maternal lacunae (Fig. 16C), suggesting a partial rescue by FOXO1 disruption under HG. The interhemal membrane thickness in each group was further measured. The IHM is associated with the exchange efficiency of the placenta. Within the WT-WT group, the IHM thickness was found to be significantly higher in response to a HG condition, but no differences among other genotype groups were observed (Fig. 16D). These results indicate that the hyperglycemia can regulate fetal growth through increasing fetal vascularization and IHM thickness changes, and FOXO1 may have a role of intermediator during this physiological process.

*FOXO1 disruption did not affect mice heart development under normal or hyperglycemic conditions.*

Previous reports indicate that a FOXO1 global knockout would lead to heart malformations and embryonic lethality at early embryonic stages [169], while others, employing a cardiac cell specific knockout of FOXO1, demonstrated that this conditional knockout model does not cause a higher heart defect rate during embryonic development. Because of this literary discrepancy, the question of whether a FOXO1

disruption would affect the normal heart development under normal or maternal hyperglycemic condition was further investigated. Heart morphologies were examined by serial sections of embryos from WT NG, FOXO1$^{+/-}$ NG, WT HG and FOXO1$^{+/-}$ HG groups at E14.5. As a result, ventricular septal defects (VSD) were observed in all four groups. Atrial septal defects (ASD) were also observed, except in the FOXO1$^{+/-}$ HG group, and only one embryo in WT HG group exhibited double outlet right ventricle (DORV) (Fig. 17A-D). However, there were no significant differences among the incidences of each heart defect (Fig. 17E). Furthermore, there is evidence showing that the ventricular wall thickness is increased in a diabetic pregnancy [234]. Therefore, the ventricular thickness was also evaluated in the different groups by measuring the compact tissue area as a ratio of the entire ventricular chamber. However, there were no significant differences between any two groups (Fig. 17F).

## Discussion

FOXO1 is an important transcriptional factor that regulates cell survival and metabolism in many tissues. This study investigated the role of FOXO1 on placental development under normal and hyperglycemic conditions. Specifically, FOXO1 was found to be expressed in the labyrinth and decidua of the placenta during mid to late gestational stages. Disrupting FOXO1 expression resulted in increased embryo weight and placenta weight under both normoglycemia and hyperglycemia. However, increased cell proliferation and survival in the labyrinth zone was only observed under normoglycemia at E12.5. Though open questions were left to understand the molecular mechanism of placenta enlargement under hyperglycemia, findings in this study provided new knowledge in understanding placental development in health people or gestational diabetes patients.

In this study, the localization and expression of FOXO1 in the mouse placenta was reported at different gestational stages. This suggests that FOXO1 could have a regulatory role throughout gestation, not only in the early stage of placenta development [160]. It has been suggested that there is a strong association between a diabetic pregnancy and increased birth weight [235]. In addition to that, placental weight was also increased during pregestational diabetes or gestational diabetes [235, 236]. In this study, STZ-induced diabetes in mice caused the embryonic weight to increase when compared to the non-treated mice from E14.5 to term, but the placenta weight remained unchanged at E14.5, which indicated that the increase in placental weight occurred gradually during mid to late gestation. This finding was similar with clinical

observations of which the newborns from diabetic mothers tend to be larger [237]. Under FOXO1 disruption, the embryonic weight displayed a significant increase at term, but not E16.5 or E14.5. Although we did not check the body composition of the embryo, Embryonic weight at later stage is likely due to the fat deposition in the adipose tissue. It has been shown that FOXO1 suppression release the inhibition of PPARγ and other target genes which are associated with lipid metabolism [154, 155], therefore the activation of downstream targets related with lipogenesis can be a potential mechanism of the weight change observed in FOXO1 disruption mice. Accordingly, the placenta weights for these embryos were higher at E16.5 and term, consistent with the unchanged placenta efficiency at E16.5 and term. These results suggest that FOXO1 disruption did not interfere the matched growth between placenta and embryo under either NG or HG. However, increased offspring weight may potentiate the higher risk for future health complications including obesity and diabetes [238, 239].

The important role of FOXO1 has been studied during early placental development [160], while no studies investigating the function of FOXO1 at a later stage of placenta development. That FOXO1 expression reaches to the peak at E14.5 suggested an important role of FOXO1 in supporting the placenta maturation. Indeed, we showed that FOXO1 disruption caused increased placental weight after E14.5, but not before E14.5. Increased placenta weight might be due to activated cell proliferation. We find that FOXO1 disruption can cause decreased apoptosis and promoted proliferation in the labyrinth zone under normal glucose condition. These findings are consistent with previous reports to show an up-regulation of FOXO1 inhibits cell proliferation and

induces apoptosis in other tissues [240, 241]. We also noticed that the disrupted effects on cell proliferation and survival caused by FOXO1 disruption was released under hyperglycemia. This phenotype could be a result of the upregulation of FOXO1 expression under hyperglycemia condition. However, our data at E12.5 is insufficient to explain the placental weight change under hyperglycemia at E16.5 and afterwards. Future study to measure the cell proliferation and survival rate at later stages will provide important evidence to elucidate the important role of FOXO1 on regulating the development of labyrinth layer.

It has been reported that the loss of FOXO1 would lead to severe vasculature malformation during early placental development [160]. In addition, there are literatures demonstrating that hyperglycemia can induce endothelial cell dysfunction and promote angiogenesis [242-246]. Similarly, we found that the placentas of WT-WT HG group showed significant more fetal vasculature and less maternal lacunae space compared with WT-WT NG group, but other groups showed no difference among each other. However, there were clear decreasing trends of the fetal vasculature and increasing trend of the maternal lacunae area in F-WT HG and F-F HG groups, showing similar levels as the normal situation. This result suggests a partial rescue of the abnormal vasculature under HG by FOXO1 disruption. It is possible that FOXO1 deficiency interacts with hyperglycemia to mediate the vasculature development. A two-way ANOVA analysis should be conducted to disclosure this interaction between FOXO1 expression levels and hyperglycemia. In addition, limited sample size of the current study (n=3) provides less

power of the analysis. Thus, we will increase sample size to 6-8 in the following study to achieve a power analysis great than 90%.

As for the heart phenotypes observed in this study, we did not see a significant higher heart defect rate in WT HG group compared with WT NG group. Although there has been reported that the risk of congenital heart defect are 2-5 times higher in women with diabetes [40], the overall defect rate is low which is reported to be 4 to 9 cases per 1000 liver birth [247]. Previous reports showed that FOXO1 deletion lead to embryonic death due to cardiac malformation, suggesting an important role of FOXO1 in heart development [248, 249]. In our study, disrupting FOXO1 expression did not resulted in higher incidence of CHDs, neither more severe heart abnormalities. Possibly, the sample size we collected is not large enough to test if hyperglycemia plays a synergic effect to promote CHDs. It is also possible that the FOXO1 heterozygote is sufficient to support normal heart development under both normoglycemia and hyperglycemia. Future studies with FOXO1 deletion in specific cardiac cell lineages may illustrate detailed molecular mechanisms of how FOXO1 contributes to embryonic heart development.

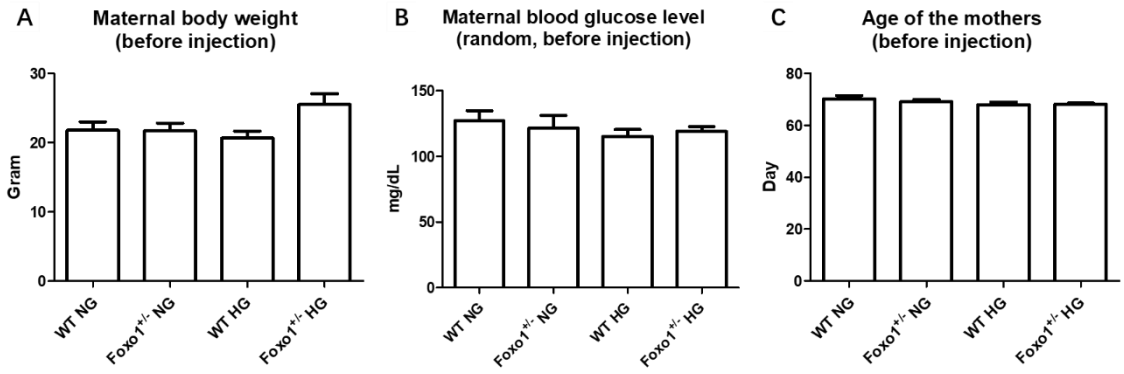


Figure 7. No significant difference in maternal weights, glucose levels and ages.

A. Body weights of the female mice at one day before injection in different groups.

B. Random blood glucose levels of the female mice at one day before injection in different groups.

C. Ages of female mice at one day before injection in different groups.

Data is presented as Mean±SE, N=6-7, #$p<0.1$, *$p<0.05$.

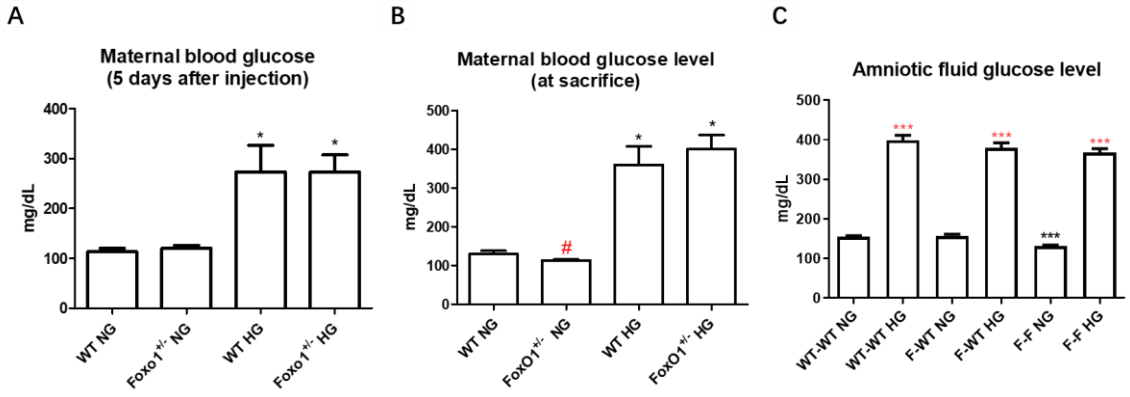


Figure 8. Maternal blood glucose and fetal amniotic fluid glucose levels were upregulated under STZ treatment.

A. Random blood glucose levels of the female mice at 5 days after the second injection in different groups.

B. Random blood glucose levels of the female mice at sacrifice in different groups.

C. Amniotic fluid glucose levels of the embryos in different groups.

Data is presented as Mean±SE, N=6-7, #p<0.1, *p<0.05, **p<0.01, ***p<0.001. black pond and star indicate the comparison between different genotype under same treatment condition, red pond and star indicated the comparison between different treatments of the same genotype conditions.

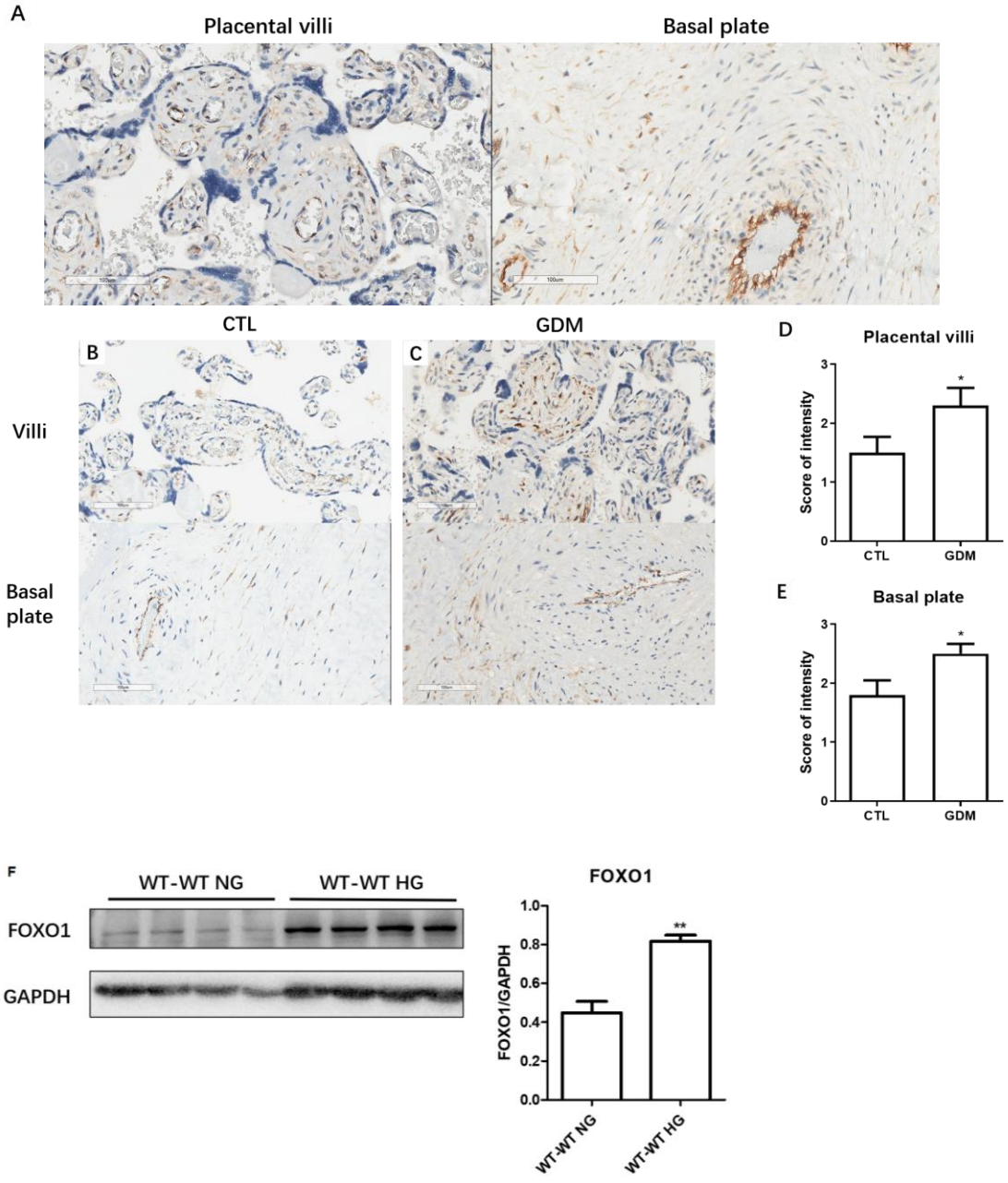


Figure 9. FOXO1 expression in mice and human placenta.
A. FOXO1 IHC staining in human term placenta.
B-C. FOXO1 IHC staining performed in healthy and GDM women.
D. Score of staining intensity in the placental villi.
E. Score of staining intensity in the basal plate.
F. Western blot analysis of FOXO1 in WT placentas in NG and HG groups.
Data is presented as Mean±SE, N=10, #p<0.1, *p<0.05.

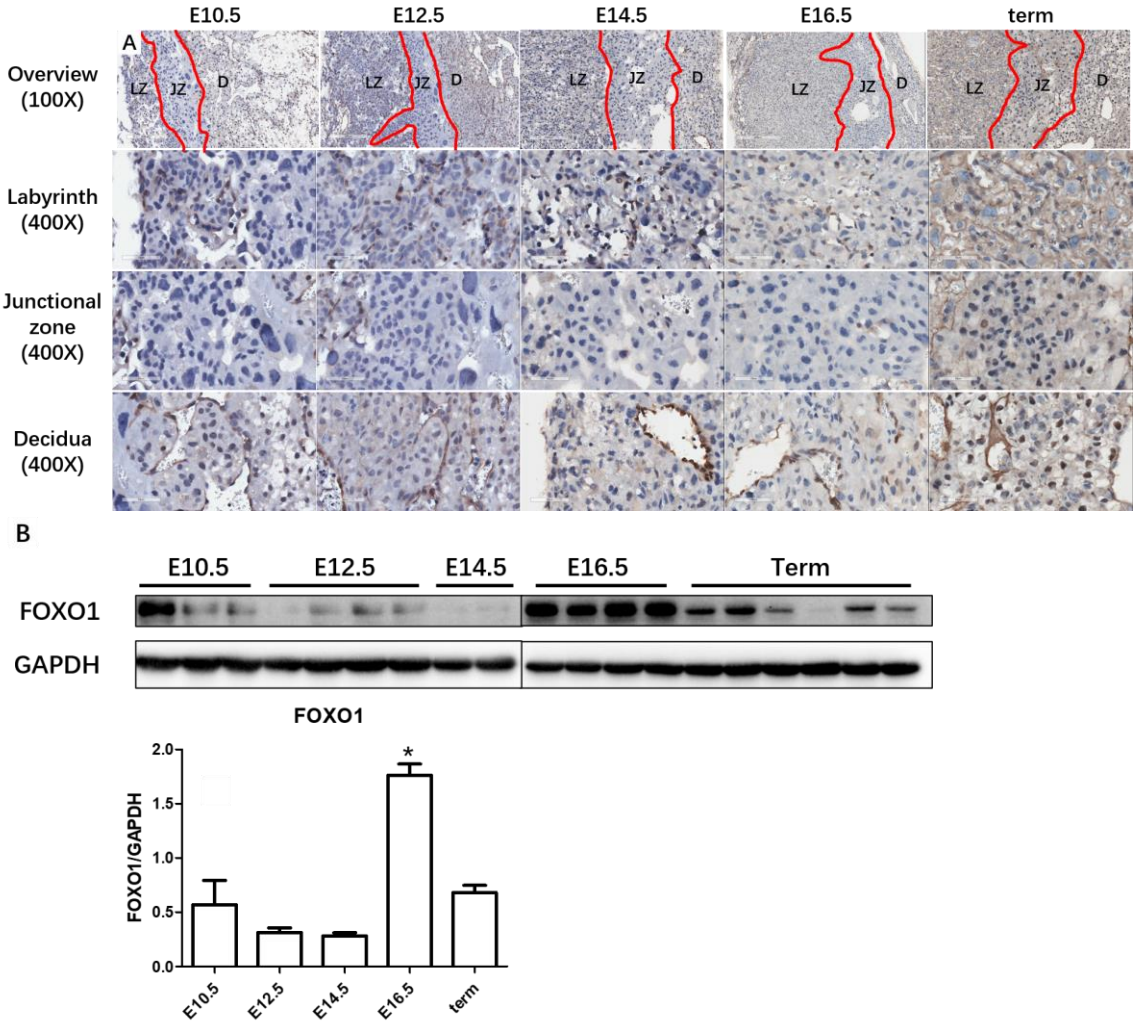


Figure 10. FOXO1 expression in WT and *FOXO1*$^{+/-}$ placentas.

A. FOXO1 IHC staining in mice placentas at E10.5, E12.5, E14.5, E16.5 and term. Red lines indicate the borderline of different layers in the placenta. LZ, labyrinth; JZ, junctional zone; D, maternal decidua.

B. Western blot analysis of FOXO1, pFOXO1, GAPDH in WT placentas at indicated gestational days.

Data is presented as Mean±SE, N=3-4, *p<0.05.

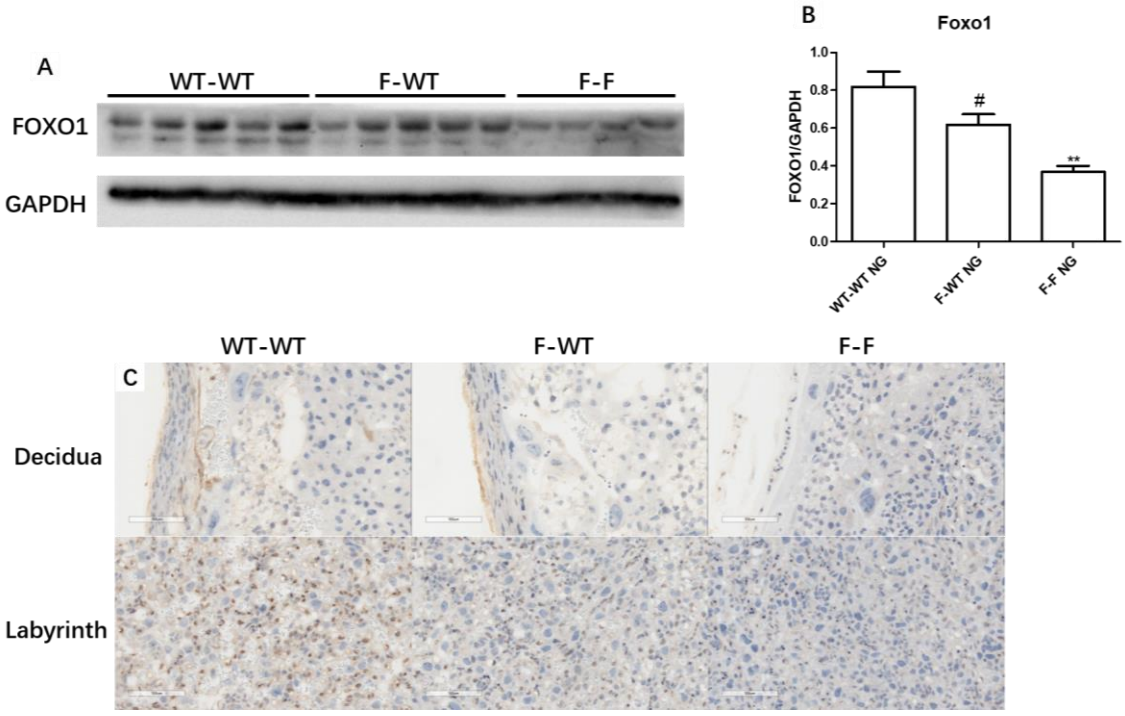


Figure 11. FOXO1 expression in WT and *FOXO1*$^{+/-}$ placentas.

A. Western blot analysis of FOXO1 in placentas with indicated genotypes without STZ treatment. WT-WT, WT embryo from WT female; F-WT, WT embryo from *FOXO1*+/- female; F-F, *FOXO1*+/- embryo from *FOXO1*+/- female.

B. Statistic quantifications of FOXO1/GAPDH was performed with ImageJ. Data is presented as Mean±SE, N=4-5, #p<0.1, **p<0.01.

C. FOXO1 IHC staining in decidua and labyrinth of mice placentas with indicated genotypes

.

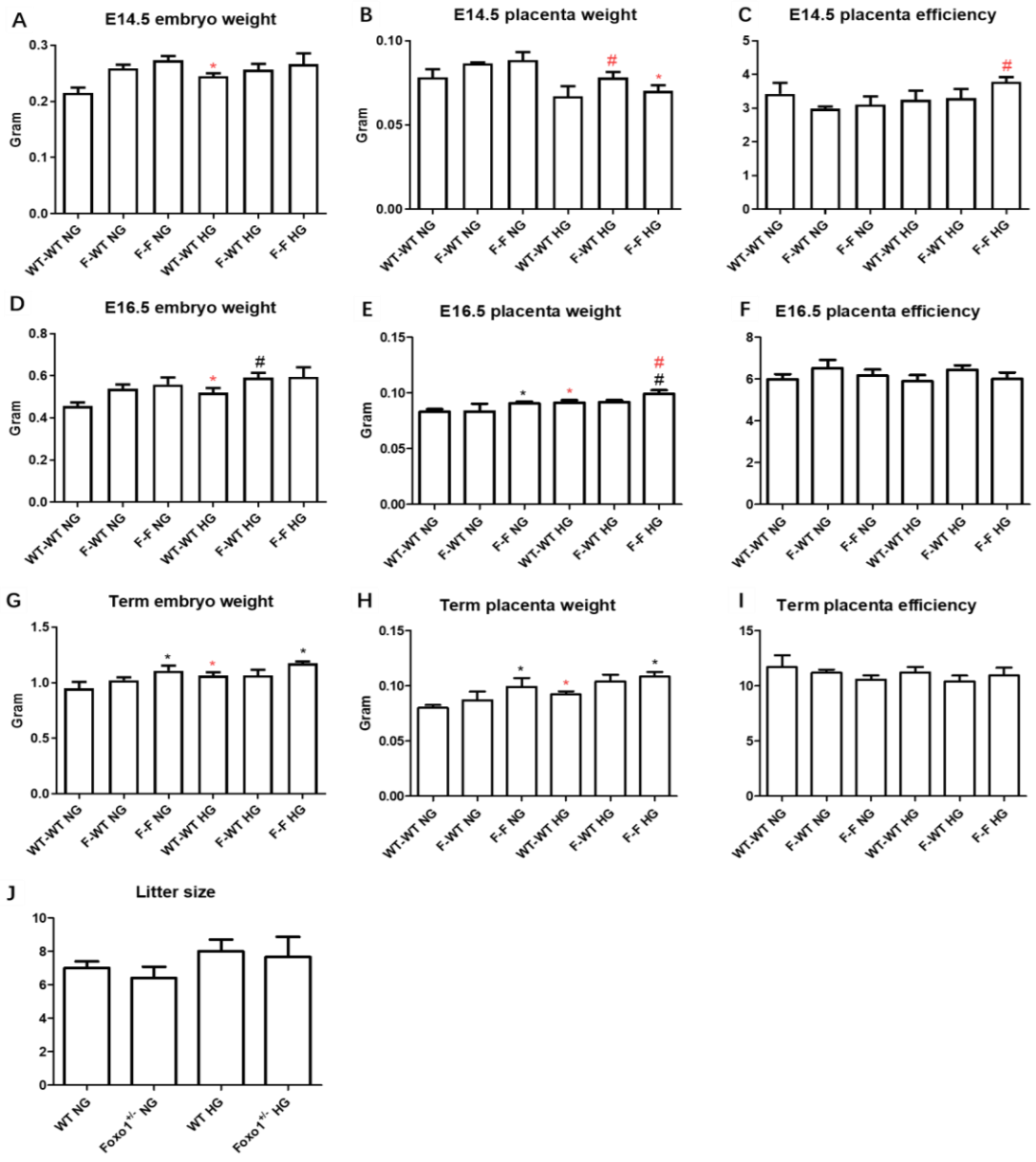


Figure 12. FOXO1 disruption and maternal hyperglycemia caused embryo and placenta weight changed at different gestational stages.

A-C. Embryo weights, placenta weights and placenta efficiency at E14.5.

D-F. Embryo weights, placenta weights and placenta efficiency at E16.5.

G-I. Embryo weights, placenta weights and placenta efficiency at term.

J. Litter size of the female in different groups.

Data is presented as Mean±SE, N=6-7, #p<0.1, *p<0.05, **p<0.01, ***p<0.001. black ponds and stars indicate the comparison between different genotype under same treatment condition, red ponds and stars indicated the comparison between different treatments of the same genotype conditions.

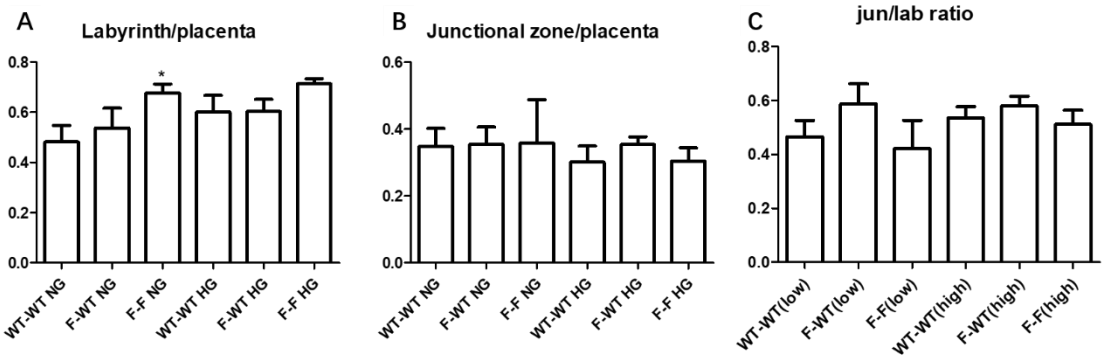


Figure 13. FOXO1 deficiency caused relative labyrinth volume increasing under euglycemic condition, but not under hyperglycemic condition.

A. Relative labyrinth volumes were evaluated by labyrinth area/placenta area ratio.

B. Relative junctional zone volumes were evaluated by junctional zone area/placenta area ratio.

C. The ratio of junctional zone volume to labyrinth volume.

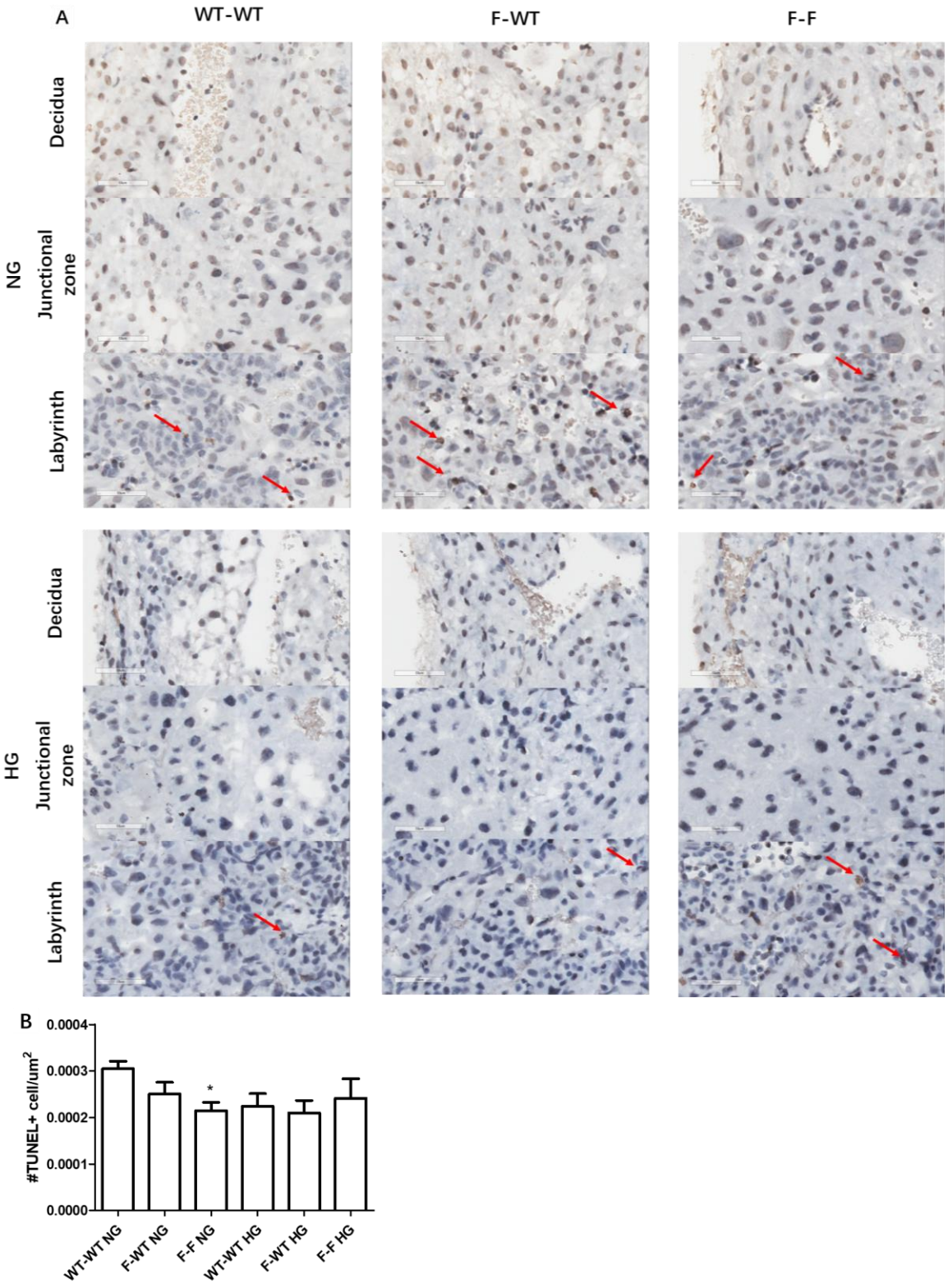
A
WT-WT
F-WT
F-F
NG
HG
Decidua
Junctional zone
Labyrinth
B
#TUNEL+ cell/um2
0.0004
0.0003
0.0002
0.0001
0.0000
*
WT-WT NG
F-WT NG
F-F NG
WT-WT HG
F-WT HG
F-F HG

Figure 14. FOXO1 disruption caused apoptotic cell number decreasing under euglycemic condition, but not under hyperglycemic condition.

A. TUNEL staining in decidua, junctional zone, and labyrinth for placenta at E12.5. red arrows indicate the cell with TUNEL positive staining.

B. The number of TUNEL+ cells per μm2 in the labyrinth layer. Data is presented as Mean±SE, N=4, *$p<0.05$.

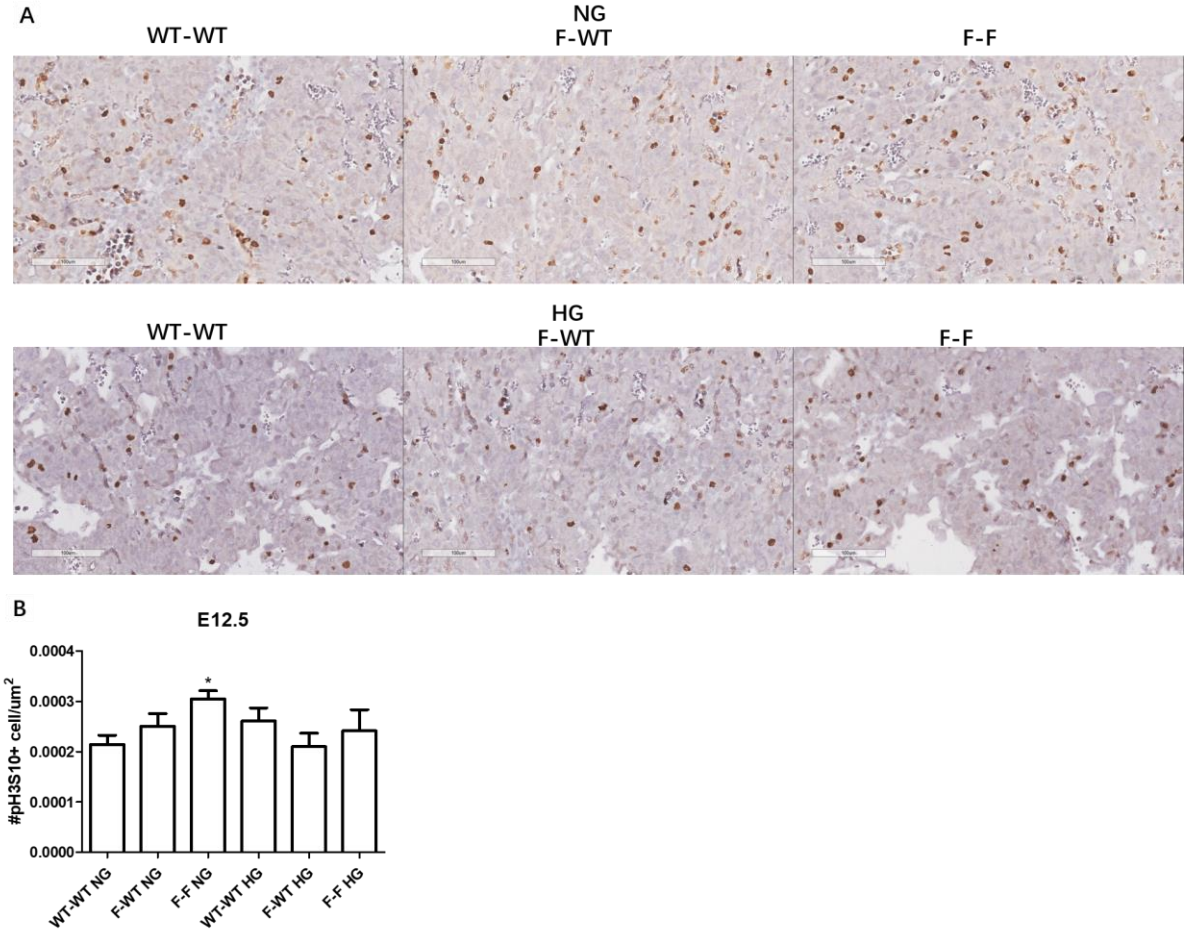


Figure 15. FOXO1 disruption increased relative labyrinth volume under euglycemic condition, but not under hyperglycemic condition.

A. pH3S10 staining in labyrinth for placenta at E12.5.

B. The number of pH3S10+ cells per μm2 in the labyrinth layer. Data is presented as Mean±SE, N=4, *p<0.05.

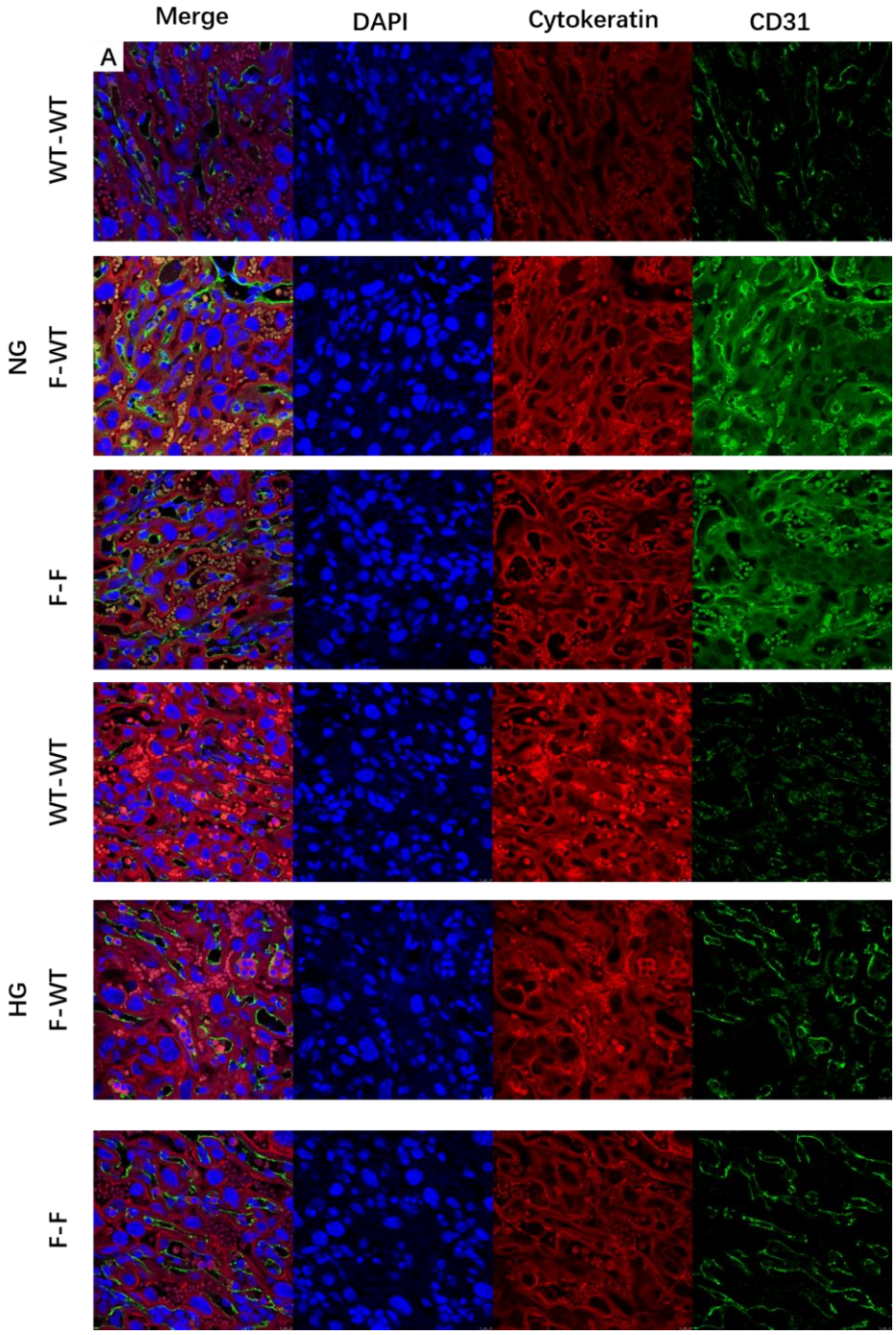

Figure 16. FOXO1 disruption promoted labyrinth angiogenesis.

(Figure 16 Continued)

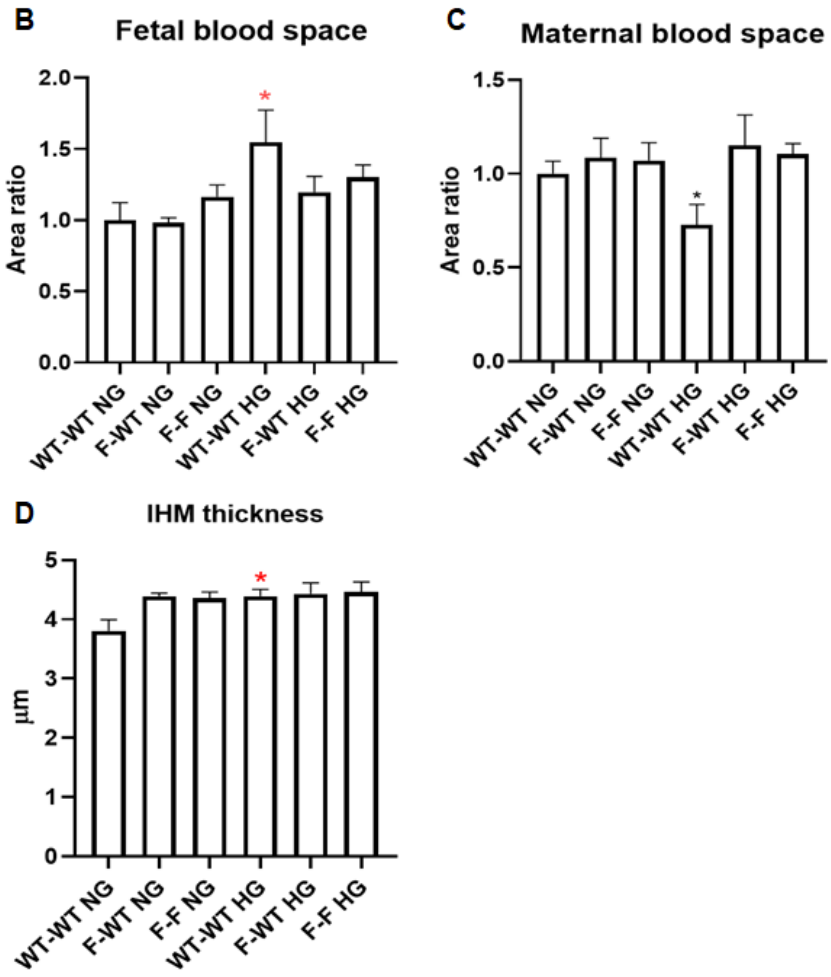


A. PECAM (green) and Cytokeratin (red) co-IF staining in the labyrinth, counterstained with DAPI (blue).

B. Relative fetal blood space (normalized to WT-WT NG group) observed in 0.025 mm2 area.

C. Relative materal blood space (normalized to WT-WT NG group) observed in 0.025 mm2 area.

D. Interhemal membrane (IHM) thickness in E14.5 placentas.

Data is presented as Mean±SE, N=3-7, #p<0.1, *p<0.05.

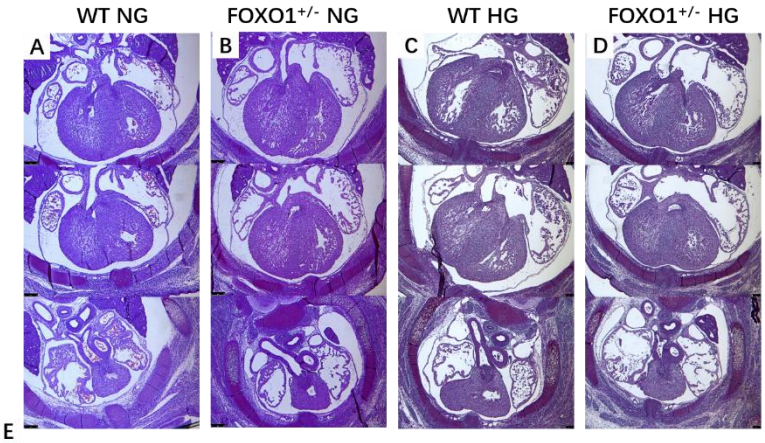


E

| | VSD | ASD | DORV | PTA | Total |
|---|---|---|---|---|---|
| WT NG | 4 | 1 | 0 | 0 | 16 |
| FOXO1$^{+/-}$ NG | 6 | 2 | 0 | 0 | 20 |
| WT HG | 5 | 1 | 1 | 0 | 18 |
| FOXO1$^{+/-}$ HG | 6 | 0 | 0 | 0 | 17 |

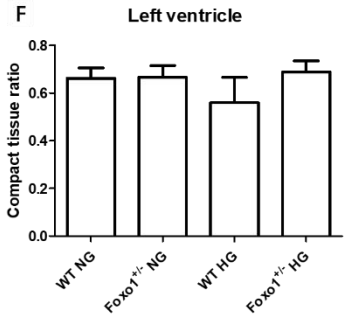


Figure 17. FOXO1 disruption or maternal hyperglycemia did not cause higher heart defect rate at E14.5

A-D. H&E staining of E14.5 hearts from indicated groups.

E. Table of the occurrence times of VSD, ASD, DORV and PTA. VSD, ventricular septal defect; ASD, atrial septal defect; DORV, double outlet right ventricle; PTA, persistent truncus arteriosus.

F. The ratio of compact tissue to the entire left ventricle area.

Data is presented as Mean±SE, N=10, #p<0.1, *p<0.05, **p<0.01, ***p<0.001.

# CHAPTER IV

# PREGESTATIONAL DIET TRANSITION TO NORMAL-FAT DIET AVOIDS THE DETERIORATION OF PANCREATIC B-CELL FUNCTION IN MALE OFFSPRING INDUCED BY MATERNAL HF DIET*

## Introduction

The Developmental Origins of Health and Disease (DOHaD) hypothesis postulates that the *in utero* environment influences postnatal health and plays a role in disease etiology [250]. The Pregnancy Risk Assessment Monitoring System created by the Centers for Disease Control and Prevention (CDC) indicates that nearly half of the women are either overweight or obese at the time they become pregnant [251]. The adverse consequences of maternal overnutrition on the developing fetus, in conjunction with the rising prevalence of these pregnancies, are alarming. Therefore, an intervention strategy needs to be systematically evaluated.

Recent animal studies have reported that a prolonged HF diet before and during pregnancy predisposes the offspring to excessive weight gain, hyperglycemia, and insulin resistance [252-255]. Insulin-producing β-cells play an essential role in maintaining glucose homeostasis in healthy individuals. Under obesity-induced insulin resistance, β-cells respond to the metabolic changes by increasing their number, at least in part, via proliferation [256-258]. In response to chronic insulin insufficiency, β-cells

*Reprinted with permission from " Pregestational diet transition to normal-fat diet avoids the deterioration of pancreatic β-cell function in male offspring induced by maternal high-fat diet." by Liu, Z., et al, (2020). *The Journal of Nutritional Biochemistry* 86: 108495. Copyright 2020 by Elsevier Inc.

proceed to de-granulate by de-differentiating into a progenitor cell type; this further contributes to β-cell failure [259, 260].

Rodents have been a great model to investigate the effects of maternal overnutrition on the pancreatic β-cell. Upon exposure to maternal HF diet, offspring were found to have sex-dependent phenotypes in islet remodeling [252, 255]. Only the male offspring displayed enlarged islet area indicating increased oxidative stress in islets [252, 255]. Male offspring also showed a lower level of pancreatic and duodenal homeobox 1 (PDX-1) mRNA in isolated islets, whereas female had a higher level [255]. Furthermore, male offspring showed impaired insulin-signaling in the islet, evidenced by decreased protein expressions of insulin receptor substrate 1 (IRS-1), phosphoinositide 3-kinases (PI3K), p-AKT, programmed cell death protein 1 (Pd-1), and Glut2 proteins [252].

Although progress has been made to understand the pathophysiological changes in the pancreas of offspring exposed to over-nutrition *in utero*, no study has evaluated the possibility of maternal diet interventions in preventing adverse effects on offspring β-cell function. Similar to humans, "metabolic memory" ranging from 1 week to 5 months is observed in mice, depending on different diets or biometrics being evaluated [261-263]. In our previous studies, we have explored the impacts of various maternal diet interventions on offspring obesity, glucose tolerance, and non-alcoholic fatty liver disease [199, 264-268]. From our study, maternal HF diet was shown to reprogram the offspring's glucose and fatty acid metabolism, increasing their risks of obesity, insulin resistance, and NAFLD. Early transition from a HF diet to a NF diet (9-week before pregnancy, H9N diet) before pregnancy prevents this effect. In contrast, rushed

transition (1-week or 5-week before pregnancy) worsens these effects [199, 264-268]. These studies prove that pre-conception diet intervention reduces the risk of offspring obesity, and its associated complications, by preventing the reprogramming of metabolism, and inflammation of multiple organs, including adipose tissue and liver. These studies also suggest sufficient duration of dietary intervention to be crucial in successfully preventing the obesogenic effects of maternal HF diet on the offspring. Here, we tested our hypothesis that early dietary transition (9-week) prevents the disruptive effects of maternal HF diet on offspring pancreas β-cells. We investigated the effectiveness of, and mechanisms behind, pre-conception maternal diet transition from HF to NF in preventing the adverse effects of maternal HF diet on offspring β-cell function. Ultimately, we hope to evaluate the success of pre-conceptional dietary intervention in reducing the risk of offspring metabolic syndrome.

## Experimental methods

### *Experimental design*

Four-week-old female mice of mixed background (B6/129/SvEv) were fed with either the control diet (NF, 10% fat) or the HF diet (60% fat) for 12 weeks and randomly mated with male mice with mixed background and similar age. A group of female breeders were fed HF diet for 12 weeks before pregnancy, during gestation, and lactation (HF group). Another group of female breeders were placed on HF diet for 3 weeks, then transitioned to NF diet 9 weeks prior to pregnancy, and stayed on NF diet through gestation and lactation (H9N group). A separate group of female breeders on the NF diet continued that diet through gestation and lactation, and were utilized as a control group (NF group). All offspring were weaned at 3 weeks after birth, and were given a post-weaning HF diet for 12 weeks. In addition, a group of offspring from breeding pairs on normal chow diet (CD) diet were fed the CD, and served as the reference group (REF group, n=3) to show normal ranges of a given characteristic (Table 5). At least five litters per treatment group were used in this study (n=5-7 per treatment group) with each litter size ranging from 6-8 pups. All mice experiments were conducted under the protocol approved by the Institutional Animal Care and Use Committee at Texas A&M University which is in compliance with the USA Public Health Service Policy on Humane Care and Use of Laboratory Animals.

### *Diet Composition*

Diets were purchased from Research Diets, LLC (New Brunswick, NJ) to implement a diet-induced obesity (DIO) model. The HF diet (Catlog#D12492) has an energy

density of 5.24 kcal/g (60% fat energy, 20% carbohydrate energy, and 20% protein energy). The fat source is composed of 54% lard and 6% soybean oil. The normal fat diet (Catlog#D12450J) was designed to match the sucrose component of the HF diet with only 10 kcal% fat. The diets were matched by micronutrient and macronutrient content (Table 6).

*Antibodies and Reagents*

Primary antibodies used were: anti-insulin (Catlog#14976982, IF/IHC, 1:200 dilution) and anti-glucagon (Catlog#14974382, IF/IHC, 1:200 dilution) from Thermo Fisher Scientific (Waltham, MA, United States), anti-p-H3S10 (Catlog#5176, IHC, 1:200 dilution) from Abcam (Cambridge, United Kingdom), and anti-Glut2 (Catlog#sc-9117, IF, 1:1000 dilution) from Santa Cruz Biotechnology (Dallas, TX, United States). Secondary antibodies used were: F(ab')2-Goat anti-Mouse IgG-Alexa 594 (Catlog#A11020, IF, 1:800 dilution) and Goat anti-Rabbit IgG-Alexa 488 (Catlog#A31628, IF, 1:800 dilution) from Thermo Fisher Scientific (Waltham, MA, United States), anti-AKT (Catlog#9272, Western blot, 1:1000 dilution), anti-p-AKT (Ser473) (Catlog#9271, Western blot, 1:1000 dilution), and anti-Gapdh (Catlog#2218, Western blot, 1:1000 dilution) from Cell Signaling Technology (Danvers, MA, USA). Chemical reagents used were BSA (Catlog#A2153) and DAPI (Catlog#F6057) from Sigma-Aldrich (Oakville, ON, Canada).

*Intraperitoneal injected glucose tolerance test (IPGTT)*

IPGTT was performed as previously described [264].

*Homeostatic model assessment (HOMA)*

Offspring serum was collected and stored at -80°C. Plasma insulin concentrations were measured via insulin enzyme-linked immunosorbent assay (ELISA) commercial kit (P01325) from RayBiotech (Peachtree Corners, GA, United States) using the manufacture's protocol. The HOMA insulin resistance index was calculated using the following equation:

$$HOMA\ IR\ Index = \frac{Fasting\ blood\ glucose\ concentration \times insulin\ concentration}{22.5}$$

*Pancreas histology*

The pancreas samples, specifically the head portion, were fixed in 10% formalin from Thermo Fisher Scientific (Waltham, MA, United States) for 24 hours. For hematoxylin and eosin (H&E) staining of the pancreas tissue, five serial 5 µm paraffin sections were deparaffinized by xylene and stained by standard procedures. Islet morphology was observed using a Leica DM2500 light-microscope. The area of each pancreas section and islet were measured using Image J at 100x magnification. The pancreas area, area of each islet, and islet count were recorded for each mouse (n=4-5 per treatment group). Calculations were performed as follow:

$$Area\ ratio\ of\ islet/pancreas = \frac{sum\ (area\ of\ each\ islet)}{pancreas\ area}$$

$$Average\ size\ of\ islet = \frac{sum\ (area\ of\ each\ islet)}{islet\ count}$$

$$Number\ of\ islet/mm^2 = \frac{islet\ count}{pancreas\ area}$$

*Immunofluorescent staining*

The slides of pancreas sections were deparaffinized with xylene before staining. Antibodies were used at the aforementioned concentrations. Primary antibody incubation took place in a humidified box overnight at 4℃. Secondary antibody incubation took place at room temperature for 30 minutes in a dark box. Incubation was stopped by washing the slides with PBS.

β-cell was marked as insulin positive (Ins+) and α-cells were marked as glucagon positive (Gcg+) in the islet. The number of Ins+ β-cells and Gcg+ α-cells in every 1000 $\mu m^2$ islet area were counted and analyzed.

β-cell proliferation rate was evaluated using the Image J count of total number of H3S10+Ins+ cells and total number of Ins+ cells in five randomly selected islets at 200x magnification. The percentile of proliferating islet cells was calculated by dividing the number of H3S10+Ins+ cells with the number of Ins+ cells. The percentile of proliferating non-islet cells in non-islet regions of the pancreas was generated from the number of H3S10+ cells within 500 randomly selected DAPI+ cells. For each treatment group, five to six mouse samples were analyzed.

β-cell degranulation rate was calculated by dividing the total number of Glut2+Ins- cells with the total number of Glut2+ cells counted in ten randomly selected islets per pancreas sample. For each treatment group, three to four mouse samples were analyzed.

TUNEL staining was performed using ApopTag® Red In Situ Apoptosis Detection Kit (Catlog#S7165, Millipore Sigma, Burlington, MA, United States).

*Statistical analysis*

At least three litters per treatment group were included in this study (n=3-7). Differences from REF to NF, HF, and H9N group, and differences from NF to REF, HF, and H9N group were analyzed by one-way analysis of variance (ANOVA). The post-hoc test we used for the ANOVA was Fisher's LSD test. For all statistical tests, results were considered significant when the *P*-values were less than 0.05. All analyses were carried out by using SAS JMP software (SAS Institute Inc., Cary, NC, USA) and R statistical programming language.

**Results**

*Maternal H9N diet avoided the early emergence of insulin resistance primed by maternal HF-diet in offspring fed a post-weaning HF diet.*

Male offspring from all groups had similar body weights at the time of weaning (Fig. 18A). After 12 weeks of post-weaning HF diet, offspring from all groups continuously gained bodyweight. The mean bodyweight at the time of sacrifice ranking from the highest to the lowest was: HF≈H9N>NF≈REF (Fig. 18B). These two data sets indicate that maternal H9N diet is unable to slow down body weight gain of the male offspring (Fig. 18A and B). Consistently, the maternal HF diet significantly enlarged the offspring visceral fat mass, and the H9N diet failed to prevent this effect (Fig. 18C). Next, glucose tolerance was measured by performing IPGTT before termination at week 12. Fasting glucose levels were not significantly different between any two groups (Fig. 18D). Unlike REF and NF offspring that reached peak glucose levels at 30-minutes post-glucose challenge, both HF and H9N offspring maintained high glucose levels until 60-minutes post-glucose challenge (Fig. 18D). Blood glucose levels of all groups were able to return to basal level at 120-minute post-challenge. From the area under the curve (AUC) analysis, both NF and HF offspring displayed glucose intolerance, while H9N offspring was glucose tolerant (Fig. 18E). We then performed homeostasis model assessment (HOMA) to investigate β-cell function and insulin resistance (IR) from basal (fasting) glucose and insulin levels. The HOMA-IR values were increased in NF offspring, but the changes were insignificant. However, HF offspring had significantly higher HOMA-IR values compared to those of REF offspring. Importantly, H9N

offspring showed HOMA-IR values similar to those of REF offspring (Fig. 18F). This suggests that H9N diet can prevent the impairment of β-cell function and insulin resistance seen in HF offspring.

Unlike male offspring, REF female offspring had a mean body weight at weaning that was significantly lower than that of the other three groups (Fig. 19A). After 12-weeks on the HF diet, the NF female offspring maintained a lower body weight, similar to that of REF offspring. However, HF female offspring experienced significant body weight gain compared to NF female offspring. Interestingly, maternal H9N diet prevents this body weight gain. Instead, H9N offspring had similar body weights to those of NF offspring (Fig. 19B). Similarly, maternal HF diet significantly enlarged the visceral fat mass in female offspring, while the maternal H9N diet completely prevented such effect (Fig. 19C). The female offspring had similar glucose tolerance test results as the male offspring (Fig. 19D and E).

*Maternal H9N diet prevents the enlargement of islet primed by maternal HF-diet in offspring fed a post-weaning HF diet.*

Within the pancreas head portion of male NF offspring, the 12-week post-weaning HF diet increased neither the islet/pancreas ratio (Fig. 20B) nor the average islet size (Fig. 20C). However, HF offspring had increased islet area evidenced by both higher islet/pancreas ratio and larger islet size compared to REF offspring (Fig. 20B and C). In contrary, H9N offspring had a similar islet/pancreas ratio and average islet size to those of REF or NF offspring (Fig. 20B and C). We did not observe significant differences in islet density (number of islets per $1mm^2$ pancreas area) among the four groups (Fig.

20D). These results suggest that maternal and post-weaning HF diets have a synergistic effect on offspring islet size enlargement.

Interestingly, we did not observe changes in the islet areas or the number of islets per $1mm^2$ pancreas field of females among the four groups (Fig. 21B-D).

*Maternal H9N diet prevents the loss of β-cells (Ins+) primed by maternal HF-diet in offspring fed a post-weaning HF diet.*

Since the histological changes of the islet were only observed in the male offspring, but not the female offspring, histological changes in islet β and α-cell were evaluated only in male offspring. While the post-weaning HF diet significantly decreased the number of Gcg+ α-cells in offspring of NF compared to REF, the H9N diet completely blocked this effect (Fig. 22A and B). Unlike the Gcg+ α-cells, lower numbers of Ins+ β-cells were observed in HF offspring but not NF offspring (Fig. 22A and C). This suggests that maternal and post-weaning HF diets have a synergistic effect on β-cell number reduction. Interestingly, the maternal H9N diet completely avoided this effect (Fig. 22A and C). There were no differences in the ratio of Ins+ β-cells to Gcg+ α-cells among different treatment groups (Fig. 22D).

Since the enlarged islet area observed in HF offspring was not explained by β-cell hyperplasia, we investigated if there were changes in the size of individual Ins+ β-cells or Gcg+ α-cells. The NF offspring showed a slight, but not significant, increase in the size of Ins+ β-cells compared to REF offspring (Fig. 22E). As for HF offspring, the size of Ins+ β-cells was significantly larger compared to REF offspring. This suggests that maternal HF diet causes offspring β-cell hypertrophy. Interestingly, the size of Ins+ β-

cells of H9N offspring was smaller than that of NF offspring. Instead, the size of Ins+ β-cells were similar between H9N and REF offspring (Fig. 22E). Unlike Ins+ β-cells, the size of Gcg+ α-cells were not different among any of the treatment groups (Fig. 22F).

*Maternal H9N diet avoided β-cell degranulation which was observed in NF and HF offspring.*

The variances in number of the Ins+ β-cells in offspring from different maternal diets led us to the following question: does maternal nutritional status affect β-cell degranulation in the offspring? Glut2 is required for glucose-stimulated insulin secretion and is selectively expressed in the islet β-cells [269, 270]. Therefore, we detected β-cell degranulation by the colocalization of Glut2 and insulin. β-cell degranulation was marked by positive Glut2 expression and negative insulin expression (Fig. 23A-M, a typical "degranulation" is indicated by the yellow arrow in Fig. 21M). There was no difference in the total number of Glut2+ cells per 1000 $\mu m^2$ islet area among all four groups (Fig. 23A-D and N). The ratio of undifferentiated β-cell per pancreas was calculated by dividing the total number of Glut2+Ins- cells by the total number of Glut2+ cells in each islet. Compared to REF offspring, NF and HF offspring had significantly more $Glut2^{+}Ins^{-}$ β-cells that indicated increased β-cell degranulation. However, H9N diet prevented such effect as H9N offspring had similar β-cell degranulation levels as REF offspring.

*Maternal H9N diet avoided islet cell proliferation defects primed by maternal HF-diet in offspring fed a post-weaning HF diet.*

Next, the effects of varying maternal diets on offspring islet cell proliferation were examined with Co-IF staining of p-H3S10 and Insulin. Positive staining for p-H3S10 indicated cells in the G2-M phase, and was observed in both islet and non-islet cells (Fig. 24A). The cell count ratio of H3S10+ β-cells to Ins+ cells per islet (Fig. 24B) or to every 500 non-islet cells (Fig. 24C) were analyzed. The post-weaning HF diet (NF offspring) slightly increased the ratio of proliferating islet β-cells, but not significantly. HF offspring had significantly lower ratios of p-H3S10$^{+}$ cells to islet β-cells compared to either REF or NF offspring (Fig. 24A and B). This suggests that maternal HF diet primes the inhibition of islet cell proliferation. Strikingly, H9N offspring had significantly lower ratios of p-H3S10$^{+}$ to Ins+ β-cells compared to NF offspring. Instead, ratios of p-H3S10$^{+}$ to Ins+ β-cells were similar between H9N and REF offspring (Fig. 24A and B). The proliferation rate within non-islet cells was not different among the four groups (Fig. 24A and C).

TUNEL staining was performed to assess if different maternal diets affect cell survival. No programmed cell death was observed in the pancreas tissues regardless of different treatment groups (Fig. 25A). This suggests that different maternal dietary conditions tested in our study do not affect cell apoptosis in the offspring's pancreas.

*Maternal H9N diet avoided AKT signaling deactivation primed by maternal HF-diet in offspring fed a post-weaning HF diet.*

The AKT signaling pathway is important for pancreatic β-cell proliferation, mass, and cell size [271]. Western blot analysis revealed that the AKT expression was unaffected by different treatments (Fig. 26D and E). However, there was a significant decrease in the level of p-AKT in the pancreas of HF offspring when compared to that of the REF group. This suggests that maternal HF diet and post-weaning HF diet have a synergistic effect on inhibiting the AKT signaling in offspring. In contrast, H9N offspring had a similar level of p-AKT to that of REF offspring suggesting that maternal H9N diet prevents such deleterious effect (Fig. 26D and F).

## Discussion

In this study, we proved the predisposing effects of maternal HF diet in deteriorating the offspring pancreas islet function in male offspring fed a post-weaning HF diet (HF group). Most importantly, this effect was prevented via early pre-conceptional dietary transition from HF to NF (H9N group). This was evidenced by the fact that H9N offspring was protected from developing an abnormal metabolic profile, including glucose intolerance and insulin resistance. Alarmingly, maternal HF diet and the post-weaning HF diet had synergistic effects in promoting hypoplasia and hypertrophy of islet Ins+ β-cells in male offspring, whereas the maternal H9N diet prevented such effects. Islet Ins+ β-cell hypoplasia is likely associated with increased degranulation and reduced cell proliferation of the islet β-cells in HF offspring. Interestingly, these changes in islet β-cells were not seen in H9N offspring. At the molecular level, HF offspring displayed deactivated AKT signaling in their pancreas tissue, whereas H9N offspring presented normal AKT signaling. In summary, the results support the idea that early maternal diet transition from HF to NF before pregnancy is effective in preventing maternal HF diet from reprograming offspring pancreatic function. However, it is also possible that maternal physiological state, such as weight loss and insulin resistance, differentially impacts the risk for offspring obesity and insulin resistance. We addressed and excluded this possibility in our previous study using the same mouse model, since mother dams from different treatment groups did not show differences in body weight change nor glucose tolerance during pregnancy [15].

Proliferation of β-cells occur at a high rate near the end of embryogenesis, which leads to a massive increase in β-cell mass, and then slows down considerably in adult mice [272]. Previous studies have demonstrated a decrease in β-cell mass among newborns from mothers fed a HF diet compared to those from mothers fed a chow diet. However, the rapid β-cell growth in the newborns exposed to *in utero* over-nutrition eliminates this difference within 10-days after birth [273]. These results suggest a possibility that HF offspring have lower β-cell capability to respond to increased insulin demand associated with different physiological and pathological status, including pregnancy, obesity, and overfeeding by HF diet. In our study, HF offspring which were exposed to HF diet during gestation, lactation, and post-weaning, displayed significantly increased islet mass. This result suggests a synergistic effect of maternal HF diet and post-weaning HF diet in promoting islet enlargement. Previous studies have reported that increasing β-cell proliferation expands β-cell population and islet area, and meets the increased demand of insulin prior to developing insulin resistance [274]. However, HF offspring displayed β-cell proliferation defects due to inhibited AKT phosphorylation. This suggests that the β-cell is unable to proliferate in response to the increased demand of insulin caused by combined maternal and post-weaning HF diet. Indeed, this hypothesis was further supported by β-cell hypertrophy in HF offspring. The β-cell damage might be attributed to various mechanisms such as oxidative stress and endoplasmic reticulum (ER) stress [275, 276]. Interestingly, H9N offspring, which also underwent post-weaning HF diet, completely prevents islet enlargement. Overall, this suggests that early pre-gestational maternal diet transition can prevent adverse *in utero*

reprogramming caused by maternal HF diet which leads to abnormal islet β-cell proliferation in offspring induced by post-weaning HF diet.

In our study, HF male offspring, but not H9N, displayed increased islet mass alongside decreased Ins+ β-cell density. This observed islet remodeling is likely due to β-cell de-granulation. Previous studies have demonstrated that β-cell dysfunction in type 2 diabetes may be associated with alterations in β-cell phenotype through de-differentiation or de-granulation, wherein the β-cell loses insulin expression and gains expressions of various embryonic progenitor markers [260, 277-279]. In our report, we showed that both NF and HF, but not H9N, offspring had more β-cell de-granulation evidenced by an increase in Glut2+Ins- cells in the islet. This suggests a new mechanism behind β-cell de-granulation that leads to β-cell failure induced by post-weaning HF diet. The number of de-granulated β-cells of HF offspring was not different from NF offspring suggesting an absence of synergistic effects of maternal and post-weaning HF diets. However, we could not rule out the possibility that maternal diet pre-disposed the β-cells to these cellular events. A supporting evidence was that β-cell de-granulation was avoided in offspring of maternal diet transition (H9N group). Further investigation on the effect of maternal HF diet on the gain of islet progenitor features, such as Neurogenin 3 expression (i.e., Ngn3) and Nanog transcription factor production [277], will provide insight to this important question.

In summary, our study discovered that maternal HF diet can modify the phenotype and function of offspring β-cell via cell hypertrophy, proliferation defects, and de-granulation. Maternal and post-weaning HF diets synergistically prompt offspring

insulin resistance, whereas maternal H9N transition avoids this effect. Our study provides evidence that pre-conception maternal diet transition from HF to NF is effective in preventing the adverse metabolic “fetal-programming” seen among maternal HF offspring. This study proves that pre-conceptional maternal dietary intervention is effective in preventing transgenerational insulin resistance and normalizing the β-cell proliferation and function. Human studies that aim to seek effective nutritional prevention strategies should be carefully designed and investigated in the near future.

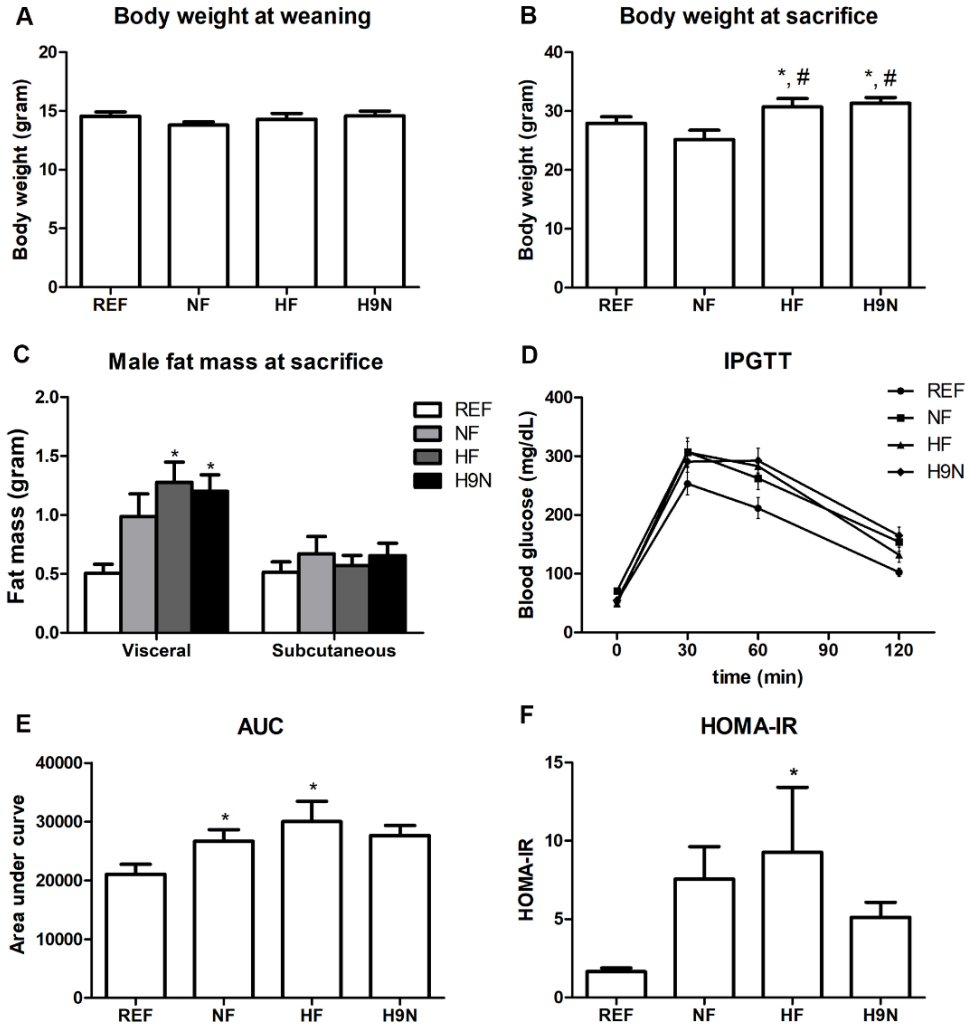


Figure 18. Maternal H9N diet avoided the development of insulins resistance in maternal HF diet offspring fed a post-weaning HF diet.

A. Body weight of male offspring at the time of weaning.

B. Body weight of male offspring before sacrifice.

C. Visceral and subcutaneous fat mass of male offspring before sacrifice.

D. Male offspring IPGTT results after 12 weeks of HF diet.

E. Area under curve (AUC) of IPGTT results from four groups. NF and HF offspring showed glucose intolerance while H9N offspring did not.

F. Homeostasis model assessment (HOMA) results after 12 weeks of HF diet. HF offspring had significantly higher scores compared to REF offspring.

Data are reported as Mean±SEM, n=5-7. * indicates significance level of $P<0.05$ against REF. # indicates significance level of $P<0.05$ against NF.

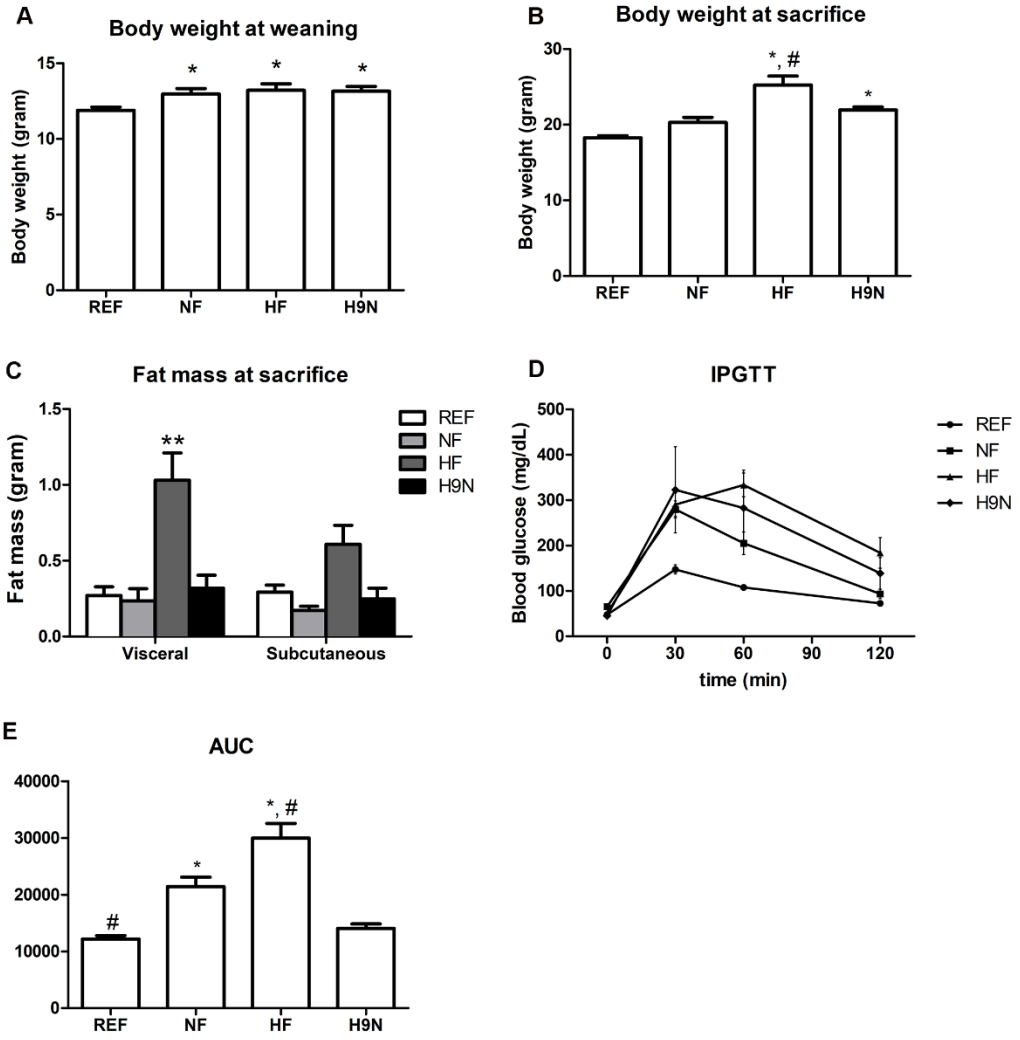


Figure 19. Maternal H9N diet avoided the development of insulins resistance in maternal HF diet offspring fed a post-weaning HF diet.

A. Body weight of female offspring at the time of weaning.

B. Body weight of female offspring before sacrifice.

C. Visceral and subcutaneous fat mass of female offspring before sacrifice.

D. Female offspring IPGTT results after 12 weeks of HF diet.

E. Area under curve (AUC) of IPGTT results from four groups. NF and HF offspring showed glucose intolerance while H9N offspring did not.

Data are reported as Mean±SEM, n=5-7. * indicates significance level of $P<0.05$ against REF. # indicates significance level of $P<0.05$ against NF.

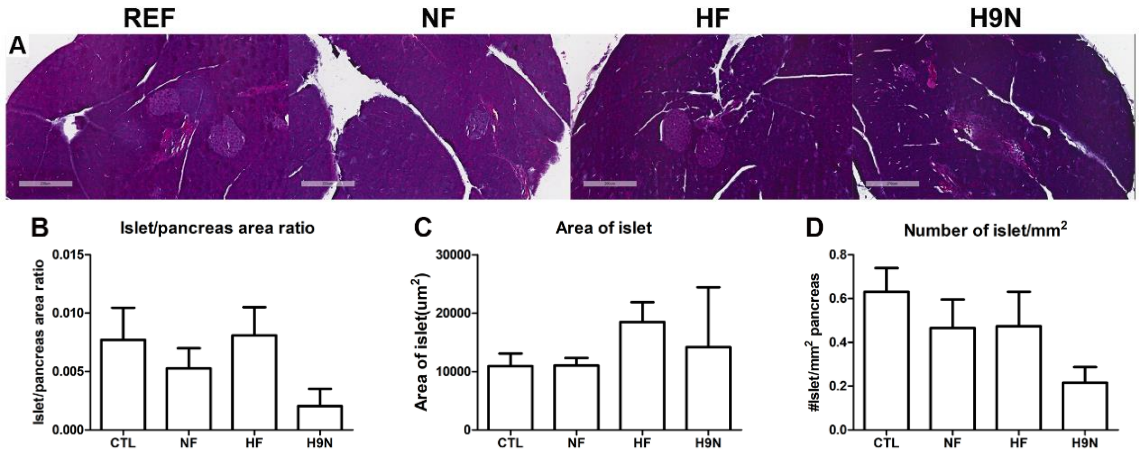


Figure 20. There were no changes of islet number and area of the female offspring among four groups.

A. H&E staining of pancreas tissue from female offspring.

B. Islet area/pancreas area ratio of four groups.

C. Average area of islets of four groups.

D. Number of islets in every $1mm^2$ of pancreas from four groups.

Data are reported as Mean±SEM, n=4-5. * indicates significance level of $P<0.05$ against REF. # indicates significance level of $P<0.05$ against NF.

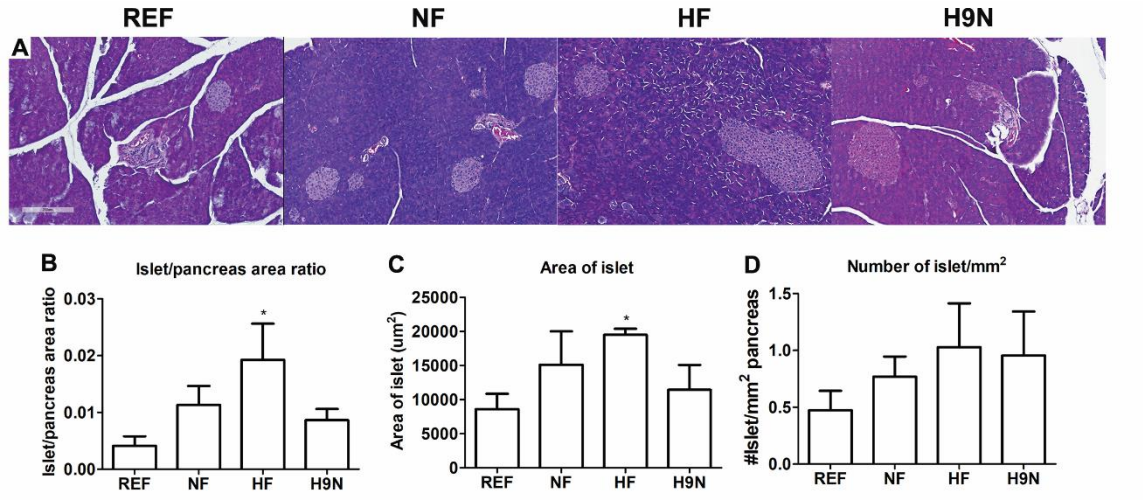


Figure 21. HF offspring, but not NF or H9N offspring, showed enlarged islets area in male offspring.

A. H&E staining of pancreas tissue from male offspring.

B. Islet area/pancreas area ratio of four groups. Only HF offspring had increased area of islet per pancreas compared to REF offspring.

C. Average area of islets of four groups. Only HF offspring showed a significantly larger area of islet, while H9N offspring had a similar islet area compared to REF group.

D. Number of islets in every $1mm^2$ of pancreas from four groups.

Data are reported as Mean±SEM, n=4-5. * indicates significance level of $P<0.05$ against REF. # indicates significance level of $P<0.05$ against NF.

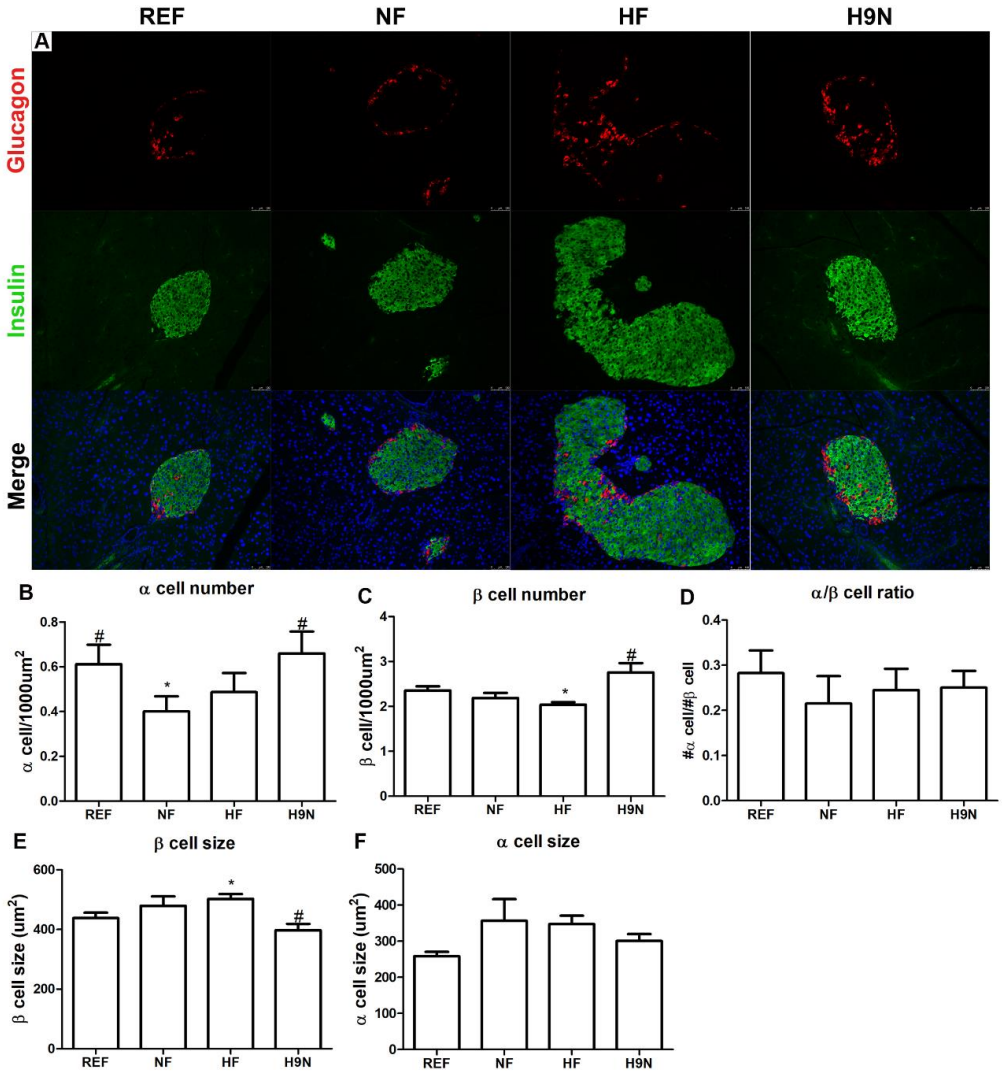


Figure 22. HF offspring, but not H9N offspring, showed a decrease in insulin positive β-cell number in islets.

A. Insulin (green) and Glucagon (red) immunofluorescence staining of pancreas tissue from male offspring.

B. Gcg+ α cell number was counted in every 1000μm$^2$ islet area. The number of Gcg+ α cells of the NF offspring significantly decreased compared to the REF group.

C. Ins+ β-cell number was counted in every 1000μm$^2$ islet area. Ins+ β-cells in the HF offspring significantly decreased compared to the REF group.

D. The ratio of the number of Ins+ β-cells to the number of Gcg+ α cells.

E. The average size of individual Ins+ β-cell. The HF offspring showed a significantly enlarged β-cell size compared to the REF offspring.

F. The average size of individual Gcg+ α cell.

* indicates significance level of $P<0.05$ against REF. # indicates significance level of $P<0.05$ against NF.

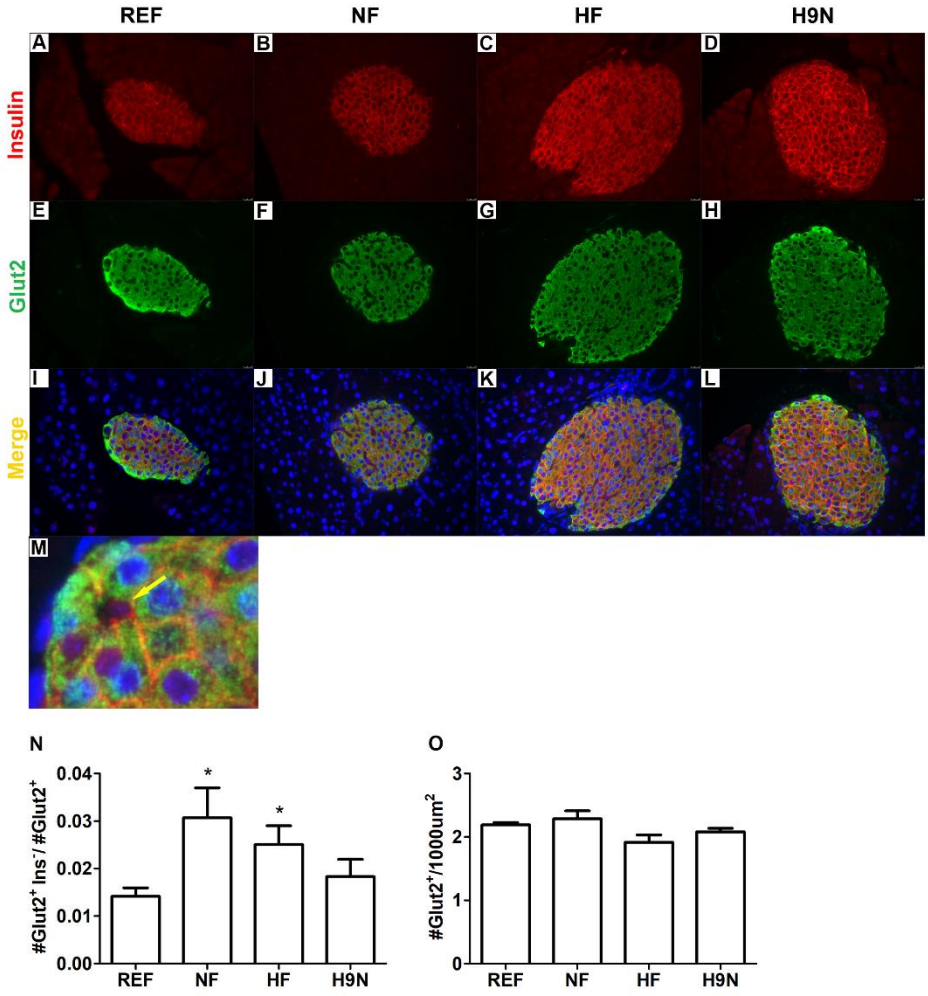


Figure 23. Maternal H9N diet avoided Ins+ β-cell degranulation in maternal HF-diet offspring fed a post-weaning HF diet.

A-L. Insulin (red) and Glut2 (green) immunofluorescence staining of pancreas tissue from male offspring.

M. A typical degranulated β-cell marked by Glut2 positive but insulin negative was indicated by yellow arrow.

N. The number of Glut2+cells per 1000 $\mu m^2$ of islet.

O. The number of Glut2+Ins- cells per 100 randomly picked Glut2+ cells.

Data are reported as Mean±SEM, n=4-5. * indicates significance level of $P<0.05$ against REF. # indicates significance level of $P<0.05$ against NF.

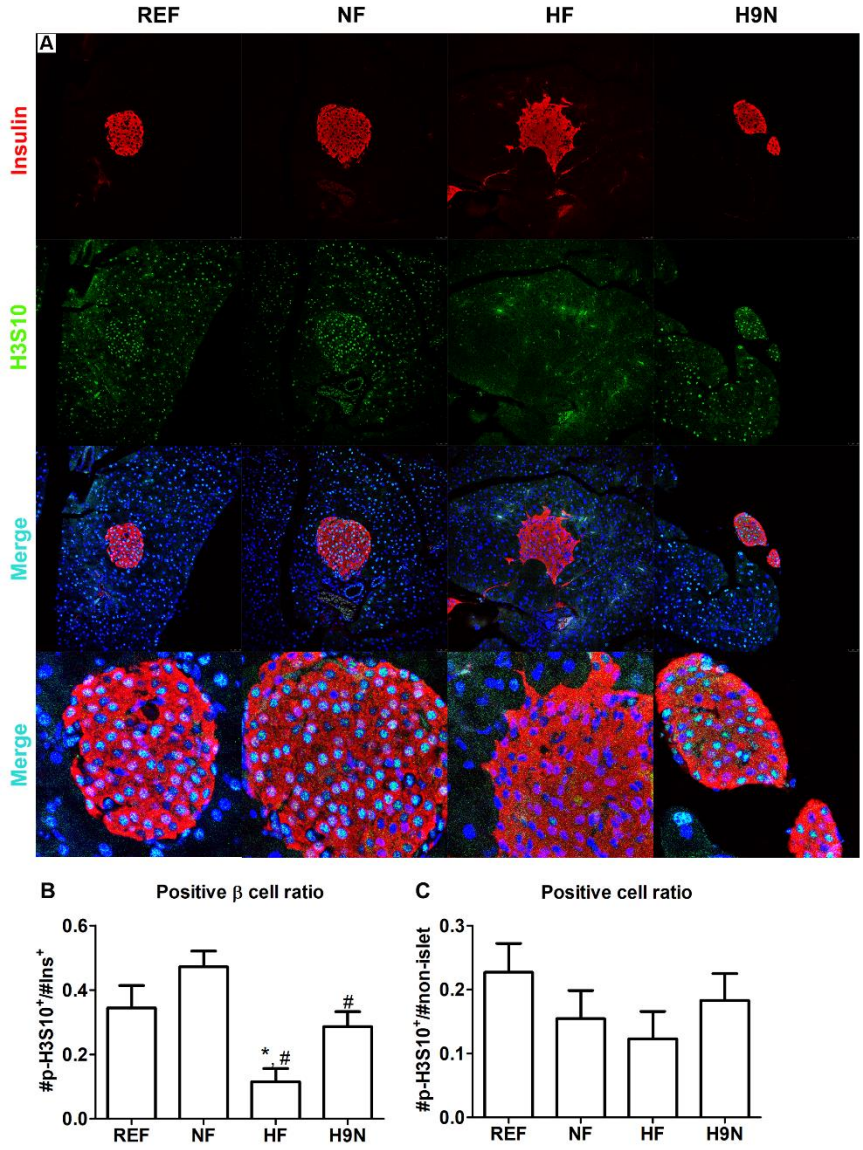


Figure 24. Maternal H9N diet avoided islet cell proliferation defects and deactivation of AKT signaling in maternal HF-diet offspring fed a post-weaning HF diet.

A. Insulin (red) and pH3S10 (green) immunofluorescence staining of pancreas tissue from male offspring.

B. The ratio of the H3S10+ cells to the Ins+ β-cells in islet.

C. The ratio of the number of H3S10+ cells to every 500 randomly selected non-islet cells.

Data are reported as Mean±SEM, n=4-7. * indicates significance level of $P<0.05$ against REF. # indicates significance level of $P<0.05$ against NF.

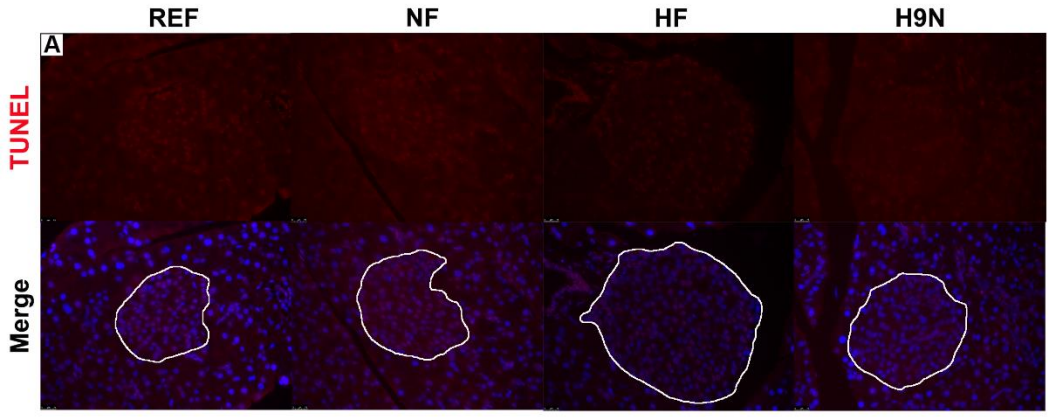


Figure 25. HF and H9N group showed no effects on pancreatic cell apoptosis in male offspring.

A. TUNEL staining of pancreas tissue. n=4-5. White lines indicate the islet areas.

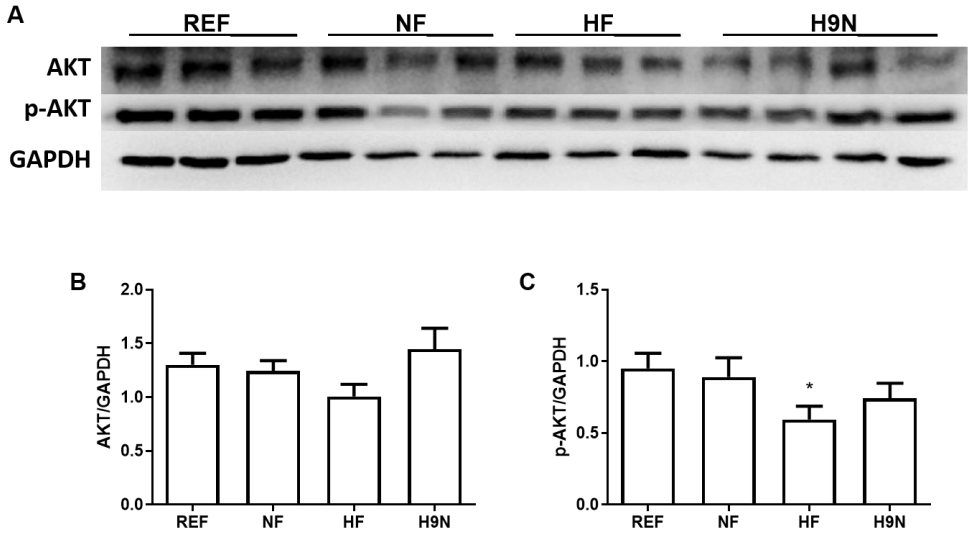


Figure 26. Maternal H9N diet avoided AKT signaling deactivation induced in HF groups.

A. Pancreatic AKT and p-AKT473 expression detection by Western Blot.

B. Relative AKT expression against GAPDH expressed as the ratio AKT/GAPDH.

C. Relative p-AKT473 expression expressed as the ratio p-AKT473/GAPDH.

Data are reported as Mean±SEM, n=4-7. * indicates significance level of $P<0.05$ against REF.

Table 5. Study Design

| | Maternal Diet | | | Offspring Diet |
|---|---|---|---|---|
| | Pre-pregnancy | Transition | Pregnancy/Lactation | After Weaning |
| REF | CD | - | CD | CD |
| NF | NF | - | NF | HF |
| HF | HF | - | HF | HF |
| H9N | HF | NF (9 weeks) | NF | HF |

*Diet description:
REF Rodent diet: normal chow diet (4% kcal. from fat)
NF Rodent diet: 10% kcal from fat.
HF Rodent diet: 60% kcal from fat.

Table 6. Nutrition content

| | NF Rodent diet (10% fat) | HF Rodent diet (60% fat) |
|---|---|---|
| Protein | 203 g | 203 g |
| Carbohydrate (from corn starch) | 506.2 g | 0 g |
| Carbohydrate | 125 g | 125 g |
| Carbohydrate (from sucrose) | 72.8 g | 72.8 g |
| Fiber | 50 g | 50 g |
| Fat (from soybean oil) | 25 g | 245 g |
| Fat (from lard) | 20 g | 25 g |
| Mineral | 50 g | 50 g |
| Vitamin | 3 g | 3 g |

REFERENCES

1. Connor, K.L., et al., *Maternal metabolic, immune, and microbial systems in late pregnancy vary with malnutrition in mice.* Biol Reprod, 2018. **98**(4): p. 579-592.

2. Mallmann, A.L., et al., *Maternal nutrition during early and late gestation in gilts and sows under commercial conditions: impacts on maternal growth and litter traits1.* J Anim Sci, 2019. **97**(12): p. 4957-4964.

3. Basu, M., et al., *Epigenetic mechanisms underlying maternal diabetes-associated risk of congenital heart disease.* JCI Insight, 2017. **2**(20).

4. Gohir, W., et al., *High-fat diet intake modulates maternal intestinal adaptations to pregnancy and results in placental hypoxia, as well as altered fetal gut barrier proteins and immune markers.* J Physiol, 2019. **597**(12): p. 3029-3051.

5. Xie, R., et al., *Maternal High Fat Diet Alters Gut Microbiota of Offspring and Exacerbates DSS-Induced Colitis in Adulthood.* Front Immunol, 2018. **9**: p. 2608.

6. Clapp, J.F., 3rd, *Maternal carbohydrate intake and pregnancy outcome.* Proc Nutr Soc, 2002. **61**(1): p. 45-50.

7. *Reprint: 2013 AHA/ACC Guideline on Lifestyle Management to Reduce Cardiovascular Risk.* J Am Pharm Assoc (2003), 2014. **54**(1): p. e2.

8. Chen, Y.Q., et al., *Dietary fat-gene interactions in cancer.* Cancer Metastasis Rev, 2007. **26**(3-4): p. 535-51.

9. Elias, S.L. and S.M. Innis, *Infant plasma trans, n-6, and n-3 fatty acids and conjugated linoleic acids are related to maternal plasma fatty acids, length of gestation, and birth weight and length.* Am J Clin Nutr, 2001. **73**(4): p. 807-14.

10. Stephens, T.V., et al., *Protein requirements of healthy pregnant women during early and late gestation are higher than current recommendations.* J Nutr, 2015. **145**(1): p. 73-8.

11. Butte, N.F. and J.C. King, *Energy requirements during pregnancy and lactation.* Public Health Nutr, 2005. **8**(7a): p. 1010-27.

12. Kunz, L.H. and J.C. King, *Impact of maternal nutrition and metabolism on health of the offspring.* Semin Fetal Neonatal Med, 2007. **12**(1): p. 71-7.

13. Reveiz, L., et al., *Treatments for iron-deficiency anaemia in pregnancy.* Cochrane Database Syst Rev, 2011(10): p. Cd003094.

14. Mishra, V., et al., *Effect of iron supplementation during pregnancy on birthweight: evidence from Zimbabwe.* Food Nutr Bull, 2005. **26**(4): p. 338-47.

15. Smithells, R.W., S. Sheppard, and C.J. Schorah, *Vitamin deficiencies and neural tube defects.* Arch Dis Child, 1976. **51**(12): p. 944-50.

16. Kanter, R. and B. Caballero, *Global gender disparities in obesity: a review*. Advances in nutrition (Bethesda, Md.), 2012. **3**(4): p. 491-498.

17. Branum, A., S. Kirmeyer, and E. Gregory, *Prepregnancy body mass index by maternal characteristics and state: data from the birth certificate, 2014.* National vital statistics reports: from the Centers for Disease Control and Prevention, National Center for Health Statistics, National Vital Statistics System, 2016. **65**(6): p. 1-11.

18. Tschöp, M. and M.L. Heiman, *Rodent obesity models: an overview.* Experimental and Clinical Endocrinology & Diabetes, 2001. **109**(06): p. 307-319.

19. Kothari, V., et al., *High fat diet induces brain insulin resistance and cognitive impairment in mice.* Biochim Biophys Acta Mol Basis Dis, 2017. **1863**(2): p. 499-508.

20. Kang, C., et al., *Gut Microbiota Mediates the Protective Effects of Dietary Capsaicin against Chronic Low-Grade Inflammation and Associated Obesity Induced by High-Fat Diet.* mBio, 2017. **8**(3).

21. Napoli, C., et al., *Maternal hypercholesterolemia during pregnancy promotes early atherogenesis in LDL receptor-deficient mice and alters aortic gene expression determined by microarray.* Circulation, 2002. **105**(11): p. 1360-1367.

22. Zheng, J., et al., *Maternal high-fat diet regulates glucose metabolism and pancreatic β cell phenotype in mouse offspring at weaning.* PeerJ, 2020. **8**: p. e9407.

23. Cordner, Z.A., et al., *Maternal high-fat diet results in cognitive impairment and hippocampal gene expression changes in rat offspring.* Exp Neurol, 2019. **318**: p. 92-100.

24. Cho, N.H., et al., *IDF Diabetes Atlas: Global estimates of diabetes prevalence for 2017 and projections for 2045.* Diabetes Research and Clinical Practice, 2018. **138**: p. 271-281.

25. Weissgerber, T.L. and L.M. Mudd, *Preeclampsia and diabetes.* Curr Diab Rep, 2015. **15**(3): p. 9.

26. Liu, B., et al., *History of spontaneous miscarriage and the risk of diabetes mellitus among middle-aged and older Chinese women.* Acta Diabetol, 2018. **55**(6): p. 579-584.

27. Correa, A., *Pregestational Diabetes Mellitus and Congenital Heart Defects.* Circulation, 2016. **133**(23): p. 2219-21.

28. Billionnet, C., et al., *Gestational diabetes and adverse perinatal outcomes from 716,152 births in France in 2012.* Diabetologia, 2017. **60**(4): p. 636-644.

29. Nezu, M., et al., *Nrf2 inactivation enhances placental angiogenesis in a preeclampsia mouse model and improves maternal and fetal outcomes.* Science Signaling, 2017. **10**(479): p. eaam5711.

30. Bardin, N., P. Murthi, and N. Alfaidy, *Normal and pathological placental angiogenesis.* Biomed Res Int, 2015. **2015**: p. 354359.

31. Edu, A., et al., *Placenta changes in pregnancy with gestational diabetes.* Rom J Morphol Embryol, 2016. **57**(2): p. 507-12.

32. Gauster, M., et al., *The placenta and gestational diabetes mellitus.* Curr Diab Rep, 2012. **12**(1): p. 16-23.

33. Ornoy, A., et al., *Effect of maternal diabetes on the embryo, fetus, and children: congenital anomalies, genetic and epigenetic changes and developmental outcomes.* Birth Defects Res C Embryo Today, 2015. **105**(1): p. 53-72.

34. Basu, M. and V. Garg, *Maternal hyperglycemia and fetal cardiac development: Clinical impact and underlying mechanisms.* Birth Defects Res, 2018. **110**(20): p. 1504-1516.

35. Ornoy, A., S.B. Rand, and N. Bischitz, *Hyperglycemia and hypoxia are interrelated in their teratogenic mechanism: studies on cultured rat embryos.* Birth Defects Res B Dev Reprod Toxicol, 2010. **89**(2): p. 106-15.

36. Bell, R., et al., *Peri-conception hyperglycaemia and nephropathy are associated with risk of congenital anomaly in women with pre-existing diabetes: a population-based cohort study.* Diabetologia, 2012.

37. Eriksson, U.J., J. Cederberg, and P. Wentzel, *Congenital malformations in offspring of diabetic mothers--animal and human studies.* Rev Endocr Metab Disord, 2003. **4**(1): p. 79-93.

38. Gilboa, S.M., et al., *Mortality resulting from congenital heart disease among children and adults in the United States, 1999 to 2006.* (1524-4539 (Electronic)).

39. Yang, Q., et al., *Racial differences in infant mortality attributable to birth defects in the United States, 1989-2002.* Birth Defects Res A Clin Mol Teratol, 2006. **76**(10): p. 706-13.

40. Sharpe, P.B., et al., *Maternal diabetes and congenital anomalies in South Australia 1986-2000: a population-based cohort study.* (1542-0752 (Print)).

41. Loffredo, C.A., P.D. Wilson, and C. Ferencz, *Maternal diabetes: an independent risk factor for major cardiovascular malformations with increased mortality of affected infants.* Teratology, 2001. **64**(2): p. 98-106.

42. Liu, S., et al., *Association between maternal chronic conditions and congenital heart defects: a population-based cohort study.* Circulation, 2013. **128**(6): p. 583-9.

43. Macintosh, M.C., et al., *Perinatal mortality and congenital anomalies in babies of women with type 1 or type 2 diabetes in England, Wales, and Northern Ireland: population based study.* Bmj, 2006. **333**(7560): p. 177.

44. Reece, E.A., C.J. Homko, and Y.K. Wu, *Multifactorial basis of the syndrome of diabetic embryopathy.* Teratology, 1996. **54**(4): p. 171-82.

45. Inkster, M.E., et al., *Poor glycated haemoglobin control and adverse pregnancy outcomes in type 1 and type 2 diabetes mellitus: systematic review of observational studies.* BMC Pregnancy Childbirth, 2006. **6**: p. 30.

46. Saiyin, T., et al., *Maternal voluntary exercise mitigates oxidative stress and incidence of congenital heart defects in pre-gestational diabetes.* Journal of cellular and molecular medicine, 2019. **23**(8): p. 5553-5565.

47. Starikov, R., et al., *Hemoglobin A1c in pregestational diabetic gravidas and the risk of congenital heart disease in the fetus.* Pediatr Cardiol, 2013. **34**(7): p. 1716-22.

48. Canfield, M.A., et al., *National estimates and race/ethnic-specific variation of selected birth defects in the United States, 1999–2001.* Birth Defects Research Part A: Clinical and Molecular Teratology, 2006. **76**(11): p. 747-756.

49. Ermito, S., et al., *Prenatal diagnosis of limb abnormalities: role of fetal ultrasonography.* J Prenat Med, 2009. **3**(2): p. 18-22.

50. Shi, Y., et al., *Prenatal limb defects: Epidemiologic characteristics and an epidemiologic analysis of risk factors.* Medicine, 2018. **97**(29): p. e11471-e11471.

51. Frías, J.L., et al., *Infrequently studied congenital anomalies as clues to the diagnosis of maternal diabetes mellitus.* Am J Med Genet A, 2007. **143a**(24): p. 2904-9.

52. Allen, V.M. and B.A. Armson, *Teratogenicity associated with pre-existing and gestational diabetes.* J Obstet Gynaecol Can, 2007. **29**(11): p. 927-934.

53. Mai, C.T., et al., *National population-based estimates for major birth defects, 2010–2014.* Birth Defects Research, 2019. **111**(18): p. 1420-1435.

54. Becerra, J.E., et al., *Diabetes mellitus during pregnancy and the risks for specific birth defects: a population-based case-control study.* Pediatrics, 1990. **85**(1): p. 1-9.

55. Hendricks, K.A., et al., *Effects of hyperinsulinemia and obesity on risk of neural tube defects among Mexican Americans.* Epidemiology, 2001. **12**(6): p. 630-5.

56. Shaw, G.M., et al., *Neural tube defects associated with maternal periconceptional dietary intake of simple sugars and glycemic index.* Am J Clin Nutr, 2003. **78**(5): p. 972-8.

57. Yazdy, M.M., et al., *Maternal dietary glycaemic intake during pregnancy and the risk of birth defects.* Paediatr Perinat Epidemiol, 2011. **25**(4): p. 340-6.

58. Yu, J., Y. Wu, and P. Yang, *High glucose-induced oxidative stress represses sirtuin deacetylase expression and increases histone acetylation leading to neural tube defects.* J Neurochem, 2016. **137**(3): p. 371-83.

59. *<2003 Different diabetogenic response to moderate doses of streptozotocin in pregnant rats, and its long-term consequences in the offspring.pdf>*.

60. Wu, Y., et al., *Type 2 diabetes mellitus induces congenital heart defects in murine embryos by increasing oxidative stress, endoplasmic reticulum stress, and apoptosis.* Am J Obstet Gynecol, 2016. **215**(3): p. 366 e1-366 e10.

61. Scott-Drechsel, D.E., et al., *Hyperglycemia slows embryonic growth and suppresses cell cycle via cyclin D1 and p21.* Diabetes, 2013. **62**(1): p. 234-42.

62. Illsley, N.P. and M.U. Baumann, *Human placental glucose transport in fetoplacental growth and metabolism.* Biochim Biophys Acta Mol Basis Dis, 2020. **1866**(2): p. 165359.

63. Costa, M.A., *The endocrine function of human placenta: an overview.* Reprod Biomed Online, 2016. **32**(1): p. 14-43.

64. Watson, E.D. and J.C. Cross, *Development of structures and transport functions in the mouse placenta.* Physiology (Bethesda), 2005. **20**: p. 180-93.

65. Brosens, I., et al., *The "Great Obstetrical Syndromes" are associated with disorders of deep placentation.* Am J Obstet Gynecol, 2011. **204**(3): p. 193-201.

66. Knöfler, M., et al., *Human placenta and trophoblast development: key molecular mechanisms and model systems.* Cell Mol Life Sci, 2019. **76**(18): p. 3479-3496.

67. Gude, N.M., et al., *Growth and function of the normal human placenta.* Thromb Res, 2004. **114**(5-6): p. 397-407.

68. Challier, J.C., C. Vervelle, and S. Uzan, *Ontogenesis of villi and fetal vessels in the human placenta.* Fetal Diagn Ther, 2001. **16**(4): p. 218-26.

69. Chaddha, V., et al., *Developmental biology of the placenta and the origins of placental insufficiency.* Semin Fetal Neonatal Med, 2004. **9**(5): p. 357-69.

70. Rossant, J. and J.C. Cross, *Placental development: lessons from mouse mutants.* Nat Rev Genet, 2001. **2**(7): p. 538-48.

71. Coan, P.M., A.C. Ferguson-Smith, and G.J. Burton, *Ultrastructural changes in the interhaemal membrane and junctional zone of the murine chorioallantoic placenta across gestation.* Journal of Anatomy, 2005. **207**(6): p. 783-796.

72. Lescisin, K.R., S. Varmuza, and J. Rossant, *Isolation and characterization of a novel trophoblast-specific cDNA in the mouse.* Genes and Development, 1988. **2**: p. 1639-1646.

73. Simmons, D.G., et al., *Spatial and temporal expression of the 23 murine Prolactin/Placental Lactogen-related genes is not associated with their position in the locus.* BMC Genomics, 2008. **9**: p. 352.

74. Aykroyd, B.R.L., S.J. Tunster, and A.N. Sferruzzi-Perri, *Igf2 deletion alters mouse placenta endocrine capacity in a sexually dimorphic manner.* J Endocrinol, 2020. **246**(1): p. 93-108.

75. Coan, P.M., et al., *Origin and characteristics of glycogen cells in the developing murine placenta.* Dev Dyn, 2006. **235**(12): p. 3280-94.

76. McLellan, A.S., et al., *Structure and evolution of the mouse pregnancy-specific glycoprotein (Psg) gene locus.* BMC Genomics, 2005. **6**: p. 4.

77. Dyer, L.A., et al., *BMP signaling modulates hedgehog-induced secondary heart field proliferation.* Dev Biol, 2010. **348**(2): p. 167-76.

78. Hemberger, M., *IFPA award in placentology lecture–characteristics and significance of trophoblast giant cells.* Placenta, 2008. **29**: p. 4-9.

79. Erlebacher, A., *Immunology of the maternal-fetal interface.* Annu Rev Immunol, 2013. **31**: p. 387-411.

80. Ramathal, C.Y., et al., *Endometrial decidualization: of mice and men.* Semin Reprod Med, 2010. **28**(1): p. 17-26.

81. Grigsby, P.L., *Animal Models to Study Placental Development and Function throughout Normal and Dysfunctional Human Pregnancy.* Semin Reprod Med, 2016. **34**(1): p. 11-6.

82. Orendi, K., et al., *Placental and trophoblastic in vitro models to study preventive and therapeutic agents for preeclampsia.* Placenta, 2011. **32 Suppl**: p. S49-54.

83. Hannan, N.J., et al., *Models for study of human embryo implantation: choice of cell lines?* Biol Reprod, 2010. **82**(2): p. 235-45.

84. Handwerger, S., et al., *Development of the sheep as an animal model to study placental lactogen physiology.* J Pediatr, 1975. **87**(6 Pt 2): p. 1139-43.

85. Berezowsky, J., et al., *DNA ploidy of hydatidiform moles and nonmolar conceptuses: a study using flow and tissue section image cytometry.* Mod Pathol, 1995. **8**(7): p. 775-81.

86. Harrison, S.E., et al., *Assembly of embryonic and extraembryonic stem cells to mimic embryogenesis in vitro.* Science, 2017. **356**(6334).

87. Anson-Cartwright, L., et al., *The glial cells missing-1 protein is essential for branching morphogenesis in the chorioallantoic placenta.* Nat Genet, 2000. **25**(3): p. 311-4.

88. Lu, J., et al., *A positive feedback loop involving Gcm1 and Fzd5 directs chorionic branching morphogenesis in the placenta.* PLoS biology, 2013. **11**(4): p. e1001536-e1001536.

89. Outhwaite, J.E., V. McGuire, and D.G. Simmons, *Genetic ablation of placental sinusoidal trophoblast giant cells causes fetal growth restriction and embryonic lethality.* Placenta, 2015. **36**(8): p. 951-955.

90. Simmons, D.G., et al., *Spatial and temporal expression of the 23 murine Prolactin/Placental Lactogen-related genes is not associated with their position in the locus.* BMC Genomics, 2008. **9**(1): p. 352.

91. Goolam, M., et al., *The transcriptional repressor Blimp1/PRDM1 regulates the maternal decidual response in mice.* Nature Communications, 2020. **11**(1): p. 12.

92. Tanaka, M., et al., *Mash2 Acts Cell Autonomously in Mouse Spongiotrophoblast Development.* Developmental Biology, 1997. **190**(1): p. 55-65.

93. Scott, I.C., et al., *The HAND1 basic helix-loop-helix transcription factor regulates trophoblast differentiation via multiple mechanisms.* Mol Cell Biol, 2000. **20**(2): p. 530-41.

94. Ma, G.T., et al., *Nodal Regulates Trophoblast Differentiation and Placental Development.* Developmental Biology, 2001. **236**(1): p. 124-135.

95. Papadaki, C., et al., *Transcriptional Repressor Erf Determines Extraembryonic Ectoderm Differentiation.* Molecular and Cellular Biology, 2007. **27**(14): p. 5201.

96. Simmons, D.G. and J.C. Cross, *Determinants of trophoblast lineage and cell subtype specification in the mouse placenta.* Developmental Biology, 2005. **284**(1): p. 12-24.

97. Salamonsen, L.A., et al., *Complex Regulation of Decidualization: A Role for Cytokines and Proteases—A Review.* Placenta, 2003. **24**: p. S76-S85.

98. Dimitriadis, E., et al., *Cytokines, chemokines and growth factors in endometrium related to implantation.* Human reproduction update, 2005. **11**(6): p. 613-630.

99. Adamson, S.L., et al., *Interactions between trophoblast cells and the maternal and fetal circulation in the mouse placenta.* Developmental biology, 2002. **250**(2): p. 358-373.

100. Harris, L., *Review: trophoblast-vascular cell interactions in early pregnancy: how to remodel a vessel. Placenta 31 (Supplement) S93–S98*. 2010.

101. Robson, A., et al., *Uterine natural killer cells initiate spiral artery remodeling in human pregnancy.* The FASEB Journal, 2012. **26**(12): p. 4876-4885.

102. Carmeliet, P., et al., *Abnormal blood vessel development and lethality in embryos lacking a single VEGF allele.* Nature, 1996. **380**(6573): p. 435-9.

103. Shalaby, F., et al., *Failure of blood-island formation and vasculogenesis in Flk-1-deficient mice.* Nature, 1995. **376**(6535): p. 62-6.

104. Forsythe, J.A., et al., *Activation of vascular endothelial growth factor gene transcription by hypoxia-inducible factor 1.* Mol Cell Biol, 1996. **16**(9): p. 4604-13.

105. Barros, L.F., et al., *Quantitation and immunolocalization of glucose transporters in the human placenta.* Placenta, 1995. **16**(7): p. 623-33.

106. Ericsson, A., et al., *Glucose transporter isoform 4 is expressed in the syncytiotrophoblast of first trimester human placenta.* Hum Reprod, 2005. **20**(2): p. 521-30.

107. Jansson, T., M. Wennergren, and T.L. Powell, *Placental glucose transport and GLUT 1 expression in insulin-dependent diabetes.* American Journal of Obstetrics and Gynecology, 1999. **180**(1): p. 163-168.

108. Hauguel-de Mouzon, S. and E. Shafrir, *Carbohydrate and fat metabolism and related hormonal regulation in normal and diabetic placenta.* Placenta, 2001. **22**(7): p. 619-27.

109. Dilworth, M.R. and C.P. Sibley, *Review: Transport across the placenta of mice and women.* Placenta, 2013. **34 Suppl**: p. S34-9.

110. Jansson, T. and T.L. Powell, *Role of placental nutrient sensing in developmental programming.* Clin Obstet Gynecol, 2013. **56**(3): p. 591-601.

111. Herrera, E. and G. Desoye, *Maternal and fetal lipid metabolism under normal and gestational diabetic conditions.* Horm Mol Biol Clin Investig, 2016. **26**(2): p. 109-27.

112. Desforges, M., et al., *The SNAT4 isoform of the system A amino acid transporter is functional in human placental microvillous plasma membrane.* The Journal of physiology, 2009. **587**(1): p. 61-72.

113. Cleal, J., et al., *Facilitated transporters mediate net efflux of amino acids to the fetus across the basal membrane of the placental syncytiotrophoblast.* The Journal of physiology, 2011. **589**(4): p. 987-997.

114. Jansson, T., et al., *Alterations in the activity of placental amino acid transporters in pregnancies complicated by diabetes.* Diabetes, 2002. **51**(7): p. 2214-2219.

115. Jansson, N., et al., *Activation of placental mTOR signaling and amino acid transporters in obese women giving birth to large babies.* The Journal of Clinical Endocrinology & Metabolism, 2013. **98**(1): p. 105-113.

116. Gude, N.M., et al., *Growth and function of the normal human placenta.* Thrombosis Research, 2004. **114**(5): p. 397-407.

117. Desoye, G. and S. Hauguel-de Mouzon, *The human placenta in gestational diabetes mellitus. The insulin and cytokine network.* Diabetes Care, 2007. **30 Suppl 2**: p. S120-6.

118. Soares, M.J., K. Iqbal, and K. Kozai, *Hypoxia and Placental Development.* Birth Defects Res, 2017. **109**(17): p. 1309-1329.

119. Sato, Y., *Endovascular trophoblast and spiral artery remodeling.* Mol Cell Endocrinol, 2020. **503**: p. 110699.

120. Tessier, D.R., J. Yockell-Lelièvre, and A. Gruslin, *Uterine Spiral Artery Remodeling: The Role of Uterine Natural Killer Cells and Extravillous Trophoblasts in Normal and High-Risk Human Pregnancies.* Am J Reprod Immunol, 2015. **74**(1): p. 1-11.

121. Reuter, S., et al., *Oxidative stress, inflammation, and cancer: how are they linked?* Free Radic Biol Med, 2010. **49**(11): p. 1603-16.

122. Samimi, M., et al., *The role of inflammation, oxidative stress, angiogenesis, and apoptosis in the pathophysiology of endometriosis: Basic science and new insights based on gene expression.* J Cell Physiol, 2019. **234**(11): p. 19384-19392.

123. Atègbo, J.M., et al., *Modulation of Adipokines and Cytokines in Gestational Diabetes and Macrosomia.* The Journal of Clinical Endocrinology & Metabolism, 2006. **91**(10): p. 4137-4143.

124. Chang, S.-C. and W.-C. Vivian Yang, *Hyperglycemia induces altered expressions of angiogenesis associated molecules in the trophoblast.* Evidence-Based Complementary and Alternative Medicine, 2013. **2013**.

125. Hellwig-bürgel, T., *Interleukin-1 β and Tumor Necrosis Factor-? Stimulate DNA Binding of Hypoxia-Inducible Factor-1.* Blood, 2013. **92**: p. 1561-1567.

126. Lea, R., et al., *Placental leptin in normal, diabetic and fetal growth-retarded pregnancies.* Molecular human reproduction, 2000. **6**(8): p. 763-769.

127. Fasshauer, M., et al., *Hormonal regulation of adiponectin gene expression in 3T3-L1 adipocytes.* Biochemical and biophysical research communications, 2002. **290**(3): p. 1084-1089.

128. Hiden, U., et al., *Fetal insulin and IGF-II contribute to gestational diabetes mellitus (GDM)-associated up-regulation of membrane-type matrix metalloproteinase 1 (MT1-MMP) in the human feto-placental endothelium.* The Journal of Clinical Endocrinology & Metabolism, 2012. **97**(10): p. 3613-3621.

129. Eijkelenboom, A. and B.M. Burgering, *FOXOs: signalling integrators for homeostasis maintenance.* Nature reviews Molecular cell biology, 2013. **14**(2): p. 83-97.

130. Lee, S. and H.H. Dong, *FoxO integration of insulin signaling with glucose and lipid metabolism.* The Journal of endocrinology, 2017. **233**(2): p. R67.

131. Kousteni, S., *FoxO1: a molecule for all seasons.* J Bone Miner Res, 2011. **26**(5): p. 912-7.

132. Edgerton, D.S., K.M. Johnson, and A.D. Cherrington, *Current strategies for the inhibition of hepatic glucose production in type 2 diabetes.* Front Biosci (Landmark Ed), 2009. **14**: p. 1169-81.

133. Liu, Y., et al., *A fasting inducible switch modulates gluconeogenesis via activator/coactivator exchange.* Nature, 2008. **456**(7219): p. 269-73.

134. Dong, X.C., et al., *Inactivation of hepatic Foxo1 by insulin signaling is required for adaptive nutrient homeostasis and endocrine growth regulation.* Cell Metab, 2008. **8**(1): p. 65-76.

135. Matsumoto, M., et al., *Impaired regulation of hepatic glucose production in mice lacking the forkhead transcription factor Foxo1 in liver.* Cell Metab, 2007. **6**(3): p. 208-16.

136. Cheng, Z. and M.F. White, *Foxo1 in hepatic lipid metabolism.* Cell Cycle, 2010. **9**(2): p. 219-20.

137. Matsumoto, M., et al., *Dual role of transcription factor FoxO1 in controlling hepatic insulin sensitivity and lipid metabolism.* J Clin Invest, 2006. **116**(9): p. 2464-72.

138. Brown, M.S. and J.L. Goldstein, *Selective versus total insulin resistance: a pathogenic paradox.* Cell Metab, 2008. **7**(2): p. 95-6.

139. Converso, D.P., et al., *HO-1 is located in liver mitochondria and modulates mitochondrial heme content and metabolism.* Faseb j, 2006. **20**(8): p. 1236-8.

140. Wei, Y., et al., *Nonalcoholic fatty liver disease and mitochondrial dysfunction.* World J Gastroenterol, 2008. **14**(2): p. 193-9.

141. Kamagate, A., et al., *FoxO1 mediates insulin-dependent regulation of hepatic VLDL production in mice.* J Clin Invest, 2008. **118**(6): p. 2347-64.

142. Zhang, W., et al., *FoxO1 regulates multiple metabolic pathways in the liver: effects on gluconeogenic, glycolytic, and lipogenic gene expression.* J Biol Chem, 2006. **281**(15): p. 10105-17.

143. Puthanveetil, P., et al., *Cardiac triglyceride accumulation following acute lipid excess occurs through activation of a FoxO1-iNOS-CD36 pathway.* Free Radic Biol Med, 2011. **51**(2): p. 352-63.

144. Alhosin, M., et al., *Redox-sensitive up-regulation of eNOS by purple grape juice in endothelial cells: role of PI3-kinase/Akt, p38 MAPK, JNK, FoxO1 and FoxO3a.* PLoS One, 2013. **8**(3): p. e57883.

145. Yamagata, K., et al., *Arginine methylation of FOXO transcription factors inhibits their phosphorylation by Akt.* Mol Cell, 2008. **32**(2): p. 221-31.

146. Tabatabaie, P.S. and R. Yazdanparast, *Teucrium polium extract reverses symptoms of streptozotocin-induced diabetes in rats via rebalancing the Pdx1 and FoxO1 expressions.* Biomed Pharmacother, 2017. **93**: p. 1033-1039.

147. Butler, A.E., et al., *Beta-cell deficit and increased beta-cell apoptosis in humans with type 2 diabetes.* Diabetes, 2003. **52**(1): p. 102-10.

148. Nakae, J., et al., *The forkhead transcription factor Foxo1 regulates adipocyte differentiation.* Dev Cell, 2003. **4**(1): p. 119-29.

149. Kitamura, T., et al., *The forkhead transcription factor Foxo1 links insulin signaling to Pdx1 regulation of pancreatic beta cell growth.* J Clin Invest, 2002. **110**(12): p. 1839-47.

150. Nakae, J., et al., *Forkhead transcription factor FoxO1 in adipose tissue regulates energy storage and expenditure.* Diabetes, 2008. **57**(3): p. 563-76.

151. Ludikhuize, M.C., et al., *Mitochondria Define Intestinal Stem Cell Differentiation Downstream of a FOXO/Notch Axis.* Cell Metab, 2020. **32**(5): p. 889-900.e7.

152. Kim, M.K., et al., *Comparison of pancreatic beta cells and alpha cells under hyperglycemia: Inverse coupling in pAkt-FoxO1.* Diabetes Res Clin Pract, 2017. **131**: p. 1-11.

153. Guo, S., *Insulin signaling, resistance, and the metabolic syndrome: insights from mouse models into disease mechanisms.* J Endocrinol, 2014. **220**(2): p. T1-t23.

154. Chen, J., et al., *Molecular mechanisms of FOXO1 in adipocyte differentiation.* J Mol Endocrinol, 2019. **62**(3): p. R239-r253.

155. Boughanem, H., et al., *Transcriptional Analysis of FOXO1, C/EBP-α and PPAR-γ2 Genes and Their Association with Obesity-Related Insulin Resistance.* Genes (Basel), 2019. **10**(9).

156. Gu, L., et al., *Glucagon receptor antagonism increases mouse pancreatic δ-cell mass through cell proliferation and duct-derived neogenesis.* Biochem Biophys Res Commun, 2019. **512**(4): p. 864-870.

157. O'Neill, B.T., et al., *FoxO Transcription Factors Are Critical Regulators of Diabetes-Related Muscle Atrophy.* Diabetes, 2019. **68**(3): p. 556-570.

158. Shi, Y., et al., *FOXO1 inhibition potentiates endothelial angiogenic functions in diabetes via suppression of ROCK1/Drp1-mediated mitochondrial fission.* Biochim Biophys Acta Mol Basis Dis, 2018. **1864**(7): p. 2481-2494.

159. Li, W., et al., *FoxO1 Promotes Mitophagy in the Podocytes of Diabetic Male Mice via the PINK1/Parkin Pathway.* Endocrinology, 2017. **158**(7): p. 2155-2167.

160. Ferdous, A., et al., *Forkhead factor FoxO1 is essential for placental morphogenesis in the developing embryo.* Proc Natl Acad Sci U S A, 2011. **108**(39): p. 16307-12.

161. Gurtner, G.C., et al., *Targeted disruption of the murine VCAM1 gene: essential role of VCAM-1 in chorioallantoic fusion and placentation.* Genes Dev, 1995. **9**(1): p. 1-14.

162. Yang, J.T., H. Rayburn, and R.O. Hynes, *Cell adhesion events mediated by alpha 4 integrins are essential in placental and cardiac development.* Development, 1995. **121**(2): p. 549-60.

163. Inoguchi, Y., et al., *Poorly controlled diabetes during pregnancy and lactation activates the Foxo1 pathway and causes glucose intolerance in adult offspring.* Scientific Reports, 2019. **9**(1): p. 10181.

164. Kajihara, T., J.J. Brosens, and O. Ishihara, *The role of FOXO1 in the decidual transformation of the endometrium and early pregnancy.* Med Mol Morphol, 2013. **46**(2): p. 61-8.

165. Christian, M., et al., *Cyclic AMP-induced forkhead transcription factor, FKHR, cooperates with CCAAT/enhancer-binding protein β in differentiating human endometrial stromal cells.* Journal of Biological Chemistry, 2002. **277**(23): p. 20825-20832.

166. Kim, J.J., et al., *Role of FOXO1A in the regulation of insulin-like growth factor-binding protein-1 in human endometrial cells: interaction with progesterone receptor.* Biol Reprod, 2005. **73**(4): p. 833-9.

167. Takano, M., et al., *Transcriptional cross talk between the forkhead transcription factor forkhead box O1A and the progesterone receptor coordinates cell cycle regulation and differentiation in human endometrial stromal cells.* Mol Endocrinol, 2007. **21**(10): p. 2334-49.

168. Lappas, M., et al., *Localisation and expression of FoxO1 proteins in human gestational tissues.* Placenta, 2009. **30**(3): p. 256-62.

169. Furuyama, T., et al., *Abnormal angiogenesis in Foxo1 (Fkhr)-deficient mice.* J Biol Chem, 2004. **279**(33): p. 34741-9.

170. Dharaneeswaran, H., et al., *FOXO1-mediated activation of Akt plays a critical role in vascular homeostasis.* Circ Res, 2014. **115**(2): p. 238-251.

171. Wilhelm, K., et al., *FOXO1 couples metabolic activity and growth state in the vascular endothelium.* Nature, 2016. **529**(7585): p. 216-20.

172. Incalza, M.A., et al., *Oxidative stress and reactive oxygen species in endothelial dysfunction associated with cardiovascular and metabolic diseases.* Vascul Pharmacol, 2018. **100**: p. 1-19.

173. Ji, L., et al., *FOXO1 Overexpression Attenuates Tubulointerstitial Fibrosis and Apoptosis in Diabetic Kidneys by Ameliorating Oxidative Injury via TXNIP-TRX.* Oxid Med Cell Longev, 2019. **2019**: p. 3286928.

174. Force, U.S.P.S.T., *Screening for gestational diabetes mellitus: recommendation and rationale.* Am Fam Physician, 2003. **68**(2): p. 331-5.

175. Hami, J., et al., *Some of the experimental and clinical aspects of the effects of the maternal diabetes on developing hippocampus.* World J Diabetes, 2015. **6**(3): p. 412-22.

176. DeSisto, C.L., S.Y. Kim, and A.J. Sharma, *Prevalence estimates of gestational diabetes mellitus in the United States, Pregnancy Risk Assessment Monitoring System (PRAMS), 2007-2010.* Prev Chronic Dis, 2014. **11**: p. E104.

177. Zhao, Z. and E.A. Reece, *New concepts in diabetic embryopathy.* Clin Lab Med, 2013. **33**(2): p. 207-33.

178. Salman, L., et al., *The impact of first trimester fasting glucose level on adverse perinatal outcome.* J Perinatol, 2018. **38**(5): p. 451-455.

179. Martinez-Frias, M.L., E. Bermejo, and A. Cereijo, *Preaxial polydactyly of feet in infants of diabetic mothers: epidemiological test of a clinical hypothesis.* Am J Med Genet, 1992. **42**(5): p. 643-6.

180. Adam, M.P., et al., *Preaxial hallucal polydactyly as a marker for diabetic embryopathy.* Birth Defects Res A Clin Mol Teratol, 2009. **85**(1): p. 13-9.

181. Correa, A., et al., *Diabetes mellitus and birth defects.* Am J Obstet Gynecol, 2008. **199**(3): p. 237 e1-9.

182. Canfield, M.A., et al., *National estimates and race/ethnic-specific variation of selected birth defects in the United States, 1999-2001.* Birth Defects Res A Clin Mol Teratol, 2006. **76**(11): p. 747-56.

183. Erickson, J.D., *Risk factors for birth defects: data from the Atlanta Birth Defects Case-Control Study.* Teratology, 1991. **43**(1): p. 41-51.

184. Lisowski, L.A., et al., *Congenital heart disease in pregnancies complicated by maternal diabetes mellitus. An international clinical collaboration, literature review, and meta-analysis.* Herz, 2010. **35**(1): p. 19-26.

185. Simeone, R.M., et al., *Diabetes and congenital heart defects: a systematic review, meta-analysis, and modeling project.* Am J Prev Med, 2015. **48**(2): p. 195-204.

186. Ewart-Toland, A., et al., *Oculoauriculovertebral abnormalities in children of diabetic mothers.* Am J Med Genet, 2000. **90**(4): p. 303-9.

187. Boutte, P., et al., *[The Vater association in a newborn infant of a diabetic mother].* Pediatrie, 1985. **40**(3): p. 219-22.

188. Weaver, D.D., C.L. Mapstone, and P.L. Yu, *The VATER association. Analysis of 46 patients.* Am J Dis Child, 1986. **140**(3): p. 225-9.

189. Castori, M., et al., *VACTERL association and maternal diabetes: a possible causal relationship?* Birth Defects Res A Clin Mol Teratol, 2008. **82**(3): p. 169-72.

190. Zhao, Z., *TGFbeta and Wnt in cardiac outflow tract defects in offspring of diabetic pregnancies.* Birth Defects Res B Dev Reprod Toxicol, 2014. **101**(5): p. 364-70.

191. Yang, P., et al., *Maternal hyperglycemia activates an ASK1-FoxO3a-caspase 8 pathway that leads to embryonic neural tube defects.* Sci Signal, 2013. **6**(290): p. ra74.

192. Wang, F., et al., *Superoxide Dismutase 1 In Vivo Ameliorates Maternal Diabetes Mellitus-Induced Apoptosis and Heart Defects Through Restoration of Impaired Wnt Signaling.* Circ Cardiovasc Genet, 2015. **8**(5): p. 665-76.

193. Kumar, S.D., S.T. Dheen, and S.S. Tay, *Maternal diabetes induces congenital heart defects in mice by altering the expression of genes involved in cardiovascular development.* Cardiovasc Diabetol, 2007. **6**: p. 34.

194. Zhao, Z., *Cardiac malformations and alteration of TGFbeta signaling system in diabetic embryopathy.* Birth Defects Res B Dev Reprod Toxicol, 2010. **89**(2): p. 97-105.

195. Phelan, S.A., M. Ito, and M.R. Loeken, *Neural tube defects in embryos of diabetic mice: role of the Pax-3 gene and apoptosis.* Diabetes, 1997. **46**(7): p. 1189-97.

196. Gareskog, M., et al., *Maternal diabetes in vivo and high glucose concentration in vitro increases apoptosis in rat embryos.* Reprod Toxicol, 2007. **23**(1): p. 63-74.

197. Fine, E.L., et al., *Evidence that elevated glucose causes altered gene expression, apoptosis, and neural tube defects in a mouse model of diabetic pregnancy.* Diabetes, 1999. **48**(12): p. 2454-62.

198. Morgan, S.C., et al., *Oxidative stress during diabetic pregnancy disrupts cardiac neural crest migration and causes outflow tract defects.* Birth Defects Res A Clin Mol Teratol, 2008. **82**(6): p. 453-63.

199. Xu, H., et al., *A long-term maternal diet intervention is necessary to avoid the obesogenic effect of maternal high-fat diet in the offspring.* J Nutr Biochem, 2018. **62**: p. 210-220.

200. Zuzarte-Luis, V. and J.M. Hurle, *Programmed cell death in the developing limb.* Int J Dev Biol, 2002. **46**(7): p. 871-6.

201. Ahn, S. and A.L. Joyner, *Dynamic changes in the response of cells to positive hedgehog signaling during mouse limb patterning.* Cell, 2004. **118**(4): p. 505-16.

202. Tickle, C. and M. Towers, *Sonic Hedgehog Signaling in Limb Development.* Front Cell Dev Biol, 2017. **5**: p. 14.

203. Tiecke, E., et al., *Manipulations of PKA in chick limb development reveal roles in digit patterning including a positive role in Sonic Hedgehog signaling.* Dev Biol, 2007. **305**(1): p. 312-24.

204. Tisi, D.K., et al., *Fetal exposure to altered amniotic fluid glucose, insulin, and insulin-like growth factor-binding protein 1 occurs before screening for gestational diabetes mellitus.* Diabetes Care, 2011. **34**(1): p. 139-44.

205. Fahami, F., S. Torabi, and S. Abdoli, *Prediction of glucose intolerance at 24-28 weeks of gestation by glucose and insulin level measurements in the first trimester.* Iran J Nurs Midwifery Res, 2015. **20**(1): p. 81-6.

206. Hao, M. and L. Lin, *Fasting plasma glucose and body mass index during the first trimester of pregnancy as predictors of gestational diabetes mellitus in a Chinese population.* Endocr J, 2017. **64**(5): p. 561-569.

207. Kayemba-Kay's, S., et al., *Maternal hyperinsulinism and glycaemic status in the first trimester of pregnancy are associated with the development of pregnancy-induced hypertension and gestational diabetes.* Eur J Endocrinol, 2013. **168**(3): p. 413-8.

208. Riskin-Mashiah, S., et al., *First trimester fasting hyperglycemia as a predictor for the development of gestational diabetes mellitus.* Eur J Obstet Gynecol Reprod Biol, 2010. **152**(2): p. 163-7.

209. Bohuslavova, R., et al., *Gene expression profiling of changes induced by maternal diabetes in the embryonic heart.* Reprod Toxicol, 2015. **57**: p. 147-56.

210. Versiani, B.R., et al., *Caudal dysplasia sequence: severe phenotype presenting in offspring of patients with gestational and pregestational diabetes.* Clin Dysmorphol, 2004. **13**(1): p. 1-5.

211. Schaefer-Graf, U.M., et al., *Patterns of congenital anomalies and relationship to initial maternal fasting glucose levels in pregnancies complicated by type 2 and gestational diabetes.* Am J Obstet Gynecol, 2000. **182**(2): p. 313-20.

212. Kousseff, B.G., *Gestational diabetes mellitus (class A): a human teratogen?* Am J Med Genet, 1999. **83**(5): p. 402-8.

213. Hadden, D.R., *Diabetes in pregnancy 1985.* Diabetologia, 1986. **29**(1): p. 1-9.

214. Comess, L.J., et al., *Congenital anomalies and diabetes in the Prima Indians of Arizona.* Diabetes, 1969. **18**(7): p. 471-7.

215. Chung, C.S. and N.C. Myrianthopoulos, *Factors affecting risks of congenital malformations. II. Effect of maternal diabetes on congenital malformations.* Birth Defects Orig Artic Ser, 1975. **11**(10): p. 23-38.

216. Slee, J. and J. Goldblatt, *Further evidence for preaxial hallucal polydactyly as a marker of diabetic embryopathy.* J Med Genet, 1997. **34**(3): p. 261-3.

217. Parnell, A.S., A. Correa, and E.A. Reece, *Pre-pregnancy Obesity as a Modifier of Gestational Diabetes and Birth Defects Associations: A Systematic Review.* Matern Child Health J, 2017. **21**(5): p. 1105-1120.

218.Vetter, U., et al., *Human fetal and adult chondrocytes. Effect of insulinlike growth factors I and II, insulin, and growth hormone on clonal growth.* J Clin Invest, 1986. **77**(6): p. 1903-8.

219. Lorenzo, M., et al., *IGF-I is a mitogen involved in differentiation-related gene expression in fetal rat brown adipocytes.* J Cell Biol, 1993. **123**(6 Pt 1): p. 1567-75.

220. Sifakis, S., et al., *Maternal serum insulin-like growth factor-I at 11-13 weeks in preeclampsia.* Prenat Diagn, 2010. **30**(11): p. 1026-31.

221. Sifakis, S., et al., *Maternal serum insulin-like growth factor (IGF-I) and binding proteins IGFBP-1 and IGFBP-3 at 11-13 weeks' gestation in pregnancies delivering small for gestational age neonates.* Eur J Obstet Gynecol Reprod Biol, 2012. **161**(1): p. 30-3.

222. Al Naieb, S., C.M. Happel, and T.M. Yelbuz, *A detailed atlas of chick heart development in vivo.* Ann Anat, 2013. **195**(4): p. 324-341.

223. Oyen, N., et al., *Prepregnancy Diabetes and Offspring Risk of Congenital Heart Disease: A Nationwide Cohort Study.* Circulation, 2016. **133**(23): p. 2243-53.

224. Towers, M., et al., *Integration of growth and specification in chick wing digit-patterning.* Nature, 2008. **452**(7189): p. 882-6.

225. Sanz-Ezquerro, J.J. and C. Tickle, *Autoregulation of Shh expression and Shh induction of cell death suggest a mechanism for modulating polarising activity during chick limb development.* Development, 2000. **127**(22): p. 4811-23.

226. Madazli, R., et al., *The incidence of placental abnormalities, maternal and cord plasma malondialdehyde and vascular endothelial growth factor levels in women with gestational diabetes mellitus and nondiabetic controls.* Gynecol Obstet Invest, 2008. **65**(4): p. 227-32.

227. Chan, K.K., L.F. Ho, and T.T. Lao, *Nutritional intake and placental size in gestational diabetic pregnancies--a preliminary observation.* Placenta, 2003. **24**(10): p. 985-8.

228. Coughlan, M.T., et al., *Glucose-induced release of tumour necrosis factor-alpha from human placental and adipose tissues in gestational diabetes mellitus.* Diabet Med, 2001. **18**(11): p. 921-7.

229. Carrasco-Wong, I., et al., *Placental structure in gestational diabetes mellitus.* Biochimica et Biophysica Acta (BBA) - Molecular Basis of Disease, 2020. **1866**(2): p. 165535.

230. Aoyama, H., H. Daitoku, and A. Fukamizu, *Nutrient control of phosphorylation and translocation of Foxo1 in C57BL/6 and db/db mice.* Int J Mol Med, 2006. **18**(3): p. 433-9.

231. Dharaneeswaran, H., et al., *FOXO1-Mediated Activation of Akt Plays a Critical Role in Vascular Homeostasis.* Circulation Research, 2014. **115**(2): p. 238-251.

232. Jeon, H.H., et al., *FOXO1 regulates VEGFA expression and promotes angiogenesis in healing wounds.* The Journal of pathology, 2018. **245**(3): p. 258-264.

233. Schmittgen, T.D. and K.J. Livak, *Analyzing real-time PCR data by the comparative C(T) method.* Nat Protoc, 2008. **3**(6): p. 1101-8.

234. Russell, N.E., et al., *Effect of pregestational diabetes mellitus on fetal cardiac function and structure.* American journal of obstetrics and gynecology, 2008. **199**(3): p. 312. e1-312. e7.

235. Kc, K., S. Shakya, and H. Zhang, *Gestational diabetes mellitus and macrosomia: a literature review.* Ann Nutr Metab, 2015. **66 Suppl 2**: p. 14-20.

236. Stanirowski, P.J., et al., *Impact of pre-gestational and gestational diabetes mellitus on the expression of glucose transporters GLUT-1, GLUT-4 and GLUT-9 in human term placenta.* Endocrine, 2017. **55**(3): p. 799-808.

237. Buchanan, T.A., A.H. Xiang, and K.A. Page, *Gestational diabetes mellitus: risks and management during and after pregnancy.* Nature Reviews Endocrinology, 2012. **8**: p. 639.

238. Gul, M., et al., *Histopathological, Ultrastructural and Apoptotic Changes in Diabetic Rat Placenta.* Balkan Med J, 2015. **32**(3): p. 296-302.

239. Jirkovská, M., et al., *Impact of maternal diabetes type 1 on proliferative potential, differentiation and apoptotic activity in villous capillaries of term placenta.* Placenta, 2016. **40**: p. 1-7.

240. Shi, G., et al., *FoxO1 enhances differentiation and apoptosis in human primary keratinocytes.* Exp Dermatol, 2018. **27**(11): p. 1254-1260.

241. Chen, C., et al., *The vitamin D receptor (VDR) protects pancreatic beta cells against Forkhead box class O1 (FOXO1)-induced mitochondrial dysfunction and cell apoptosis.* Biomed Pharmacother, 2019. **117**: p. 109170.

242. Ren, B., et al., *Heterogeneity of Vascular Endothelial Cells, De Novo Arteriogenesis and Therapeutic Implications in Pancreatic Neuroendocrine Tumors.* J Clin Med, 2019. **8**(11).

243. Ren, B., *FoxO1 transcriptional activities in VEGF expression and beyond: a key regulator in functional angiogenesis?* The Journal of Pathology, 2018. **245**(3): p. 255-257.

244. Xu, Y., et al., *The expression of FoxO1 in placenta and omental adipose tissue of gestational diabetes mellitus.* Exp Clin Endocrinol Diabetes, 2014. **122**(5): p. 287-94.

245. Callaghan, M.J., D.J. Ceradini, and G.C. Gurtner, *Hyperglycemia-induced reactive oxygen species and impaired endothelial progenitor cell function.* Antioxid Redox Signal, 2005. **7**(11-12): p. 1476-82.

246. Wang, D., et al., *Hyperglycemia inhibition of endothelial miR-140-3p mediates angiogenic dysfunction in diabetes mellitus.* J Diabetes Complications, 2019. **33**(5): p. 374-382.

247. PS, N.M., *Birth defects and maternal diabetes mellitus.* Natl Med J India, 1990. **3**(6): p. 283-284.

248. Puthanveetil, P., A. Wan, and B. Rodrigues, *FoxO1 is crucial for sustaining cardiomyocyte metabolism and cell survival.* Cardiovascular Research, 2012. **97**(3): p. 393-403.

249. Sengupta, A., et al., *FoxO1 is required in endothelial but not myocardial cell lineages during cardiovascular development.* Developmental Dynamics, 2012. **241**(4): p. 803-813.

250. Waterland, R.A. and K.B. Michels, *Epigenetic epidemiology of the developmental origins hypothesis.* Annu Rev Nutr, 2007. **27**: p. 363-88.

251. Elsakr, J.M. and M. Gannon, *Developmental programming of the pancreatic islet by in utero overnutrition.* Trends Dev Biol, 2017. **10**: p. 79-95.

252. Bringhenti, I., et al., *The insulin-signaling pathway of the pancreatic islet is impaired in adult mice offspring of mothers fed a high-fat diet.* Nutrition, 2016. **32**(10): p. 1138-43.

253. Han, J., et al., *Long-term effect of maternal obesity on pancreatic beta cells of offspring: reduced beta cell adaptation to high glucose and high-fat diet challenges in adult female mouse offspring.* Diabetologia, 2005. **48**(9): p. 1810-8.

254. Song, Y., et al., *Severe maternal hyperglycemia exacerbates the development of insulin resistance and fatty liver in the offspring on high fat diet.* Exp Diabetes Res, 2012. **2012**: p. 254976.

255. Yokomizo, H., et al., *Maternal high-fat diet induces insulin resistance and deterioration of pancreatic beta-cell function in adult offspring with sex differences in mice.* Am J Physiol Endocrinol Metab, 2014. **306**(10): p. E1163-75.

256. Saisho, Y., et al., *β-cell mass and turnover in humans: effects of obesity and aging.* Diabetes Care, 2013. **36**(1): p. 111-7.

257. Parsons, J.A., T.C. Brelje, and R.L. Sorenson, *Adaptation of islets of Langerhans to pregnancy: increased islet cell proliferation and insulin secretion correlates with the onset of placental lactogen secretion.* Endocrinology, 1992. **130**(3): p. 1459-66.

258. Saisho, Y., et al., *beta-cell mass and turnover in humans: effects of obesity and aging.* Diabetes Care, 2013. **36**(1): p. 111-7.

259. Yamauchi, T., et al., *Globular adiponectin protected ob/ob mice from diabetes and ApoE-deficient mice from atherosclerosis.* J Biol Chem, 2003. **278**(4): p. 2461-8.

260. Talchai, C., et al., *Pancreatic beta cell dedifferentiation as a mechanism of diabetic beta cell failure.* Cell, 2012. **150**(6): p. 1223-34.

261. Intine, R.V. and M.P. Sarras, Jr., *Metabolic memory and chronic diabetes complications: potential role for epigenetic mechanisms.* Curr Diab Rep, 2012. **12**(5): p. 551-9.

262. Ceriello, A., M.A. Ihnat, and J.E. Thorpe, *Clinical review 2: The "metabolic memory": is more than just tight glucose control necessary to prevent diabetic complications?* J Clin Endocrinol Metab, 2009. **94**(2): p. 410-5.

263. Cameron, K.M., et al., *Male mice retain a metabolic memory of improved glucose tolerance induced during adult onset, short-term dietary restriction.* Longev Healthspan, 2012. **1**: p. 3.

264. Fu, Q., et al., *A short-term transition from a high-fat diet to a normal-fat diet before pregnancy exacerbates female mouse offspring obesity.* Int J Obes (Lond), 2016. **40**(4): p. 564-72.

265. Summerfield, M., et al., *A long-term maternal diet transition from high-fat diet to normal fat diet during pre-pregnancy avoids adipose tissue inflammation in next generation.* PLoS One, 2018. **13**(12): p. e0209053.

266. Xie, L., et al., *Effects of prenatal low protein and postnatal high fat diets on visceral adipose tissue macrophage phenotypes and IL-6 expression in Sprague Dawley rat offspring.* PLoS One, 2017. **12**(1): p. e0169581.

267. Zhou, Y., et al., *Sex-associated preventive effects of low-dose aspirin on obesity and non-alcoholic fatty liver disease in mouse offspring with over-nutrition in utero.* Lab Invest, 2019. **99**(2): p. 244-259.

268. Zhou, Y., et al., *Maternal diet intervention before pregnancy primes offspring lipid metabolism in liver.* Lab Invest, 2020. **100**(4): p. 553-569.

269. Tal, M., et al., *Expression and function of GLUT-1 and GLUT-2 glucose transporter isoforms in cells of cultured rat pancreatic islets.* J Biol Chem, 1992. **267**(24): p. 17241-7.

270. Thorens, B., *GLUT2, glucose sensing and glucose homeostasis.* Diabetologia, 2015. **58**(2): p. 221-32.

271. Bernal-Mizrachi, E., et al., *Islet beta cell expression of constitutively active Akt1/PKB alpha induces striking hypertrophy, hyperplasia, and hyperinsulinemia.* J Clin Invest, 2001. **108**(11): p. 1631-8.

272. Dhawan, S., S. Georgia, and A. Bhushan, *Formation and regeneration of the endocrine pancreas.* Curr Opin Cell Biol, 2007. **19**(6): p. 634-45.

273. Bringhenti, I., et al., *Maternal obesity during the preconception and early life periods alters pancreatic development in early and adult life in male mouse offspring.* PLoS One, 2013. **8**(1): p. e55711.

274. Mosser, R.E., et al., *High-fat diet-induced beta-cell proliferation occurs prior to insulin resistance in C57Bl/6J male mice.* Am J Physiol Endocrinol Metab, 2015. **308**(7): p. E573-82.

275. Asghar, Z., et al., *Insulin resistance causes increased beta-cell mass but defective glucose-stimulated insulin secretion in a murine model of type 2 diabetes.* Diabetologia, 2006. **49**(1): p. 90-9.

276. Medina, A., et al., *Early deficits in insulin secretion, beta cell mass and islet blood perfusion precede onset of autoimmune type 1 diabetes in BioBreeding rats.* Diabetologia, 2018. **61**(4): p. 896-905.

277. Poitout, V., et al., *Glucolipotoxicity of the pancreatic beta cell.* Biochim Biophys Acta, 2010. **1801**(3): p. 289-98.

278. Butler, A.E., et al., *beta-Cell Deficit in Obese Type 2 Diabetes, a Minor Role of beta-Cell Dedifferentiation and Degranulation.* J Clin Endocrinol Metab, 2016. **101**(2): p. 523-32.

279. Cinti, F., et al., *Evidence of beta-Cell Dedifferentiation in Human Type 2 Diabetes.* J Clin Endocrinol Metab, 2016. **101**(3): p. 1044-54.